Integration of a Calcium Looping Carbon Capture technology with a Waste-to-Energy Power Plant

TESI DI LAUREA MAGISTRALE IN
ENERGY ENGINEERING
INGEGNERIA ENERGETICA

Author: **Eleonora Cherubini**

Student ID: 939445
Advisor: Ing. Stefano Consonni
Co-advisor: Dr. Edoardo De Lena
Co-advisor: Dr. Maurizio Spinelli
Academic Year: 2021-2022

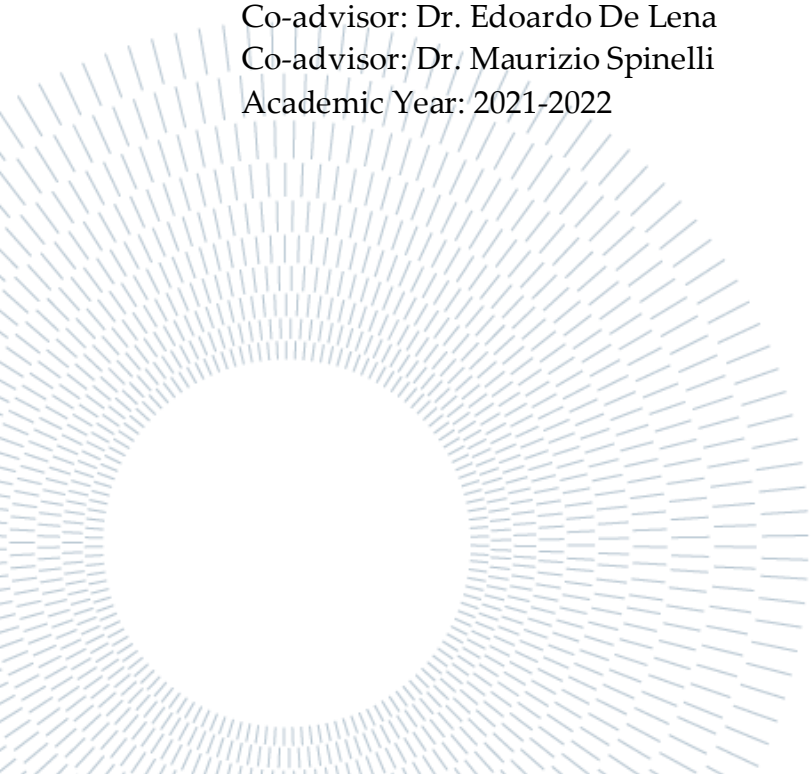

Contents

Abstract

The aim of this thesis is addressing a possible solution to boost the sustainable generation of heat and electricity, by promoting, on one hand, the development of a BECCS technology that leads to net negative emissions, and, on the other, a waste management solution that avoids landfilling.

The solution treated in this work regards the integration of a waste to energy power plant with a CO2 carbon capture technology, which is, more specifically, a calcium looping system. The modeling phase will be conducted using the GS software and MATLAB.

After an analysis of the main sections of a WTE power plant (Chapter two) and the consequences of the CO2 anthropogenic emissions to the atmosphere (Introduction), two different solutions are analysed. In both solutions, a calcium looping technology is implemented, whose functioning is well described in Chapter three.

What I will refer with the name of "Case A" considers a full integration of a post-combustion calcium looping solution, whose heat generated in the exothermic reaction of the process is recovered to generate steam toward the main steam turbine. This solution leads to a significant reduction of the CO2 emissions to the atmosphere with a contained cost for the avoided CO2.

For what concerns "Case B", it refers to an optimized solution that sees the integration of a calcium looping post-combustion technology equipped with its own steam turbine. The steam turbine, due to the presence of cleaner flue gases, is able to work at higher temperature and pressure compared to the main turbine. This condition leads to an optimization, in terms of efficiency, compared to the previous case and an increase in the net power output. However, considering a situation in which neither the carbon tax nor the gate fee is applied, case B is not only more complex in terms of plant configuration, but it is also more expensive.

A final simplified analysis gives a better understanding of the costs related to both the solutions.

Key words: Waste to Energy, Power generation, Waste Management, BECCS, Calcium looping system

Sommario

Questa tesi indaga una soluzione alternativa per la produzione di elettricità e/o calore: da un lato, si ha come obiettivo la promozione di una tecnologia BECCS, mentre, dall'altro, si propone una soluzione alternativa allo smantellamento in discarica dei rifiuti.

Nel presente lavoro si propone l'analisi dell'integrazione di un termovalorizzatore con il calcium looping utilizzato come sistema di cattura della CO2. La presente analisi sarà svolta utilizzando il software di simulazione GS e MATLAB.

Dopo una descrizione introduttiva (Introduction) delle conseguenze principali delle emissioni di CO2 in atmosfera, si procede con una descrizione del funzionamento delle varie sezioni di un termovalorizzatore (Chapter two), per poi analizzare nello specifico la tecnologia del calcium looping (Chapter three).

Il lavoro termina con la presentazione di due casi studio. In primo luogo, il caso A considera l'integrazione del termovalorizzatore di riferimento con il sistema di cattura della CO2. La presenza di una reazione esotermica è sfruttata con un recupero del calore e produzione di vapore. Il vapore prodotto è inviato in turbina e contribuisce alla produzione di energia elettrica. Questa soluzione è semplice e i costi sono contenuti.

Per quanto riguarda, invece, il caso B, la proposta fa riferimento ad un'integrazione volta all'ottimizzazione del processo di cattura: il sistema di calcium looping è equipaggiato con una turbina ausiliare che funziona a temperatura e pressione più alta. Questo è consentito dalla presenza di fumi di combustione più puliti. La soluzione proposta ha come risultato un impianto più performante, ad efficienza e potenza generata maggiore. Nonostante le migliori performance dell'impianto, questa soluzione presenta una maggiore complessità nel design e costi più elevati.

Lo studio si conclude con una breve analisi economica che permette una più completa comparazione tra i due casi studi.

Parole Chiave: Termovalorizzatore, Management dei rifiuti, BECCS, Calcium looping

Introduction

The issues related to climate change are becoming more and more visible and, with a faster pace, researchers from all over the world have been defining new scenarios to handle it. Climate change can lead to relevant consequences, which will expose people, societies, economic sectors, and ecosystems to serious risks for an undetermined period. To avoid the worst outcomes from climate change it has been highlighted the importance of reaching net-zero emissions by mid-century. The interconnection between the anthropogenic impact, such as, for example, the industrial emissions of greenhouse gases, and the warming of the planet, oceans, and atmosphere has become clearer thanks to the observation of huge amounts of historical and recent data. The International Energy Agency (IEA) has defined a Sustainable Development Scenario (SDS), as shown in Figure 1, which describe a future in which the United Nations (UN) energy-related sustainable development goals for emissions, energy access, and air quality are met.

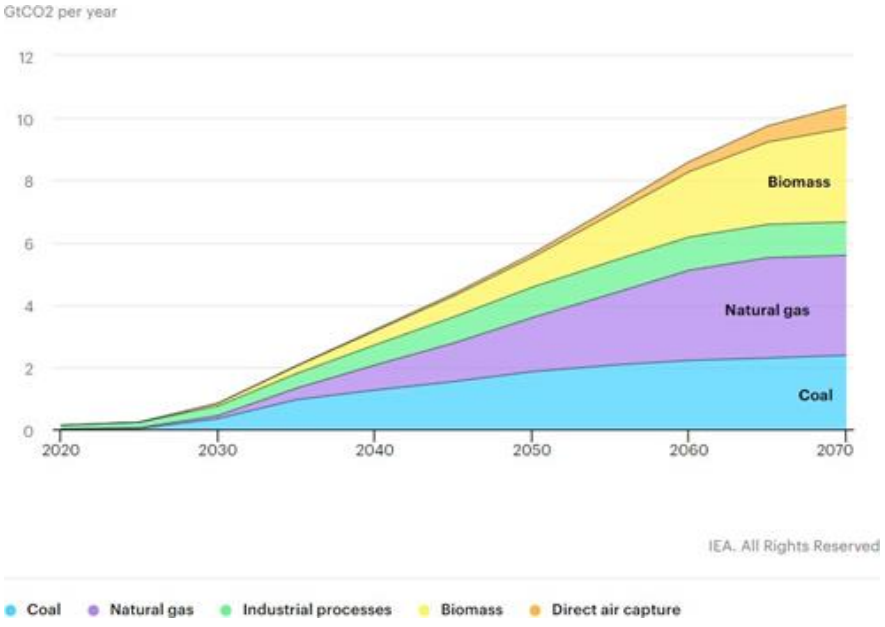

Figure 1 IEA, World captured CO2 by source in the Sustainable Development Scenario, 2020-2070, IEA, Paris https://www.iea.org/data-and-statistics/charts/world-captured-co2-by-source-in-the-sustainable-development-scenario- 2020-2070

This Scenario is based on a series of near-term emission reductions, without assuming any net negative emissions. It also integrates the stimulus incentives required for a global recovery after the COVID-19 crisis. The objective defined by this SDS define a zero emission on a net basis by 2070 and the contribution of CCUS

is expected to account around 15% of the cumulative reduction in emissions compared with the Stated Polices Scenario, involving almost all parts of the global energy system. Carbon capture utilization and storage systems can avoid carbon dioxide (CO2) emissions at their source, enabling, on one hand, the fossil-fuel-based countries to smoothen their energy transition both in the economic and technical matter and, on the other, reduces the impact of production plants whose CO2 emissions would be unavoidable otherwise. Time is running out to reach net-zero emissions and limit temperature rise to 1.5 degrees (°C) by 2050 and energy efficiency implementation, reduction of energy consumption, and waste production, together with CCUS, can push the trend toward the objective.

Although the COVID-19 crisis has resulted in unprecedented reductions in energy demand and emissions in its first phase, the long-term picture for CCUS has not changed because a rebound in CO2 production is expected. To have the greatest chance of achieving net-zero emissions, it is essential that wide use of CCUS happens quickly. Now is the time to accelerate investments in CCUS both in the energy sector and in the production plant sector. Policymakers can accelerate the low-carbon transition by supporting policies that promote carbon capture technologies in power generation, giving direction to utilities and investors, and in production plants. The latter has still a wide range of improvements. Policy actions will need to consider local and regional power market characteristics and the anticipated role of CCUS-equipped plants in the market, which may evolve over time as flexibility requirements increase. The availability of CO2 transport and storage infrastructure or demand for CO2 from users will be critical to underpin investment in CO2 capture facilities at power plants. Policymakers are likely to need a range of approaches to support successful green business cases and accelerate deployment of carbon capture technologies in power generation, including capital support, public procurement, tax credits, regulatory standards and obligations and operational subsidies.

Additionally, support for Carbon Capture Utilization and Storage (CCUS) in economic recovery plans can ensure the COVID-19 crisis does not derail recent progress. CCUS is in a much stronger position to contribute to sustainable recoveries than it was after the 2008 global financial crisis. Since then, deployment has tripled, the range of demonstrated applications has expanded, costs have declined, and new business models have emerged.

1.1. Why is it important to avoid CO2 anthropogenic emissions?

To describe the problems related to carbon dioxide anthropogenic emissions, the concept of "Carbon Cycle" needs to be addressed. Carbon circulates among the atmosphere, oceans, soil, plants, and animals as liquid and solid, in carbohydrate molecules as mineral compounds or hydrocarbons, and in the gaseous form, as carbon dioxide. It can be found in the atmosphere because of respiration, volcanos, and fossil fuels, or biomass combustion and it can also be found dissolved in water. The carbon cycle can be roughly split into two cycles, the slow component, and the fast component. The slow component is the one operating over hundreds of thousands of years, while the fast component is the one linked to a much faster release. Among the different kinds of emissions, it can be distinguished the natural emissions and human-related emissions: the latter can be direct and indirect, and they come mainly from fossil fuels combustion, fossil fuel extractions, wildfires, and land-use change.

Because anthropogenic emissions have been adding to the natural sources for centuries, an imbalance is now registered. Consequently, carbon dioxide (CO2) is the primary greenhouse gas emitted through human activities. A greenhouse gas causes the well-known "greenhouse effect": solar radiation passes largely unhindered through the atmosphere, heating the Earth's surface. In turn, energy is re-emitted as infrared, much of which is absorbed by CO2 and water vapor in the atmosphere, which thus acts as a greenhouse surrounding the Earth. The concentration of CO2 in the atmosphere is increasing year by year as we burn fossil fuels, which enhances the natural greenhouse effect and warms the planet. However, the increase in the average surface temperature of the Earth is not the only dramatic consequence. System feedbacks include changes in the circulation of the atmosphere and ocean (redistributing heat around the globe), the melting of snow and ice (altering albedo: the reflection of solar radiation from the Earth's surface), sequestration of CO2 by plants, changes to the amount and types of clouds, and altered atmospheric water vapor (a warmer atmosphere holds more water), among others.

1.2. How can CO2 anthropogenic emissions be avoided using Carbon Capture technologies?

Different approaches can be adopted to limit or avoid the CO2 emissions in the atmosphere: among those options, Carbon Capture Utilization and Storage (CCUS) solutions have become a valid and interesting option applicable in the decarbonization of different sectors, because they allow the capture of CO2 from large point sources, including power generation or industrial facilities that use fossil fuels. In Figure 2 it is clearly reported the contribution of the different sectors in the overall amount of CO2 anthropogenic emissions.

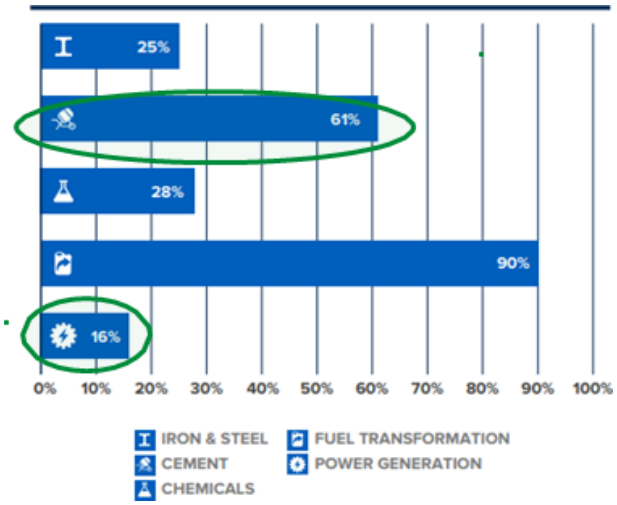

Figure 2 Contribution of CCUS to sector CO2 emissions reductions up to 2070 in the IEA Sustainable Development Scenario

Researchers have been focusing their effort on finding more efficient and less costly solutions to boost sustainable consumption and production in a pathway toward a "net-zero emission scenario" or, even better, to a "negative emission scenario".

The sectors which would be mostly impacted by the use of CCUS are the following:

- **hard-to-abate industries** (cement, iron and steel, and chemical sectors): those industries are the ones that emit carbon due to the nature of their industrial processes and high-temperature heat requirements. In the IEA's Sustainable Development Scenario, CCUS accounts for between one quarter and two-thirds of the cumulative emissions reduction in heavy industries;

- **dispatchable power**: a third of global CO2 emissions is linked to electricity generation, therefore rapid decarbonization is required to achieve net-zero

emissions. CCUS equipped power plants will help ensure that the low-carbon grid of the future is resilient and reliable. Flexible power plants with CCUS supply dispatchable and low-carbon electricity as well as grid-stabilizing services, such as inertia, frequency control, and voltage control, characteristics which cannot be provided by non-predictable renewable generation. Moreover, retrofitting fossil fuel generation with CCUS can be a cost-effective option in some cases, such as in the countries whose economy is dependent on coal.

Existing power plants and heavy industries CO2 emissions are reported in Figure 3. By reducing the CO2 emissions of existing power plants, it has been estimated by IEA that by 2030, more than half of the CO2 captured will be from retrofitted existing infrastructures, avoiding up to 600 billion tons of CO2 over the next five decades.

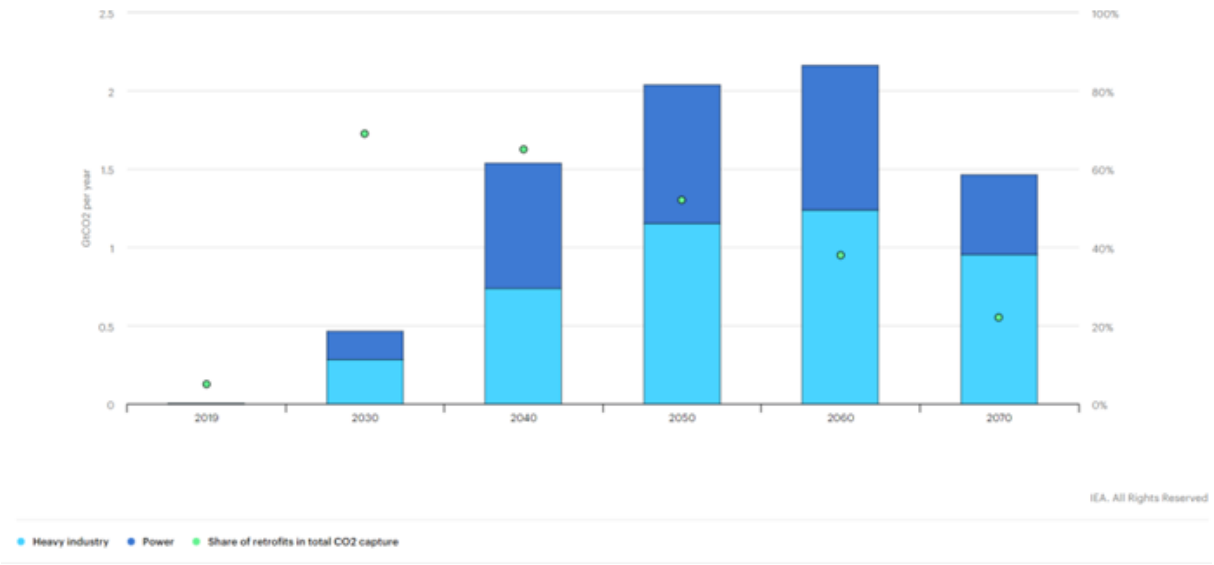

Figure 3 IEA, World CO2 emission reductions from CCUS retrofits in the power generation and heavy industry in the Sustainable Development Scenario, 2019-2070, IEA, Paris https://www.iea.org/data-and-statistics/charts/world-co2- emission-reductions-from-ccus-retro

Additionally, CCUS could be also employed to promote the spreading of **a cost-effective hydrogen production**, that could boost sustainable mobility and cleaner consumptions in industries and buildings. One of the cheapest and at the same time low-carbon emission solutions is the production of hydrogen via coal or natural gas plants with CCS. Nowadays, this solution represents around the 40% of low carbon "blue hydrogen".

1.3. What is the share of CCUS facilities around the World?

According to the IEA Report (1), the CCUS facilities around the world have a capacity to capture more than 40 MtCO2 each year: Figure 4 lists the most common technology employed.

However, to increase the development of this technology, further investments and incentives need to be destinated to building new facilities, increasing the pipeline infrastructures, and developing new hubs. Outside of targeted incentives on policies for CCUS, the introduction of carbon taxations and higher carbon prices in Europe are making CCUS a more attractive option for many industries, that see in the CCUS technology the only option to contribute to reaching the net zero emission scenario. Moreover, an increase interest in producing hydrogen safely and sustainably has resulted in a steep increase in the interest of improving the technologies availability and in building new facilities. Therefore, researchers from different sectors are starting to study a way to cut the costs: not only technical improvements, but also new business models have emerged (2), especially in the transport and storage field.

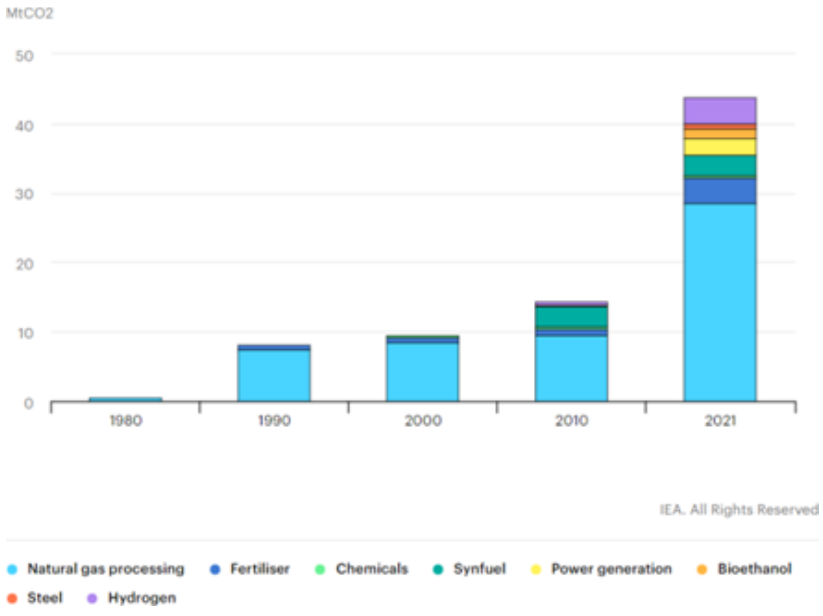

Figure 4 IEA, CCUS facilities in operation by application, 1980-2021, IEA, Paris https://www.iea.org/data-and-statistics/charts/ccus-facilities-in-operation-by-application-1980-2021

The World has reacted to the crisis in a completely different way compared to the previous years: 2021 has seen unprecedented advances for carbon capture,

utilization and storage and the tangible results could be seen in Figure 5 and Figure 6. In 2021 more than 100 new CCUS facilities have been programmed and the CO2 pipeline are going to significantly grow (it is expected to quadruple).

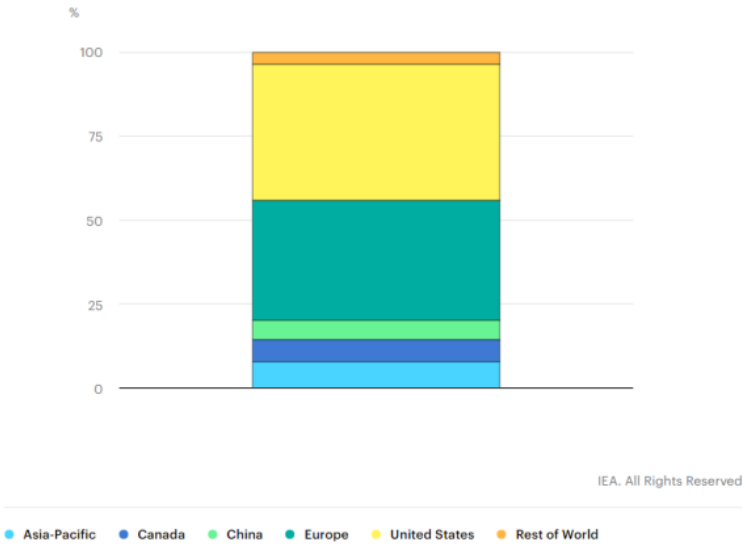

Figure 5 IEA, Global CCUS projects in development by region or country, 2021, IEA, Paris https://www.iea.org/data- and-statistics/charts/global-ccus-projects-in-development-by-region-or-country-2021

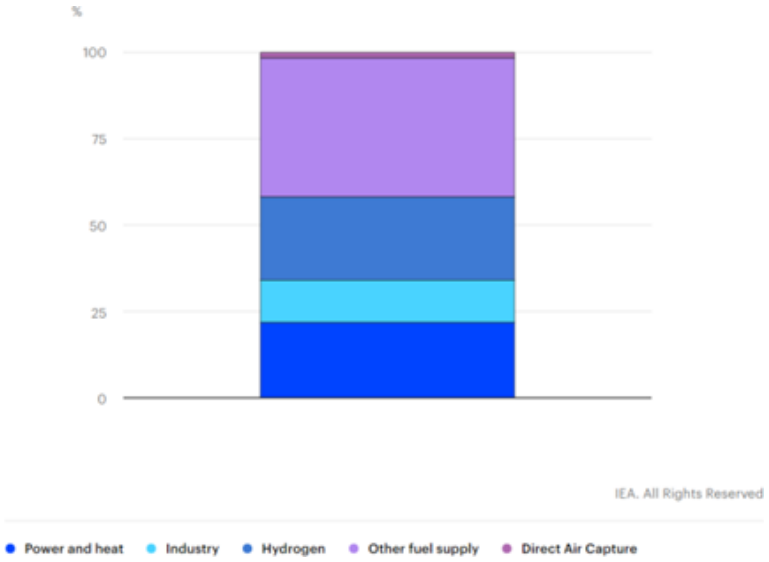

Figure 6 IEA, Global CCUS projects in development by application, 2021, IEA, Paris https://www.iea.org/data-and- statistics/charts/global-ccus-projects-in-development-by-application-2021

More specifically, what is the share of CCUS-equipped WTE power plants?

Worldwide there are 2.090 WTE power plants using MSW as fuel in 42 countries, with a treatment capacity of around 360 million tons of waste per year. According

to a literature survey that used public reports and private interaction with the plant operators (3), the benchmark technology in the field is the MEA based absorption process and the removal target is often equal to 90%. Further considerations on the advantages of this integration will be discussed in Chapter two.

1.4. Why is CCUS useful and important in the transition toward low-carbon power production? Aren't the renewable energy sources sufficient?

We are facing an era in which electricity demand is steeply increasing, but the carbon footprint of its generation needs to drastically decrease to align with the Sustainable Development Goals and the Paris Agreement targets. As shown in Figure 7, the energy production needs to change quickly, reducing the amount of energy generated by fossil fuels. Among the different options, renewable energy sources have acquired a significant recognition, thus wind and solar production power plants have been under construction for years.

However, most of the renewables are non-programmable and have a low reliability due to their unpredictability. Additionally, their life cycle impact is still under study and their production is not yet linked to net zero emissions.

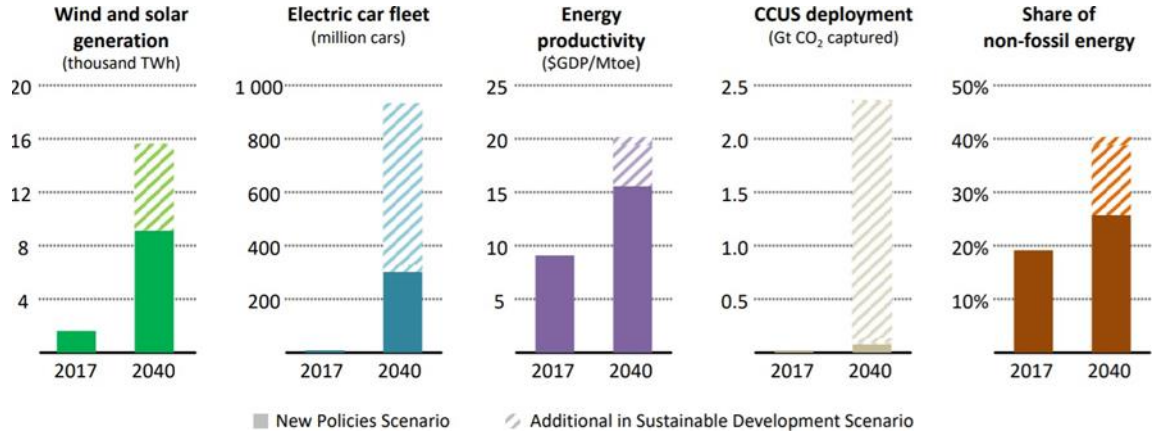

Figure 7 Energy sector transformation in the New Policy Scenario and SDS: delivering the energy transformation in the SDS requires 13% more energy sector investments due to ramped up demand-side investment. Source: (4)

As said before, the share of renewable energy sources plays a key role, but this solution drags with it several drawbacks, such as unpredictability, unreliability, heterogeneity in the spatial distribution, and in the year-based time frame. On one hand, it has increased the awareness of the need for a dramatic change in the grid

infrastructure and management, on the other, new solutions need to be integrated to handle the fluctuations and the peaks.

It is clear now that carbon capture technologies are going to undertake a key role in providing dispatchable, globally distributed low-carbon electricity, and with a lower space encumbrance and costs than other solutions. Taking these aspects under consideration, the future power generation assets will be valued not only for energy, but also for a diverse set of services like grid services, inertia, and frequency provision, or turn-down capabilities and dispatchability. All these services are essential for a reliable and affordable power supply. This is a key reason why traditional cost metrics like the Levelized cost of electricity (LCOE) are often inadequate when evaluating the economics, as they do not reflect the total cost and value of generation assets to the operation of the power system.

1.5. What are the optional steps after the CO2 is captured?

Once the CO2 has been captured, it is important to properly select the destination of the captured molecule. Figure 8 shows a general overview of the most popular destinations and use of CO2 around the world (5). Additionally, in all these cases, it is important to underline the transportation phase, that links the capture to the storage and/or utilization facility. However, the destination needs to be well evaluated prior the selection of the transportation option, because the CO2 concentration and the thermodynamic characteristics of the stream change based on the final use (paragraph 1.5.1 illustrates the different transportation's options) of the different CCUS technologies.

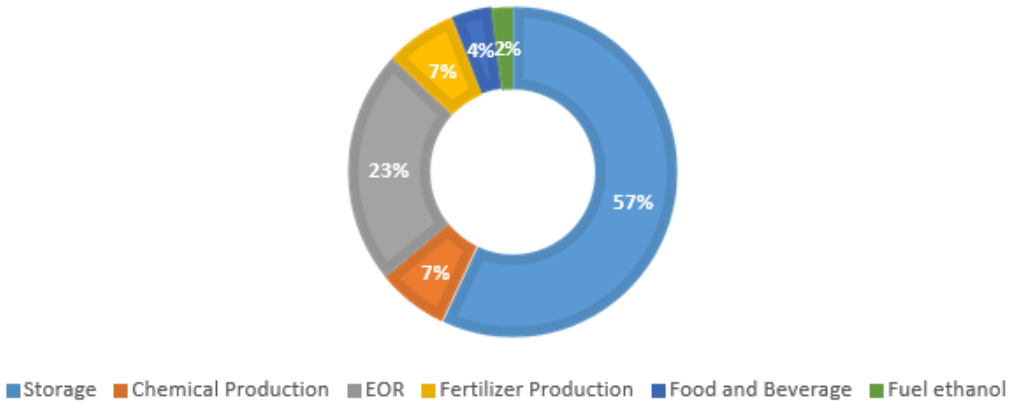

Figure 8 CO2 destination for major world countries

Once the different possibilities, in terms of destination, have been listed, what is the best approach to achieve the climate goals?

The IEA Clean Technology Scenario (CTS) (6) assumes, to achieve the climate goals, a cumulative CO2 storage of 107 GtCO2 by 2060, but that would require a significant scale-up of CO2 storage facilities from today's levels. Due to the difficulties linked to the CO2 storage availabilities a new scenario has been proposed: the Limited CO2 storage Scenario variant (LCS) considers a storage availability up to 10 Gt CO2 over the scenario period, thus considers additional measures and technologies that would be required to achieve the same emissions reductions by 2060. This scenario implies the implementation of different utilization options (in paragraph 1.5.2) that could boost the sustainable development in the power, industrial, transport and buildings sectors.

Therefore, on one hand, more specific analysis and more investments are required to study different geological sites to increase the operative sites all over the world; on the other hand, the utilization of CO2 has recently become topic of several research, because classified as renewable source, low-cost and not-toxic alternative.

1.5.1. Transport

Transport is that stage that links the sources and the storage sites (7). CO2 can be transported in the three different states: gas, liquid and solid (this specific case is not considered in the commercial-scale applications). When transported in the gaseous phase, the gas is compressed to reduce the volume occupied. This is the case of pipeline transportation. Furthermore, liquefaction, or eventually solidification, could lead to a further reduction of the volume required for transport: this solution is adopted in case shipping is selected.

Additionally, the selection of the transportation criteria is also related to safety and reliability of the technology selected.

Even if transport of CO2 already occurs daily in many parts of the world, significant investments in transportation infrastructure are required to enable large-scale deployment. Among the different solutions, three main options will be further analyzed: pipelines, ship transportation, and trucks transportation.

What is the right choice?

In terms of economic evaluation, the price needed to transport CO2 via pipeline from the site of capture to the site of storage varies between 0,5 € to 10 € per 100 km (the range is dependent on the nature of the pipelines – onshore or offshore). On the

other hand, boat transportation is less costly on greater distances, but the real convenience needs to be properly studied because of non-continuous supply.

Pipelines

Onshore and offshore pipelines are the most common method of transporting the very large quantities of CO2 involved in CCUS. There is significant experience with CO2 pipeline development and operation on land and under the sea, ensuring safety and reliability of the system.

Nowadays, 6.500 km of pipelines are actively transporting CO2. That said, the scale of pipeline infrastructure needed to support longer-term CCUS deployment around the world is considerable. The estimated CO2 transportation infrastructure to be built in the coming 30-40 years is roughly 100 times larger than currently exists.

When CO2 is transported via pipeline, the stream must be brought in the supercritical state, thus at a temperature greater than 74 bar and a temperature higher than 31 °C. Additionally, CO2 pipeline operators have established minimum specifications for the stream composition, dependent on the transportation technology, but also on the destination. In case the CO2 is going to be used for EOR a low content of nitrogen is required, while in case of CCS this detail is not so important. Additionally, the humidity of the stream needs to be lower than 60% to avoid corrosion problems of the pipes. This problem could be easily solved by purification or dehydration.

Tankers

A promising method for longer distances and offshore storage is via tankers. This solution implies the ship transportation, but also the transport of CO2 via trucks and rails, if small quantities are handled. Given the large quantities of CO2 that would be captured via CCUS in the long term, it is unlikely that truck and rail transport will be significant.

Ship transportation can be an alternative option for many regions of the world. CO2 could be continuously captured and stored temporarily on land and loading facilities. The capacity, service speed, number of ships and shipping schedule is planned to take into account the CO2 capture rate, transport distance, and social and technical restrictions. If the delivery point is onshore, the CO2 is unloaded from the ships into the temporary storage tanks, otherwise, ships may unload it into the platform, to a floating storage facility. Due to the strong similarities with the transportation of the LPG, the scaling up of the system is easier. Shipment of CO2

already takes place on a small scale in Europe, where ships transport food-quality CO2 (around 1,000 tons) from large point sources to coastal distribution terminals.

1.5.2. Utilization

Because of CCS facilities' high costs, the term CCS has recently become CCUS (Carbon capture, utilization, and storage) wherein the economic value of the captured CO2 was promoted through utilization. It is worth emphasizing that CO2 utilization technologies alone cannot mitigate enough CO2 emissions and that the excessive promotion of utilization as a solution could lead to a dangerous outcome. This is also because CO2 utilization is not necessarily linked with net climate benefit, but with indirect effects that are worth to be accounted for in the energy transition. Underpinning research into CO2 conversion should continue to expand options and reduce costs.

CO2 utilization is an industrial process that makes the CO2 an economically valuable product, involving it in chemical reactions or using it directly in processes. Additionally, many CO2-using techniques, such as soil carbon sequestration, are becoming more popular, thanks to the CO2 capacity to enhance crop yields, thus, to make an economic profit.

Among the different options three pathways' categories need to be listed:

- "open" utilization pathways: CO2 is stored in leaky biological systems (purple arrows) such as biomass and soil;

- "closed" utilization pathways: CO2 is permanently stored (red arrows) in the lithosphere (via CO2-EOR or BECCS), in deep ocean, or in mineralized carbon in the built and natural environments.

- "cycling" utilization pathways: thanks to the transformation of CO2 into CO2- based fuels, carbon moves around the short cycle (yellow arrows). They don't provide net CO2 removal from the atmosphere, but they allow an emission reduction via industrial CO2 capture and by limiting the fossil fuel use. This is the most popular conventional utilization pathway.

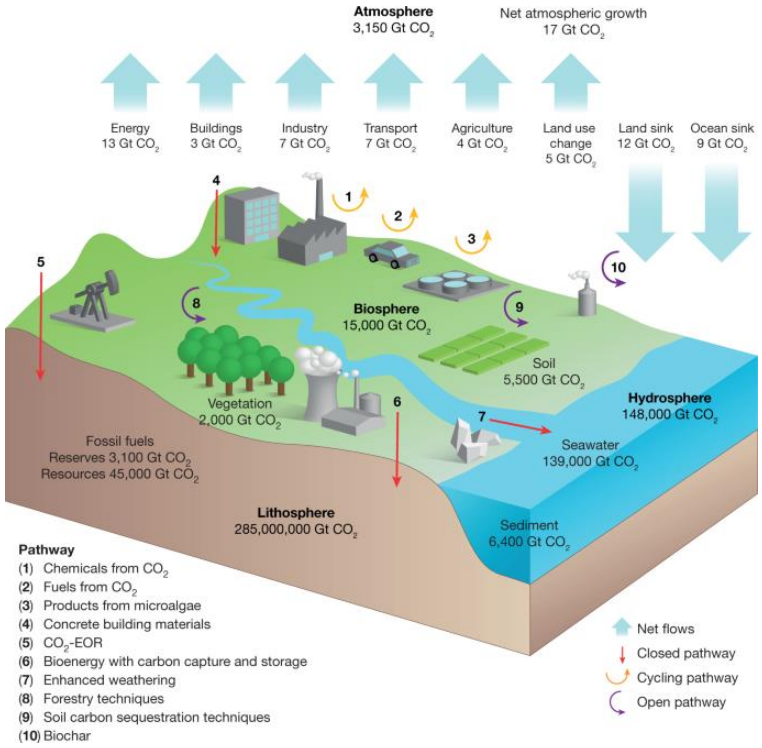

Figure 9 Stocks and net flows of CO2, including 10 numbered potential utilization and removal pathways. Source: Hepburn et al. (8)

Figure 9 shows the different removal pathways and lists the 10 main options of CO2 utilization. More specifically, the ten main utilization pathways are the following:

1) **Chemicals from CO2**: thanks to a catalytic chemical conversion of CO2 from flue gas or other sources, products, such as methanol, urea or plastics, are produced. CO2 is back released in the atmosphere through hydrolysis or decomposition of the products;

2) **Fuels from CO2**: thanks to a catalytic hydrogenation processes CO2 is converted into derived fuels, such as methane and Fischer-Tropsch derived fuels from flue gas or other sources. CO2 is re-emitted in the atmosphere through combustion;

3) **Products from microalgae**: microalgae take the CO2 from the atmosphere and allow the production of biofuels, biomass or bioproducts (aquaculture feed). CO2 is released in the atmosphere through combustion or by consumption of the specific bioproduct;

4) **Concrete building materials**: through mineralization of CO2 from flue gas or other sources CO2 could be transformed into carbonated aggregates or concrete products a material that cures concrete;

5) **CO2 – EOR**: though CO2 injection into oil reservoirs, it is allowed a geological sequestration that is continuous over time. This technique has a nearly zero re- emission in the atmosphere;

6) **Bioenergy with carbon capture and storage (BECCS)**: by burning biomass, bioenergy could be obtained, allowing a nearly zero re-emission in the atmosphere because permanent storage is involved;

7) **Enhanced weathering**: via application of pulverized silicate rock, CO2 is transformed into agricultural crop biomass through mineralization, leading to possible atmospheric acidic conditions;

8) **Forestry techniques**: growth of woody biomass via afforestation, reforestation or sustainable forest management;

9) **Soil carbon sequestration techniques**: via land management practices it could be increased the percentage of soil organic carbon;

10) **Biochar**: growth of plant biomass for pyrolysis to produce bioenergy.

Among the pathways listed above, it is expected that conventional utilization pathways, such as chemicals, fuels, microalgae, building materials and CO2-EOR, might be able to utilize around 0,5 GtCO2/year in 2050: it has also been estimated by Hepburn et al. (8) that between 0,2 and 3,5 GtCO2/year could be removed and stored for centuries.

	Pathway	Removal potential in 2050 [MtCO2/year]	Utilization potential in 2050 [MtCO2/year]	Breakeven cost of CO2 utilization [2015 US$ per ton of CO2]
Conventional utilization	Chemicals	10 to 30	300 to 600	-80$ to 320$
	Fuels	0	1000 to 4200	Up to 670$
	Microalgae	0	200 to 900	230$ to 920$
	Concrete building materials	100 to 1400	100 to 1400	-30$ to 70$
	CO2-EOR	100 to 1800	100 to 1800	-60$ to -45$
Non-conventional utilization	BECCS	500 to 5000	500 to 5000	60$ to 160$
	Enhanced weathering	2000 to 4000	n.d.	Up to 200$
	Forestry techniques	500 to 3600	70 to 1100	-40$ to 10$
	Land management	2300 to 5300	900 to 1900	-90$ to -20$
	Biochar	300 to 2000	170 to 1000	-70$ to -60$

Table 1 Range estimated of potential for CO2 utilization and present-day breakeven cost. Source: (8)

Utilization pathways often involve removal and long term or short-term storage, to limit the re-emission in the atmosphere of carbon dioxide. However, storage selection varies based on the specific utilization pathway that is considered.

From an economical point of view the "breakeven CO2 cost" is introduced (Table 1) in order to properly represent the theoretical incentive per ton of CO2 utilized that would be necessary in order to implement a specific economic pathway. The indicative breakeven cost reported above is one of the necessary parameters to underline the challenges related to scaling-up utilization. Another factor related to cost barriers is the impact that CO2 utilization has on the final price of the product, that may become not competitive in the market.

Additionally, another issue of utilization is related to the energy requirements: some of the pathways listed above require energy, which leads to further costs and emissions.

In conclusion, to boost CO2 utilization, major policy and regulatory changes need to be made to support the appropriate scale-up of the technologies, reducing the prices on one hand, and, on the other, penalizing CO2 emissions and incentivizing verifiable reductions or atmosphere removal. Thus, from the perspective of mitigating climate change, CCU can, at most, be seen as supplementing CCS to a

small extent. Any proposals for its large-scale deployment should be accompanied by a careful and thoughtful analysis of associated opportunity costs.

1.5.3. Storage

The injection and storage of CO2 have been working safely and effectively for 45 years.

CO2 is stored through a trapping mechanism that considers the injection of the CO2 into the pores of a storage reservoir. As explained by the Global CCS Institute (9) and shown in Figure 10, there are four main trapping mechanisms, depending on the geology of the reservoir and local formation conditions:

1) **Physical trapping**: free-phase CO2 is contained below an extensive low-permeability caprock.

2) **Residual trapping**: as the CO2 migrated into the reservoir, the gas is trapped in the pore space and micro-scale heterogeneities through capillary forces.

3) **Dissolution trapping**: it occurs when CO2 encounters brine and the CO2 can dissolve, forming a solution. A CO2-saturated brine solution is thicker than unsaturated brine and sinks to the bottom of the reservoir permanently.

4) **Mineral trapping**: the interaction of CO2 with the brine and the reservoir lithology can lead to chemical reaction that form stable carbonate minerals.

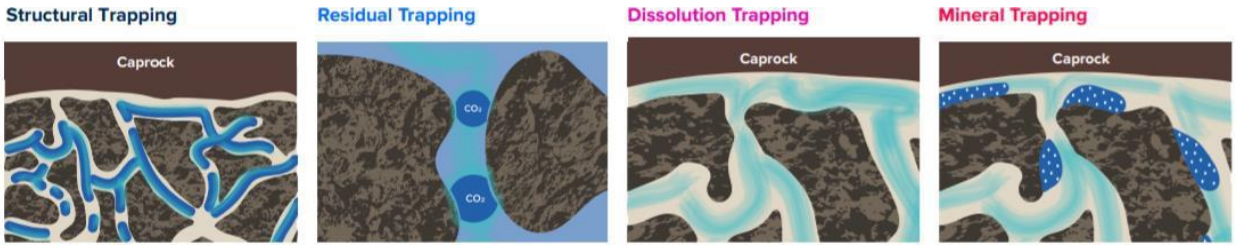

Figure 10 Trapping mechanisms during injection and storage of CO2. Source: IPCC 2005

However, to understand deeply what happens to CO2 stored underground, not only the permanent trapping needs to be studied, but also the leakages must be considered, to ensure a safe and efficient storage system.

To have a general overview of the possibilities, it must be stated that the geological sites throughout the world that can retain centuries' worth of CO2 captured from industrial processes are many. Only the global geological storage capacity for CO2

is many times larger than what is required for CCS to play its full role in supporting the achievement of net-zero emissions under any scenario. The Global CCS Institute has analyzed the different basins around the world, and they have ranked as unlikely, possible, suitable, or highly suitable, as shown in Figure 11.

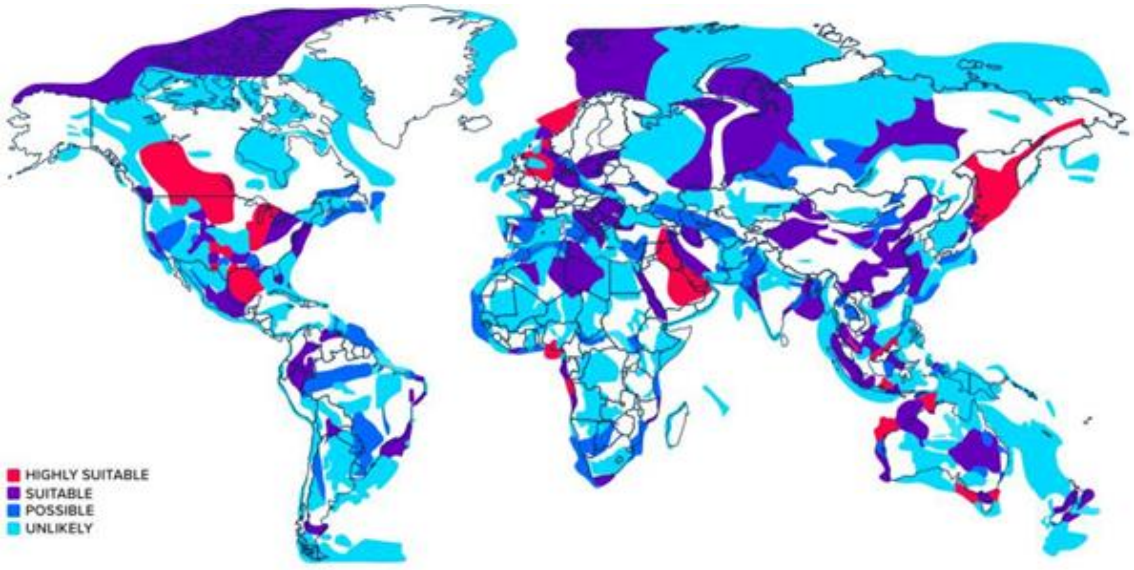

Figure 11 Suitable storage regions of the world based on the Global CCS Institute's storage basin assessment database

Additionally, by analyzing the 2021 CO2 Storage Resource Catalogue, it could be stated that the percentage of still undiscovered and unexploited surface of storage basins is in the order of Gtons of CO2 stored. Only in 2021 715 sites across 18 nations were added, resulting in a total of 13.000 GtCO2 of storage resources across the entire catalogue.

Recent studies are also exploring the potential of saline formations (more than sedimentary basins). For instance, analysis to date supports the generally held view that 98% of global storage resources are in saline formations. In fact, a large proportion of the world's key CO2 storage locations have now been vigorously assessed and almost every high-emitting nation has demonstrated substantial underground storage resources.

2 Chapter two: WTE power plant production

As the world population grows and living standards continue to rise, the consumption of goods and energy is increasing too, leading to a consequent increase in the generation of waste. The World bank has reported a value of 1,3 billion tons of waste generated annually in the world, and it is expected an increase up to 2,2 billion tons per year by 2025. The production of Municipal Solid Waste is strictly related to the economic development, the industrialization level, and the local climate (World Bank, 2018): especially countries that register a higher GDP or have a higher degree of urbanization produce larger amounts of waste (shown clearly in Figure 12).

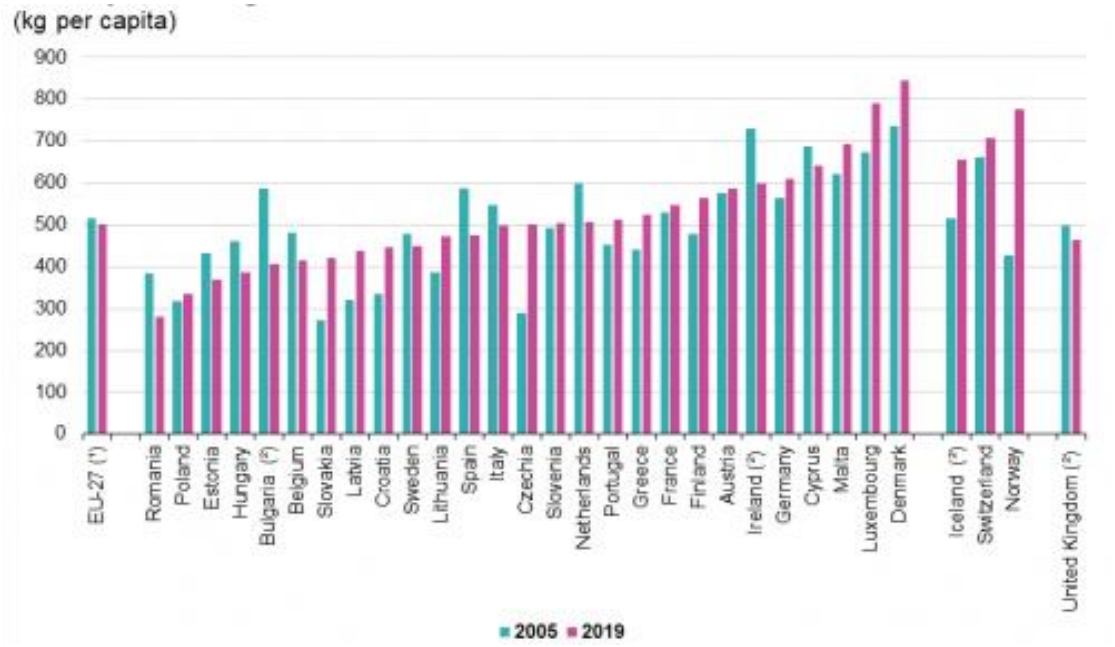

Figure 12 Municipal waste generated, 2005 and 2019

These alarming values have brought up the necessity of discovering different options in the waste management sector.

In general, with "Municipal solid waste (MSW)" we refer to the waste that is mainly collected by or on behalf of municipal authorities and it is disposed of through waste management systems. According to the EU Directive 2018/851, 2018 of the European Waste Framework Directive, MSW is defined as: (i) mixed waste and separately collected waste from households, including paper and cardboard, glass,

metals, plastics, bio-waste, wood, textiles, packaging, waste electrical and electronic equipment, waste batteries and accumulators, and bulky waste, including mattresses and furniture; (ii) mixed waste and separately collected waste from other sources, where such waste is similar in nature and composition to waste from household.

According to the World Bank (10), in 2016, the MSW composition was as described in Figure 13.

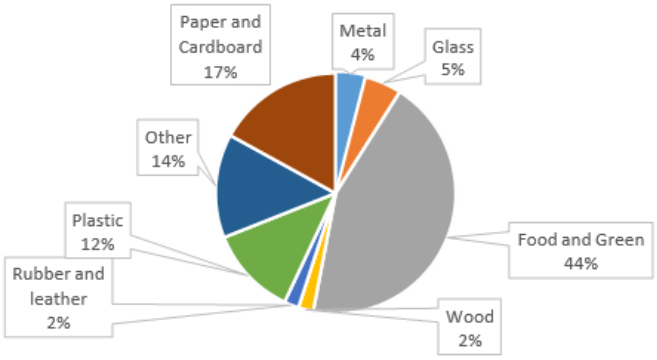

Figure 13 MSW composition worldwide in 2016. Source [11]

Proper MSW management ensures environmental, economic, and social sustainability, thus, the EU Waste Framework Directive (WFD, 2008/98/EC) has built a comprehensive legislation on the matter, and it has the purpose of guiding the European member's choices. The Directive aims at improving waste management, as well as to reduce greenhouse gas emissions and adverse health and environmental impacts, through a hierarchy of management options, which includes a legally binding prioritization of waste management activities.

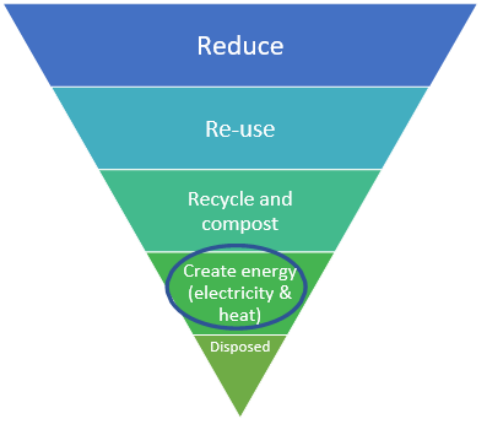

Figure 14 The Waste Hierarchy, an upside-down pyramid

The legislation, at both the EU and member states levels, has shifted from disposal of MSW to its prevention and recycling, as shown in the upside-down pyramid in Figure 14.

However, even if the waste hierarchy is very strict, Member States must always take measures to encourage the options that deliver the best overall environmental outcome. This means that it is possible to break this rigid structure by justifying the choices using the Life Cycle Assessment Approach (LCA). This tool has been classified by the international set of norms ISO 14040 as the most efficient technique to evaluate a process and to boost sustainable production and consumption. LCA focuses on the entire life cycle of a process, or a product, and it can help minimize in a transparent way the direct, indirect and avoided/substituted environmental impacts.

The evolution of the EU framework is the new Green Deal, with its ten pillars, which focuses on developing a low-carbon, low-energy economy and proposes a new resource and energy transition that foresees massive investment in clean, safe energy and energy efficiency as an explicit basis for sustainable growth across EU member states.

Why is it important to implement the shared power of WTE power plants?

Figure 14 shows clearly all the different options among all the waste management solutions prior the selection of landfilling. Waste to Energy power plants fit the fourth option of the hierarchy, and it includes the possibility to produce electricity and heat starting from waste that cannot be recycled. The solution appears interesting because (i) heat and electricity would have been generated otherwise with an alternative source i.e. fossil-based, (ii) because in every recycling process there will always be a percentage of waste material that cannot be recycled but still has a potential, especially in terms of heating value, and (iii) the management/treatment of waste would have been carried out through landfilling.

Given that the average heating value of municipal solid waste (MSW) is averagely 10 MJ/kg, the use of waste to produce energy could contribute to solving the dilemmas of waste management and energy demand, and it could ease the transition to a more sustainable model of production and consumption. By generating heat and/or electricity with MSW containing around 50% of biogenic carbon, only the fossil-derived CO2 must be considered: the biogenic-derived CO2 is considered carbon neutral. In this way, the direct emissions discharged at the stack through the flue gas are significantly reduced. With around 39 TWh of electricity and 90 TWh of heat produced in Europe annually, WTE power plants

could prevent the production of up to 50 million tons of CO2 emissions that would otherwise be generated by fossil fuels.

Indeed, because this solution also diverts waste from landfills, additional avoided emissions need to be taken into consideration. Avoiding landfilling prevents the production of methane emissions, which, according to the EPA, has a global warming potential (GWP) of 28-36 and, additionally, is the precursor to ozone (which is itself a GHG). In the end, avoiding the landfilling option, leads to savings in terms of space and visual pollution.

Finally, the possibility of further recovering solid residues from the bottom ashes, such as ferrous and non-ferrous metals (mainly aluminum) lead to an additional percentage of avoided emissions. Aluminum could be reused for many applications, like road background, landfill recovery, preparation of raw flour fed to cement kilns and raw material in the concrete or ceramic products. It could also be used for secondary metal production, avoiding the use of primary material, which is an energy intensive process.

Including WTE power plants in the future scenarios allows a clean energy transition toward a coal-free energy sector, by providing a programmable power production, stability during transients, rotating inertia and ancillary services, aspects that are becoming crucial in a world dominated by renewables and non-programmable sources.

Nowadays, what is the shared power of WTE power plants worldwide?

In the whole world around 2.090 WTE plants are active, and they have a disposal capacity of around 400 million tons of waste per year. Generation from waste is the highest in Germany (7,1 MWh in 2018), followed by the UK (4,4 MWh), France (2,5 MWh), Italy (2,4 MWh) and the Netherlands (2,2 MWh). However, it is expected a wide increase in the next years, shown by new projects that are spreading around the world. It has been estimated that nearly 2.700 plants with a capacity of more than 550 million tons per year will be operational by 2029.

2.1. General overview of the technology

WTE power plants make the conversion of a wide variety of waste into electricity and heat through a combustion process. In general, the waste combustion process appears complex and less efficient compared to coal or natural gas combustion because of its solid and heterogeneous nature, therefore the stable operation of the plant is prioritized respect to reaching the optimal efficiency, even if it has a crucial

economic and environmental value. The flue gas is used in a boiler to heat up water and send steam either to a steam turbine or to a heating system to generate electricity or/and heat. The possibility of having a cogenerated asset allows a further improvement in the environmental benefits of WTE power plants.

The operating phases of the incineration plant are essentially five: the waste receipt and storage, the combustion, the steam generation, the flue gas purification and, eventually, the cogeneration of electricity and heat.

More specifically, in this work, I'm going to analyze a power plant like the "Silla 2" WTE power plant, taken as reference plant for the Calcium looping implementation (Chapter 3). In Figure 15 a scheme of a typical WTE power plant can be seen, in order to highlight the main sections.

"Silla 2" was built in Milan in 2001 and it generates heat and electricity using the residual waste found at the outlet of a recycling process, to hence the waste management integrated system. The power plant can heat up more than 37.000 families and provide electricity to around 115.000 families per year. In 2020 the power plant treated 542.942,04 tons of waste (nearly 60% of the city's waste) generating 374.277,589 MWh_{el} and 306.737,08 MWh_{th} (11).

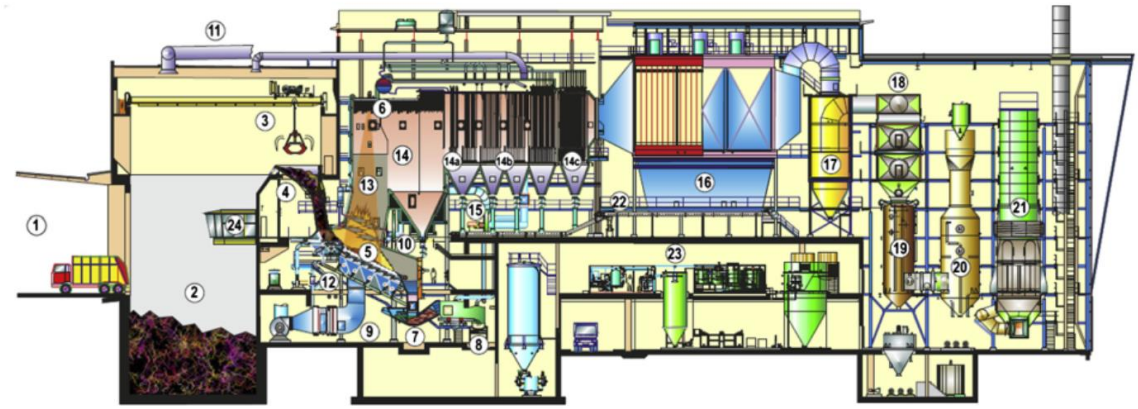

Figure 15 WTE power plant main sections description. Source (12)

The first section of the WTE power plant is the storage: after being weighted and controlled, the MSW is unloaded into the bunker which can store up to 30.000 m^3 of waste in a depressurized environment (this is needed to avoid leakages to the atmosphere). Each plant has a properly designed bunker which is needed to ensure

a continuous supply and, thanks to the cranes, to homogenize the waste in terms of composition and heating value. This last operation makes sure that the combustion process, therefore the efficiency and the power output, can be optimized. The cranes are also needed to lead the waste into the combustion chamber through the feeding system, after weighting it. Afterwards, through the feeding system, the waste is not only sent into the combustion chamber, but unwanted entrance of air into the system is controlled.

The next section of the reference power plant is the combustion chamber. In general, the combustor can be either a grate combustor or a fluidized bed combustor. While the former is preferred in case untreated waste is burned, the latter is used in case SRF is selected. In this specific case, a horizontal moving grate combustion chamber was chosen; "Silla 2" has three independent and identical combustion lines with an overall input power equal to 212 MW_{th}.

During the combustion phase the combustion heat is released and, in the boiler, it is exchanged counter currently with the water present into the boiler's tube banks. In WTE power plants the boiler is designed in a less sophisticated way compared to coal-fired power plants due to the much smaller sizes and corrosion problems. Waste is characterized by the presence of chlorine, which forms, during the combustion process, gaseous or liquid chloride-containing compounds that are well known to accelerate the corrosion rates. There is also a high presence of molten salts containing chlorine which have been considered a major cause of rapid corrosion attack. Because of this reason, not only the tube banks' asset is constrained (usually no re-heating is present), but also the optimal operating conditions, such as the maximum pressure and maximum temperature of the cycle. Thus, the efficiency can be increased up to a maximum value set by technical constraints

The asset of the boiler's tube banks must be done properly: (i) the evaporator is located in the radiative section, because evaporating water has the best heat transfer coefficient, and the wall temperature can remain low; (ii) the pressure is controlled as well because higher is the pressure higher is the risk of corrosion (in this case the pressure is set equal to 50 bar); (iii) in the convective section we have first the superheater and then the economizer, because liquid water has the worst heat transfer coefficient.

The superheating temperature is the maximum temperature of the cycle, and it remains close to 423 °C.

The last section of the power plant is the flue gas treatment line: it can have different assets based on techno-economic evaluations and each pollutant or particulate

matter emitted in the atmosphere need to be kept under control. The main gaseous pollutants emitted by a Waste to Energy power plant are the one related to the combustion process, such as CO, NOx, SO_2, Total Suspended particles (TSP), the acid gases, such as HCl, HF and HBr and the micropollutants.

The former pollutants are mainly dependent on the thermodynamics and chemical species involved in the combustion process: even if the selection of the waste characteristics is an important primary measure to reduce the emissions, their generation is unavoidable.

- CO is a tracer of the effectiveness and completeness of the combustion process, and, due to the heterogeneity of the fuel involved in the process, their percentage is higher compared to fossil fuel combustion;
- NOx are mainly generated from the nitrogen present in the atmosphere, but, in case of a high percentage of organic waste, they are also generated from the nitrogen present in the fuel. finally, the TSP are dependent only on the fuel's choice. They can be controlled through secondary measures, such as the Selective Catalytic Reduction (SCR) or the Selective Non Catalytic Reduction (SNCR),
- SO2 are mainly generated by the presence of sulfur into the fuel, and the SO2 emissions are usually controlled together with the acid gases' removal.

Acid gases' emissions, on the other hand, are a peculiar characteristic of waste to energy facilities, and they are generated by the reactions of halogens with hydrogen. Acid gases are usually removed via chemical neutralization with alkaline reactants, through dry processes or semi-dry processes: in the former method it is used hydrated lime or sodium bicarbonate as a reactant, while, in the latter, it is used the milk of lime (suspension of lime in water).

Finally, the micropollutants, are the volatile heavy metals (Hg, Cd, Pb) and the Organic compounds (PCDD/F, PCB, PAH): even if they are present in small concentrations they must be kept under control and activated carbon injections are usually used for the purpose.

Among the aforementioned gaseous pollutants, the CO2 emissions must be considered as well, as it represents one of the major greenhouse gas pollutants. This thesis focuses on the implementation of a CO2 capture facility in the flue gas treatment line: the Calcium Looping System (Chapter three) has been selected to investigate the technical and economic advantages of this technology compared to the benchmark solutions that are currently available on the market. The purpose of the study is suggesting a plausible design for a Calcium Looping post-combustion

system that well integrates with the existing power plant, increasing its environmental benefits.

"Silla 2 has already been designed to keep the direct emissions way below the limits set by both European and Italian regulations.

Finally, through three distinct stacks 120 m tall the flue gas is released in the atmosphere: a designed system takes under control with a continuous operation the emissions to verify that the limits are being respected.

WTE power plant's efficiency

In the end, a brief consideration on the efficiency of the power plant needs to be addressed: efficiency is an important parameter which must be increased as much as possible to increase the amount of CO2 avoided. It has been proven that, to have an avoidance of CO2 emitted greater than the power plant's emissions, an efficiency of more than 25% is required: the net electrical efficiency of a typical WTE power plant is in the range of 10 - 30%, because of the low energy content of the raw MSW, its fluctuation in composition and size, as well as the various corrosive species contained in the MSW reducing the effectiveness of heat recovery.

In order to increase the efficiency of WTE power plants, there are a several routes that can be followed, such as

1) increasing the size of the plant, because of reduced losses related to scale effect;

2) improvement of the steam cycle operating parameters: one option could be the increase of the evaporating pressure or SH temperature, but strong corrosion caused by meta chlorides and the HCl present in the flue gas need to be considered. To solve the problem, it could be improved the selection of the boiler's tubes material, but this is linked to higher costs. Another solution to solve the problem could be the use of a percentage between 10% and 15% of recirculated flue gases, that moderate the temperature on the walls. Beside the increase in pressure and temperature, to improve the efficiency of the steam cycle, the pressure of condensation could be reduced. This is related to the selection of the condenser and the related techno-economic analysis;

3) reduction of combustion air excess: it needs to be done considering a minimum value related to the completeness of the combustion process. Minimum air excess allows a minimization of the thermal losses at the stack,

reduced parasitic load of the plant associated with air and flue gas blowers, and reduced thermal NOx generation.

2.1.1. Advantages of CCUS-equipped WTE plants

The main advantages of CCUS-equipped WTE power plants are avoiding landfilling and reaching "net zero emissions".

First, by avoiding the landfilling option, not only the CH4 emissions (a greenhouse gas which could be referred as CO2 equivalent) are avoided but electricity and/or heat are also generated. Because of those reasons, WTE power plants could be considered an important technology in the energy transition due to its essential contribution in the emissions reduction and waste management: to enhance the environmental advantages, the introduction of a CO2 Carbon, Utilization and Storage system (CCUS) controls the CO2 emissions at the stack, significantly reducing the environmental impact. More specifically, by adding a Calcium Looping technology a CCUS facility, the environmental impacts are reduced also in terms of acid gases emissions, removing the residual compounds present in the flue gases after the proper treatment section.

Second, municipal solid waste (MSW) represents a suitable fuel source for a Bioenergy and Carbon Capture and Storage (BECCS) system considering its large organic waste fractions. According to the Global CCS Institute, emerging BECCS technologies must be considered the "best solution to decarbonize emission-intensive industries and sectors and enable negative emissions". BECCS involve the utilization of biomass, or, as in this case, a percentage of biogenic carbon as an energy source, and the capture and permanent storage of CO2 produced during the conversion of biomass to energy. The final use of biomass can vary significantly, such as transformed in biofuel or directly sent to an end user that proceeds with a combustion process. The CO2 emitted could be captured and stored. If the CO2 that is stored is greater than the CO2 emitted during biomass production, transport, conversion, and utilization, we can refer to a "negative emissions" process.

In the case of MSW combustion, the nature of the CO2 emissions needs to be specified: it could be assumed that WTE power plant emits only a 50% of fossil-derived CO2; the remaining 50% of the CO2 emitted comes from biogenic sources. Comparing MSW to other fuel solutions, it could be stated that the recovered fuels have a lower fraction of biogenic carbon, while coal and fossil fuels in general don't have any. Therefore, BECCS are foreseen as a critical pathway to limit the global warming to 1.5◦C above pre-industrial levels (IPCC, 2018), as specified in the Paris Agreement.

Moreover, WTE plants represent a stationary CO2 emitter that is reasonably large for the implementation of efficient CCUS processes. Thereby, the benefits of an efficient MSW treatment and the achievement of negative CO2 emissions are combined. Additionally, major disadvantages of BECCS applications based on cultivated energy crops, such as land system change, biosphere integrity or freshwater use, are avoided, once the already available MSW is used as the biogenic carbon source. Finally, the plant produces steam that could be used for CO2 regeneration when using solvent-based CO2 capture.

However, even if the greenhouse gas emissions significantly decrease, a series of other environmental impact categories increase because of efficiency penalty, additional infrastructures and waste generation related to the capture process. This thesis aims at providing an estimation of the main aspects of integrating a Calcium Lopping system, as CCUS technology, to finalize a balance between the positive and negative aspects of the integration.

3 Chapter three: Calcium Looping process

Calcium Looping (CaL) process may represent an important alternative option for post- combustion CO2 capture from WTE plants because it is particularly suited for being retrofitted to already existing industrial plants and it well integrates with streams containing chlorine, due to the alkaline nature of the solvent used.

It is an adsorption process which has the aim of challenging the benchmark technologies for post-combustion capture – the amine (MEA) absorption separation process and the oxyfuel combustion – trying to improve their negative aspects. Despite their maturity, both amine absorption separation process and the oxyfuel combustion are associated with several issues. On one hand, the amine scrubbing suffers of both sorbent degradation at elevated temperatures (T> 105-150 °C) and oxidation degradation, because it reacts with SO2 and NOx present in the flue gas forming highly cancerogenic compounds and, moreover, it has a low CO2 loading, causing the need of large units, a large amount of heat for solvent regeneration (3.0-5.0 GJ/ton CO2) and high circulation power consumption. On the other hand, oxyfuel combustion requires expensive cryogenic separator, stringent safety requirements, fouling, leaks affecting CO2 purity and it is suitable only for greenfield powerplants.

3.1. General overview of the CaL technology

Calcium Looping is a technology that utilizes natural or industrial waste's calcium-based sorbents to produce a highly pure stream of CO2 (> 95%). In general, this process employs twin fluidized bed reactors (Figure 16) which operate at high temperature and atmospheric pressure. They are needed to exploit the capability of Calcium Oxide-based sorbents of capturing the CO2 from combustion gases, by means of sequential carbonation-calcination cycles.

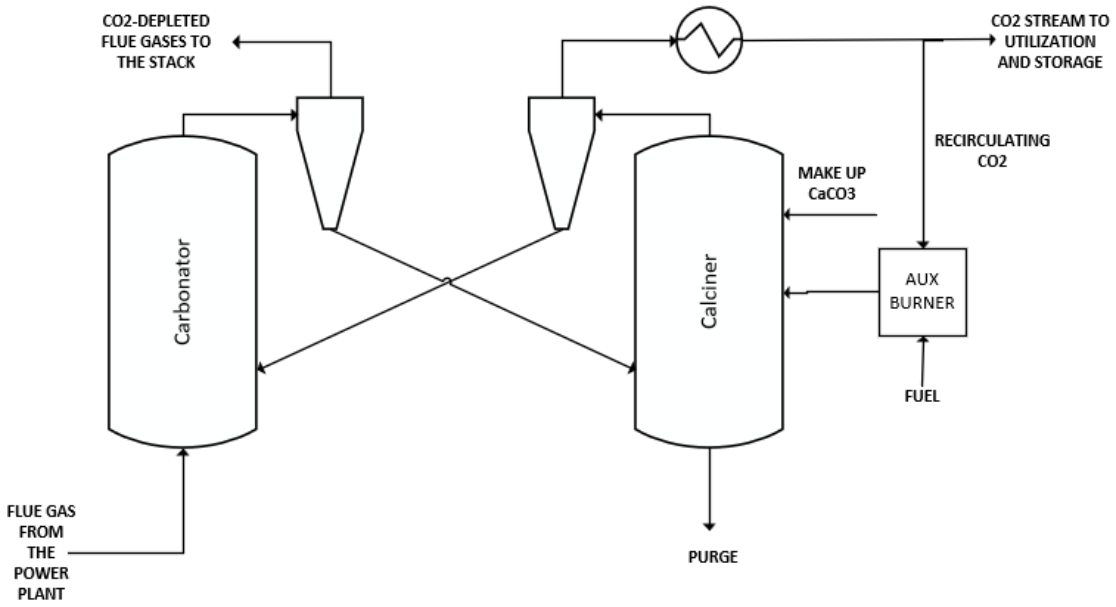

Figure 16 Conceptual scheme of a Calcium looping process focused on removing CO2 from the flue gas of an existing power plant (post-combustion CO2 capture solution)

The carbonation reaction (1) occurs into the carbonator reactor

$$CaO + CO_2 \rightarrow CaCO_3 \quad (1)$$

$$\Delta H_{298K} = -178{,}8\,\frac{kJ}{mol}$$

It is an exothermic reaction that leads to the adsorption of CO2 by CaO. It releases a great amount of energy that can be efficiently recovered to produce high pressure steam. The carbonator's optimal operating conditions, considering kinetics and the chemical equilibrium, are T=650-700 °C and high CO2 partial pressure (in general, lower temperatures lead to a more advantageous chemical equilibrium but a slower reaction rate and vice versa). Additionally, a large inventory of CaO is required.

For what concerns the structure of the reactor, it has membrane walls to remove heat and to keep the temperature constant. The products of the reaction are first separated with a cycle and then the solid stream is transported to the second reactor to be regenerated. The decarbonized flue gas can leave the carbonator toward the stack through a further heat recovery step. Because the carbon capture efficiency at the outlet of the carbonator is always lower than one, unreacted CaO will be found in the stream: from some tests performed in a 1 MWth scale plant (12) it has been seen that the efficiency of capturing the CO2 from the flue gas in the carbonator reaches up to 88% but it decreases as the number of cycles increase due to the deactivation of the sorbent.

The carbonator efficiency can be evaluated as follows:

$$\eta_{carb} = \frac{F_{CO_2 absorbed\ in\ carbonator}}{F_{CO2}} \quad (2)$$

Whilst the forward reaction (1) is exothermic, the backward reaction (2) – which is called calcination reaction - is endothermic. It needs heat from the outside that allows to reach its optimal operating conditions (T=900-950°C and partial pressure close to 1 bar).

Heat is supplied by a direct or indirect combustion in which natural gas, pulverized coal, or a recovered fuel can be burned. The main attempt of the calciner is the regeneration of the sorbent by the desorption of CO2 from CaO. Once the two streams are separated, they can be divided by another cyclone: the gaseous stream is mainly composed by the CO2 captured in the carbonator, the one generated by the auxiliary combustion, plus the one introduced by the make-up stream (if it occurs in the calciner). The carbon capture efficiency in the calciner is nearly 100%.

In the end, the CO2-rich gas leaves the calciner at 350 °C by generating superheated and reheated steam (heat is recovered increasing the overall efficiency of the system). We must underline the fact that a fraction of this nearly pure stream of carbon dioxide is recycled as fluidizing gas and temperature moderator; the other part, will be sent to a direct contact cooler for final cooling before entering the CO2 purification unit.

Finally, the CO2 stream is compressed at supercritical pressure, to reach a density of the stream comparable to the one of a liquid ($\rho = 800\ \frac{kg}{m^3}$) and it is either used for multiple applications or stored in saline formations or depleted fossil fuel reservoirs, as described in the introduction.

The overall CO2 capture efficiency of the CaL process (3) is defined as the CO2 mass flow rate leaving the calciner compared to the CO2 entering the system via the flue gas of the upstream plant, the fuel and the make-up introduced into the calciner:

$$\eta_{CO_2\ total} = \frac{m_{CO_2 calciner\ out}}{m_{CO_2 inlet} + m_{CO_2 fuel} + m_{CO_2 makeup}} \quad (3)$$

3.2. The conversion processes

During the exothermic carbonation reaction, CaO captures CO2, leading to the production of CaCO3. This reaction could be divided into two chronological steps characterized by different limiting effects on the particle conversion. The first period (fast phase regime) is mainly controlled by kinetics, and it shows a rapid CaO conversion, while the second regime (slow phase regime) is controlled by the diffusion of CO2 through the nanoscale CaCO3 layer formed during the previous phase [15]. The final aim is ensuring the achievement of full completion of the fast carbonation phase because it ensures higher conversion efficiency. It has been found that the transition to the slow kinetic regime occurs suddenly when the CaCO3 layer around the CaO micro-grains reaches the critical thickness of 49 nm (which is related to a specific level of conversion – the maximum carbonation conversion).

The particle conversion, or even better, the carrying capacity, declines along with the carbonation/calcination cycles. Because of this reason, all the experimental data collected by Abanades (13) can be retrofitted by the following expression: $X_{c,N}=fN+1+b$, where f=0,782 and b=0,174. In the aforementioned equation, b represents the residual carbonation conversion, that can be justified with the formation of a product layer of CaCO3 inside the large voids still present (the carbonation reaction is completely reversible for b≤1). The reason behind the decay of the sorbent capture capacity lies in the difference between the crystalline structure of CaO and CaCO3: the calcium carbonate grains are characterized by a higher molar volume, which reduces the particle porosity and obstructs the CO2 path through the sorbent particles.

Because of a decay in the particle conversion with an increased number of cycles, the CO2 capture efficiency needs to be introduced, with a dependency on $X_{C,N}$:

$$\eta_{CO_2} = \frac{(F_R + F_0)X_c^*}{F_{CO_2} + F_0} \qquad (4)$$

where F_{CO2} is the molar flow rate of CO2 entering into the system in the flue gases and F_R is the molar flow rate of recirculated solids, while F_0 is the molar flow rate of fresh make-up. To link the solid streams F_0 and F_R to the number of cycles, a succession of mass balance was introduced in the Abanades work (13):

$$r_N = \frac{F_0 F_R^{N-1}}{(F_0 + F_R)^N} \qquad (5)$$

Therefore, starting from equation (4) and (5) the average conversion is defined as

$$X_N^* = \sum_{k=1}^{\infty} r_k X_{c_k} \quad (6)$$

Incorporating equation (4), (5) and (6):

$$X_N^* = \frac{f\left(\frac{F_0}{F_R}\right)}{\left(\frac{F_0}{F_R}\right) + 1 - f} + b \quad (7)$$

$$\eta_{CO_2} = \frac{1 + \left(\frac{F_0}{F_R}\right)}{\left(\frac{F_0}{F_R}\right) + \left(\frac{F_{CO_2}}{F_R}\right)} \left(\frac{f\left(\frac{F_0}{F_R}\right)}{\left(\frac{F_0}{F_R}\right) + 1 - f} + b \right) \quad (8)$$

Equation (8) allows to reason on the effect of the significant parameters F0/FR and FR/FCO2 on the overall efficiency of the system and set the basis for an optimization analysis.

However, the progressive reduction of porosity and the consequent obstruction of the CO2 diffusion is also caused by the particle exposure to high temperatures during each calcination cycle. Consequently, the sorbent porosity reduction during each carbonation- calcination cycle reduces the active area available in the calciner for the CO2 diffusion, affecting the CO2 transport capacity of the sorbent particles. To take into account the active area reduction, the following equation could be considered:

$$\left(\frac{S_0 - S}{S_0}\right)^{\gamma} = K_i t \quad (9)$$

where S is the active surface at the time t and Ki is a parameter that takes into account the dependence of the CO2 diffusion from temperature, surface tension and a series of other parameters; γ is a factor that depends on the diffusion mechanism inside the sorbent grain structure and, for CaO particles, it is equal to γ = 2,7 (14).

Therefore, an updated conversion capacity XN, that consider sintering, must be introduced: according to Wang et al. (15) the decay trend could be expressed by equation (10), that relates the particle, which experiences the Nth cycle, to the number of cycles by means of a single coefficient k:

$$X_N = \frac{1}{1 + kN} \quad (10)$$

It is interesting to point out that a behavior like the one described by equation (10) is registered in the sintering phenomenon in catalysts.

However, equation (10) doesn't consider the phenomenon of deactivation of the sorbent: Grasa and Abanades (13) noticed that after 50 cycles up to 500 cycles the residual conversion remained the same. They have stated, from experimental data, that the residual conversion Xr was equal to 0,075 to 0,08 and that it is related to a product layer of around 50 nm (as stated at the beginning of the paragraph). The carrying capacity of the sorbent that considers the reduction of the active surface caused by the sintering effect is described by equation (11)

$$X_{max,N} = \frac{1}{\frac{1}{1 - X_r} + kN} + X_r \qquad (11)$$

where Xr is the residual sorbent activity after an infinite number of CaL cycles and k is the deactivation rate constant. The values of these parameters have been regressed (Figure 17) from experimental data obtaining, in the operating conditions, k=0,52 and Xr=0,075.

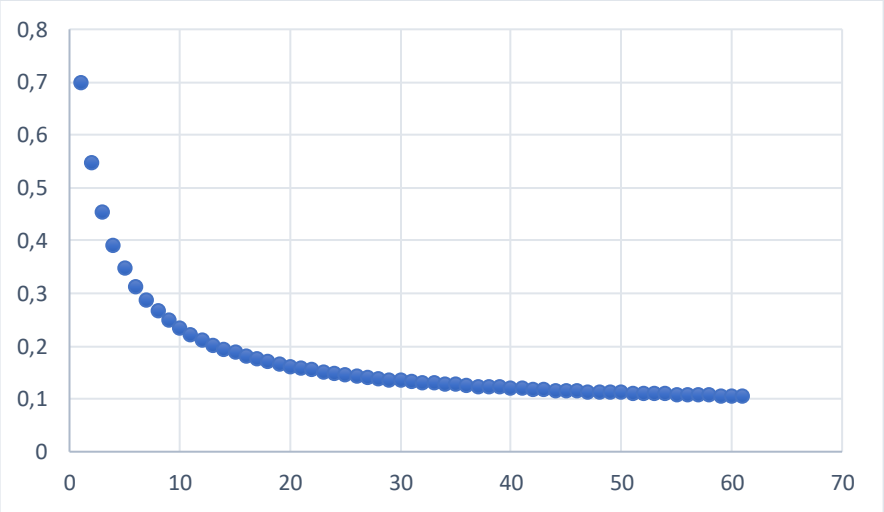

Figure 17 Carrying capacity vs number of cycles

The regressed factors are also influenced by a multitude of other side factors, as shown in Table 2, thus a variation in their value may be considered.

SIDE FACTORS	What does they influence?	Description of the process
Limestone nature	It influences the maximum conversion	*Higher is the percentage of other species beside CaCO3, lower is the reactivity. Dolomite is the best kind of sorbent.*

Sorbent's particle dimension	It influences the sorbent reactivity	*Even if the CO2 diffusion capacity is proportional to the particle surface/volume ratio, experimentally, the size of the particles is not influential.*
Calciner's operating temperature	It influences the sorbent reactivity	*The sorbent reactivity decreases if T>950°C during the first CO2 capture cycles because of an increase in the sintering phenomena and a consequent reduction of active available area for the diffusion process.*
Sorbent residence time	It influences the sorbent maximum conversion	*Higher is the residence time, higher the sintering effect*
CO2 concentration	It influences the sorbent maximum conversion	*Higher is the CO2 concentration, higher is the capture rate during the first 10 cycles.*
CO2 mass flow rate exploited in the overall process	It influences the sorbent activity	*The decay of the sorbent activity seems to depend more on the overall mass of the CO2 carried over the particle life than on the number of passages between the carbonator and the calciner*
Presence sulphur compounds	It strongly influences the sorbent performances	*Because of the CaSO4 build-up the sorbent's particles pore are obstructed reducing the participation of the particles to the carbonation process*

Table 2 Side factors influencing the X_R and k values

In the case of treating flue gas coming from a WTE power plant, two specific side events, that affect the carrying capacity, must be addressed:

1) **the degree of sulfation of the sorbent**: it has a significant influence on the evolution of the CO2 carrying capacity of the limestone due to the blockage of particle pores. Sulphur species are introduced into the CaL system by the flue gas from the WTE plant that is fed to the carbonator and by the sulfur present in the supplementary fuel that is burnt in the calciner. An appropriate flue gas cleaning system limits the first proportion, whereas the second proportion can be limited by an appropriate choice of fuel or by proper assets of indirectly heated calciner solutions. However, the formation of calcium sulphate (CaSO4) is important to be considered because it can be formed either directly or indirectly and it remains stable under typical CaL process conditions, leading to the build-up of a solid inert fraction (because

at T<1000 °C it doesn't convert back to SO2) recirculating into the CaL reactors and leading to the obstruction of particle's pores.

$$CaCO_3 + SO_2 + \frac{1}{2}O_2 \rightarrow CaSO_4 + CO_2 \qquad \Delta H_r = -324\ \frac{kJ}{mol} \quad (12)$$

$$CaO + SO_2 + \frac{1}{2}O_2 \rightarrow CaSO_4 \qquad \Delta H_r = -502\ \frac{kJ}{mol} \quad (13)$$

Equation (12) occurs when the CO2 partial pressure is higher than the CO2 concentration at equilibrium, whereas the second one, equation (13) occurs if the partial pressure is lower.

Accordingly, to account for the sulfur that leads to the sorbent deactivation, the deactivation constant and the residual conversion capacity of the sorbent need to be calculated depending on the molar sulphating level of the sorbent, x_{CaSO4}.

For this purpose, experimental data from Grasa et al. are applied to the empirical equations described above:

$$k_r = k_{r,0}\left(1 + 0{,}2962 * x_{CaSO_4}\right)$$

$$X_r = X_{r,0}\left(1 - 1{,}1536 * x_{CaSO_4}\right), for\ x_{CaSO_4} \leq 0{,}5$$

$$X_r = X_{r,0}\left(0{,}4230 - 3{,}076 * x_{CaSO_4}\right), for\ x_{CaSO_4} > 0{,}5$$

2) the presence of chlorine: both in the flue gas coming from the power plant and the additional burning of a waste-derived fuel in the calciner lead to a reaction mechanism of Ca-species with HCl. Understanding the fate of chlorine within the CaL system is crucial for an appropriate design of subsequent heat recovery systems and gas cleaning units.

$$CaCO_3 + 2HCl \leftrightarrow CaCl_2 + H_2O + CO_2$$

$$CaO + 2HCl \leftrightarrow CaCl_2 + H_2O$$

The HCl adsorption phenomenon is multi-layered, highly complex and mainly dependent on the reaction temperature, prevailing gas atmosphere and the Cl/Ca molar ratio. Several studies indicate the ability of Cl-retention by Ca-species both with the amount of chlorine coming from the flue gas and during the combustion of waste-derived fuels. During the latter, chlorine is released to the gas phase via HCl and partly absorbed by the solid phase. Part of solid phase bound chlorine is transported to the carbonator by the circulating sorbent. Thus, chlorine is released by the CaL process via gaseous and solid streams from the carbonator and from the calciner, respectively. It

has been experimentally estimated that the retention factor value is in the range of 80-85% and that it has a tendency of increasing along with increasing calciner temperatures.

3.3. Main operating parameters

Beside the selection of the calciner and carbonator's operating temperature, three main operating parameters could be introduced:

- the fresh make-up of CaCO3 $\left(\frac{F_0}{F_{CO_2}}\right)$
- the solid-stream recirculation rate to and from the carbonator and calciner $\left(\frac{F_R}{F_{CO_2}}\right)$
- the solid inventory in the carbonator $\left(\frac{W_s}{V_{gas}}\right)$

3.3.1. Fresh make-up ratio and solid recirculation rate

First, the effects of the make-up ratio (F0/FCO2) and solid recirculation rate (FR/FCO2) on the heat balance of the power plant need to be discussed.

The fresh make-up ratio is the ratio between the molar fresh CaCO3 introduced into the system and the molar CO2 entering the carbonator. It is introduced into the system, in this case into the calciner, to balance in stationary state the amount of CaO (mixed with ashes and other inert) leaving the system. This parameter could vary approximately between 0,04 and 0,4.

If the ratio increases, the purged stream needs to increase as well, reducing the recirculation of built-up compounds, such as CaSO4 and ashes. Even if the introduction of fresh stream leads to an increased efficiency, the increase in the purge stream is linked to increased losses of valuable material and of chemical energy. On the contrary, by reducing the make-up stream, the solid inert flow rate increases, leading to a poorer capture efficiency and lower reactivity of the sorbent1. This happens because of the obstruction of the pores in the carbonator, and because of the increase in the heat load in the calciner, having to heat up a bigger portion of inert.

Additionally, if we look at the global performance (net electric efficiency and specific emission) of the plant, it can be noticed that an increase of limestone make-up and circulation rate leads to lower CO2 emissions but also to lower electric efficiencies. By keeping a constant solid recirculation rate and increasing the make-

up rate, an almost asymptotic CO2 emission value is reached at a certain point: in this condition, the maximum CO2 capture efficiency allowed by thermodynamics is reached in the carbonator, thanks to the high sorbent activity. There is a maximum point after which no further increase is appreciable, whereas the electric efficiency continues reducing almost linearly. In the end, a higher value of the make-up flow leads to higher operational costs of the capture system and higher fuel consumption in the auxiliary burner.

Because the recirculation rate and the make-up rate are connected by the mass balance, the opposite approach for reducing the CO2 emissions could be presented: the make-up rate is kept fixed, and the solid recirculation rate is varied. In this case the net electric efficiency increases with a decreasing recirculation rate, that can vary between 4 and 12 approximately, and the CO2 emissions steeply increase with a decrease in the solid recirculation rate.

Among the two possible strategies for reducing the CO2 emissions, whose results are well described in Figure 18, an increase of the solid recirculation rate seems to be preferable with respect to an increase of the make-up flow.

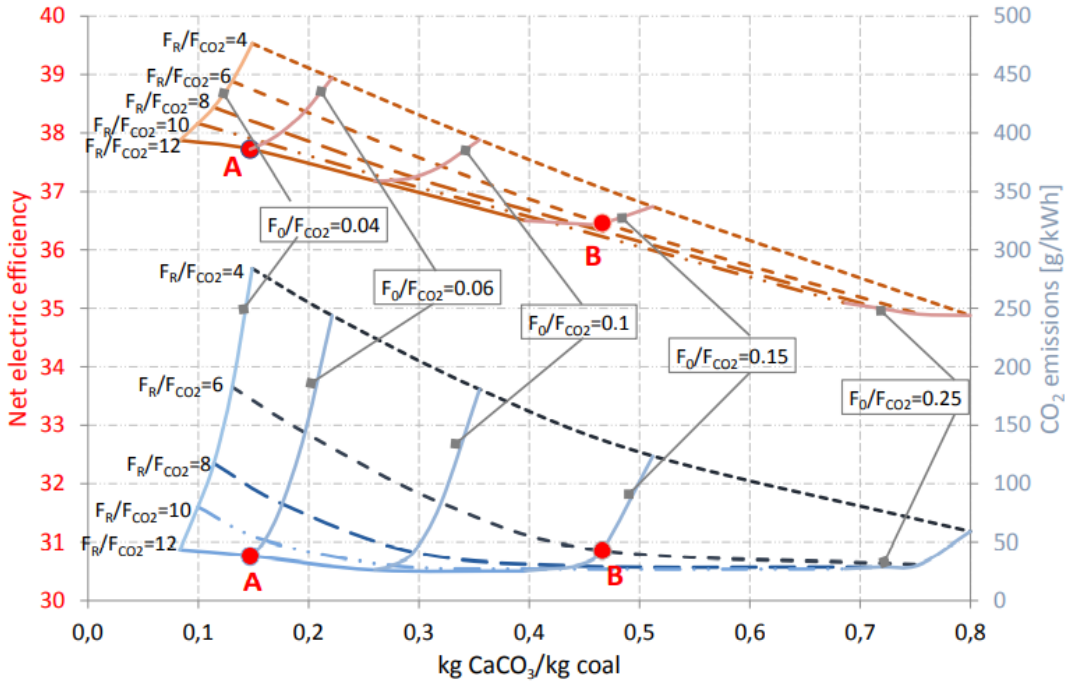

Figure 18 Electric efficiency and specific emissions of CaL power plants with fixed inventor (150 kg/(m3/s)), compact carbonator design, purge from calciner, Scottish coal and reference oxyfuel section operating conditions (Co2 recycle at 350 °C and oxygen equal to 50%). Source: (16)

3.3.2. Solid Inventory

The solid inventory has an influence on both the carbonator and the whole power plants' performances: it can be varied between 150 kg/(m3/s) and 350 kg/(m3/s). In Figure 19 it is shown how, by increasing the value of solid inventory, the emissions of CO2 decrease, especially if the make-up ratio is set equal to an intermediate value between (0,04 to 0,25). The solid recirculation rate is kept fixed and set equal to FR/FCO2 =6 or FR/FCO2 =10.

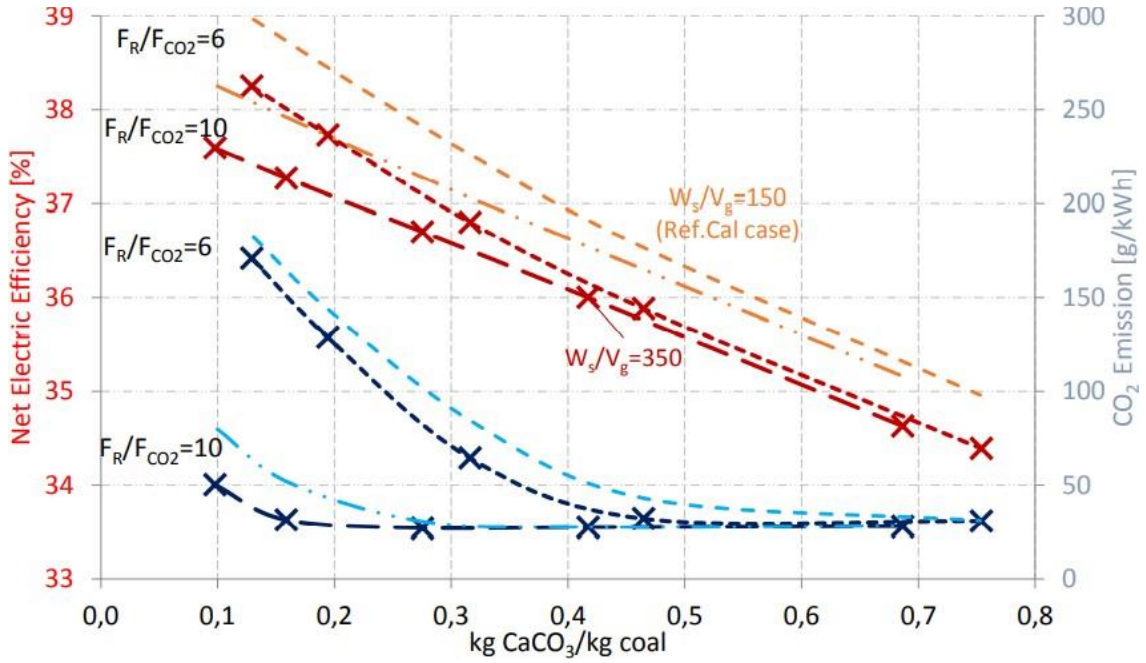

Figure 19 Electric efficiency and specific emissions of CaL equipped power plants with fixed solid inventory, varying make-up ratio and fixed solid inventory. Source: (16)

3.4. Alternative sorbent selection: waste derived calcium sorbents

While Europe has been using calcium (CaO) for the past years, other countries, such as China, are starting to study the implementation of waste-derived calcium sorbents, to cut the costs related to CCUS and increase the environmental benefits.

Several studies have been conducted using calcium carbide slag, especially in China, due to the high consumption of calcium carbine, as shown in Figure 20. Mainland China is the dominant player in the calcium carbide market. Driven by large Chinese coal reserves and the rapid development of chemical production, Chinese production and consumption of calcium carbide has grown strongly in the

past decade. Growth will moderate during the forecast period because of recent capacity rationalizations and the general slowing of economic growth in China, but global consumption of calcium carbide will continue to grow at a strong rate during 2019 – 2024.

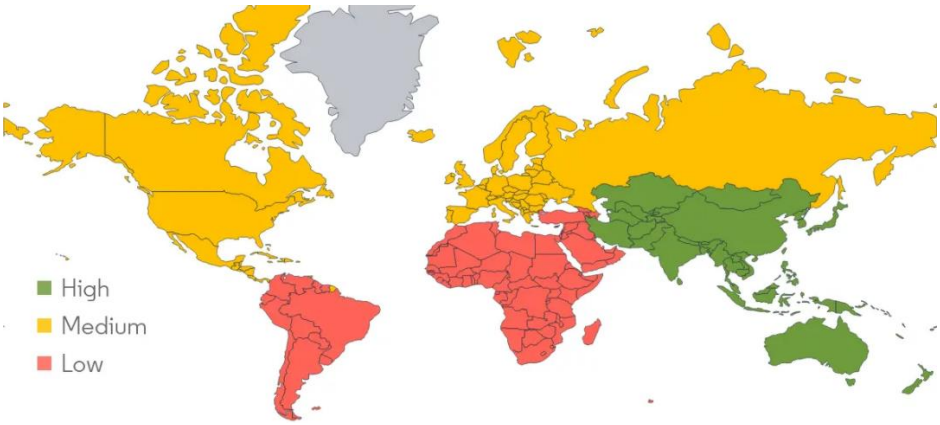

Figure 20 Calcium Carbide Market - Growth Rate by Region (2021-2026). Source: (17)

In general, the Calcium Carbide Market was estimated at 27.5 million tons in 2020 and the market is projected to register a Compound Annual Growth Rate (CAGR) of about 4% during the forecast period (2021-2026). Considering the outbreak of COVID-19, a rising demand from chemical industries is likely to drive the market demand. Chemical industries accounts for the largest share holding more than 70% of the total volume of the calcium carbide market. On the other hand, the detrimental health effects related to calcium carbide are starting to rise more and more concerns, therefore a slight shrink in the increase has been predicted.

More of our concern, it has been established that Europe is projected to witness significant growth in the calcium acetylide market. Additionally, the use of CaC2 for the desulfurization of iron and steel as a fuel, and the growing steel industry, are other key factors driving the calcium acetylide market growth in Europe. The increase in the share of calcium carbide can be boosted by the feasibility of using CaC2 to produce PVC. The current trends in the market are rising demand for PVC based plastic products, and growing chemical, steel, and agriculture industries.

Calcium carbide is an inorganic compound with the following primary commercial applications: generation of acetylene, production of calcium cyanamide (a nitrogen fertilizer), use in the iron (foundry) and steel industries as a desulfurization reagent in the production of ductile iron and steel, and as a slag modifier/conditioner (reducer) in steel production.

The main waste stream of the process (calcium carbide) is calcium carbide slag. It is formed as follows: $CaC_2 + 2H_2O \rightarrow C_2H_2 + Ca(OH)_2$.

From the above equation, we can notice that calcium hydroxide is a primary component of calcium carbide slag. One of its main characteristics is that it forms an alkaline environment when dissolved in water. Due to its basic characteristic, calcium carbide slag is mostly buried in a designated disposal area rather than being recycled. Currently, the possible recycling strategy of calcium carbide slag may include the use of it as a neutralizer of acidified soils. Nevertheless, the disposal of calcium carbide slag leads to negative effects, such as the basification of soil and subsurface water pollution due to alkaline contamination.

How could carbide slag be recycled cutting down its environmental impact?

It has been estimated that, in the production of acetylene gas, 32 g of the calcium carbide produces 13 g of acetylene gas with 37 g of the carbide slag, which indicates that a relatively large number of calcium carbide slag is generated.

Element	**Ca**	**C**	**Si**	**Al**	**Fe**	**Ti**	**Mg**	**Na**	**S**	**F**	**P**
Content (%)	75,03	6,81	5,61	4,63	3,34	0,87	0,31	0,13	0,53	0,35	0,005

Table 3 Elemental composition of carbide slag (wt%)

As indicated in Table 3, the main component of carbide slag is Ca(OH)2 and its high availability and almost free price makes it a promising CO2 capture material. Additionally, from experimental data, it has been seen that the CO2 adsorption capacity of CaO derived from carbide slag is around 0.28 molCO2/molCaO after 100 adsorption/desorption cycles and that the highest CO2 adsorption capacity was achieved at the range of 650-700°C. The adsorption process using carbide slag is shown in the reactions below. The first endothermic reaction is the dehydration of the calcium hydroxide, which is the main constituent of carbide slag. It requires a fast heat transfer in and out of the reactor to provide an acceptable power level and a suitable system integration. According to a thermodynamic analysis, Ca(OH)2 decomposes into CaO when the temperature is around 450°C, and then the CaO can capture CO2. When the temperature is higher, the product CaCO3 releases CO2 to become CaO. Thus, the Calcium looping is achieved.

$$Ca(OH)_2 \rightarrow CaO + H_2O \quad (14)$$

$$\Delta H_r = +104 \frac{kJ}{mol}$$

$$CaO + CO_2 \rightarrow CaCO_3$$

$$CaCO_3 \rightarrow CaO + CO_2$$

If the carbide slag is used as a sorbent, the carbonator's temperature can be kept around 650°C under atmospheric pressure, while, it has been theoretically and experimentally proven that the calciner's temperature should be below 900 °C. Because of this reason the calciner's temperature is usually set at around 850 °C. The value is lower than the theoretical one (900 °C) because both the thermodynamics and the kinetics affect the process, and because impurities are present in the slag, which could promote the conversion of CaCO3 into CaO.

For what concerns the recyclability of the carbide slag, it has been proved that the slag can be constantly activated during 20 cycles of CO2 capture and release, keeping the performance stable and unchanged, restoring completely in every CO2 capture process after release.

Both theoretical analysis and laboratory experiments show that carbide slag is an excellent Ca-based sorbent in the Ca-looping process for CO2 capture. In comparison to other Ca- based sorbents, this solid waste has high CO2 capture ability and stability after 20 cycles.

4 Chapter four: Integration of the WTE plant with the Calcium looping system

4.1. Methodology

The aim of this thesis is assessing the operative aspects and the functioning of a calcium looping system integrated with an existing WTE power plant. To evaluate the thermodynamics of the flows involved and ensure an energy and mass balance, the GS software developed by the Politecnico of Milan has been used. Additionally, in order to control the kinetics of the process, it has been utilized the Romano's MATLAB model.

4.1.1. GS simulation tool

The method used to model the WTE power plant equipped with the CO2 capture system is introduced: GS, a software developed by the energy department of Politecnico di Milano, was used to perform simulations of the energy system under study. It has been chosen because it allows the evaluation of the performances of the system using an iterative algorithm. The program needs an input file, an output file, and a property file to properly operate.

The input file is structured in three main sections: the first part includes the description of all the components listed in their computational order; the second section lists the first guess of all the thermodynamic characteristics of each stream involved in the energy system; the last section specifies the convergence variables.

The output file is divided into four sections: the former reports the actual thermodynamic conditions of each stream; the second section reports the compositions and the molar flow rates of each flow; the third section shows the significant outputs of each component; the latter summarizes the overall performances of the power plant.

Regarding the calculations, GS exploits two different routines: CSR and THP. The first is used to evaluate the thermodynamic properties of pure water, at any point

of the state diagram, starting from a couple of known properties; the second, the THP method, calculates the composition of multiphase and multicomponent mixtures at the equilibrium conditions: the volumetric behavior of the gaseous phase is described by the ideal gas law, while the liquids and solids are considered incompressible.

In Appendix A a complete explanation of the main modelling assumptions and the procedure for each case study have been analysed in detail.

4.1.2. MATLAB (Romano Model)

On the other hand, MTLAB has been used to assess the kinetics of the carbonation reaction and the carbonator's kinetics convergence. In particular, the Romano Model controls the kinetics and the capacity of Ca-based particles in the carbonator. The model is built on the following assumptions:

- uniform riser temperature and zero gas side mass transfer resistance that ensure a fast fluidization fluid-dynamic regime;
- perfect mixing of the particles in the reactor (typical of fast fluidized bed reactors);
- uniform particle dimension;
- uniform superficial velocity.

First, the model is used to find the average kinetic constant for the Ca-based particles and the volumetric fraction of potentially active Ca-based solids, using the main flows associated to a Ca-looping system, such as the CO2 to the stack, the CO2 to storage, the CO2 from the WTE power plant, fresh limestone, purge and the auxiliary fuel. The flows are calculated using their interdependence to the molar flow rate of CO2 going into the system, the make-up factor, the solid recirculation factor, the molar fraction of ash and CaSO4 to the calciner.

Figure 21 describes the main relationships between the input variables described before and the main flows of the system.

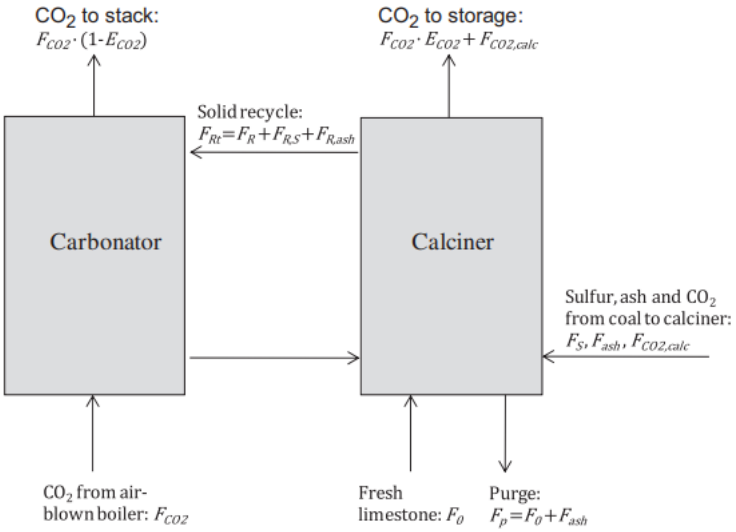

Figure 21 Main flows interdependence from the most significant parameters, defined as input variables of the system. Source: (18)

In addition to composition, Ca-based particles are classified according to two statistical distributions, the probability density function, used to calculate the fraction of particles with certain residence times in the carbonator, and the carbonation-calcination cycles distribution, used to evaluate the fraction of particles that has experienced a number N of complete carbonation-calcination cycles, to assess the so called "reaction age".

The two statistical distributions are used to evaluate the fraction of particles $r_{N,age}$ (eq. 5) which have experienced an average number of complete cycles as a function of the actual carbonation and calcination levels reached in both the carbonation and calcination reaction occurring in the process.

Knowing $r_{N,age}$ and assuming a certain value of CO2 concentration, the average conversion of the sorbent X_{ave} is evaluated in accordance with the following formula:

$$X_{ave} = \sum_{N_{age}=1}^{\infty} r_{N_{age}} \left(\int_0^{t_{limit}} f_t X\left(t, N, C^*_{CO_2}\right) dt + \int_{t_{limit}}^{\infty} f_t X_{max,N}\, dt \right)$$

Finally, thanks to an iterative procedure, the CO2 capture efficiency is found: the calculation procedure ends when it is obtained $E''_{CO2} = E'_{CO2}$, where

$$E'_{CO_2} = \frac{F_R X_{ave}}{V_{gas_{inlet}} C_{CO2_{in}}}$$

$$E''_{CO_2} = \frac{V_{gas_{inlet}} C_{CO_{2_{in}}} - V_{gas_{outlet}} C_{CO_{2_{out}}}}{V_{gas_{inlet}} C_{CO_{2_{in}}}}$$

4.2. Case study description and analysis of the main results

The GS simulation tool and the MATLAB model have been used to simulate three different case studies:

- **Base Case** (Figure 22): the model of a WTE power plant like the "Silla 2" WTE in Milan that generates, as valuable output, electricity. It has been modeled at its nominal conditions: the power plant is not equipped with a CO2 capture system. In this thesis, it will be referred as "reference case" (4.2.1).

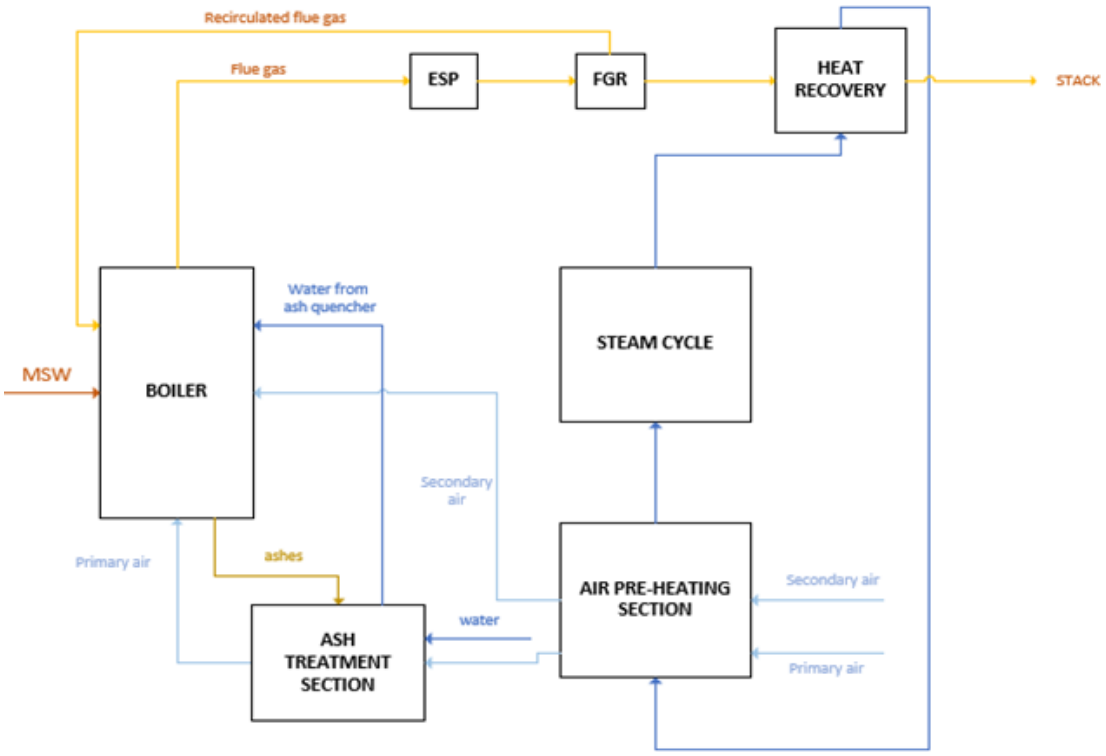

Figure 22 Base Case: block diagram describing the main fluxes. In brown the inlet mass flow rate of fuel entering the power plant; in yellow the flue gases; in blue the water streams; in light blue the primary and secondary air entering the three combustion lines.

- **Case A** (Figure 23): the reference case is equipped with a Calcium Looping system as a post-combustion CO2 capture process. Two out of three combustion lines of the WTE power plant are active. Thanks to a CaL heat recovery boiler, additional steam is sent to the steam turbine up to reaching the turbine's nominal operating conditions (4.2.2).

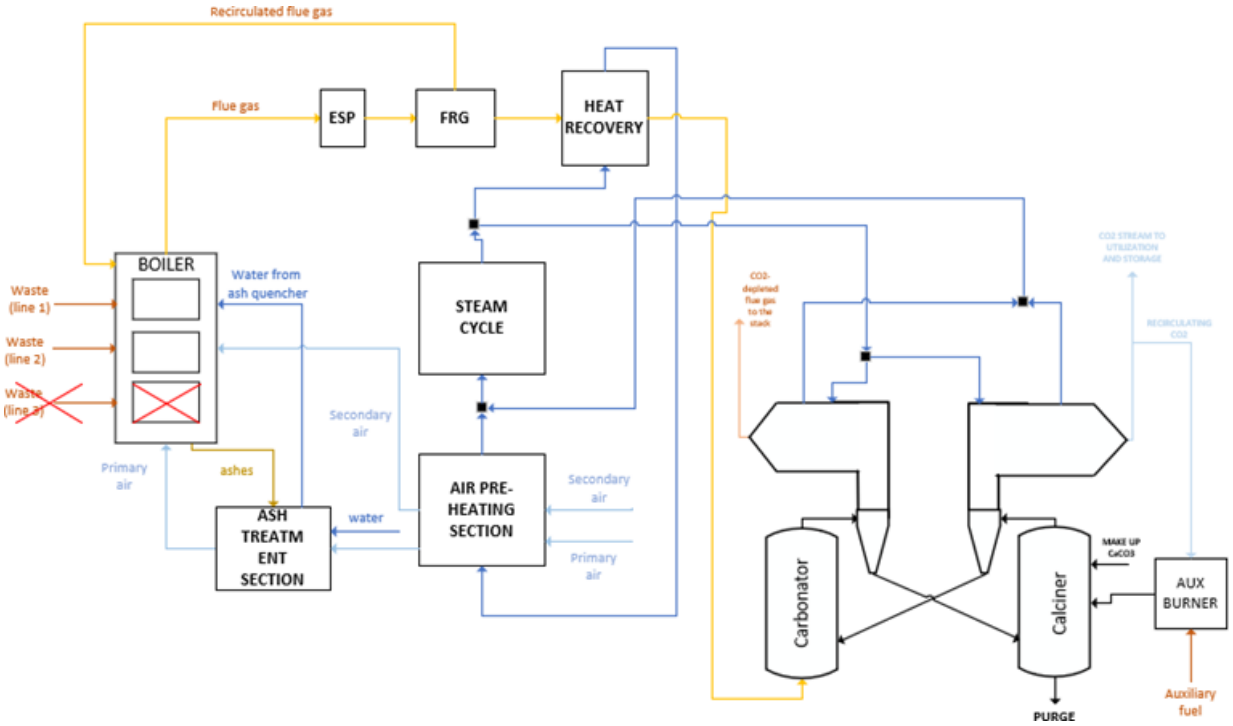

Figure 23 Case A: block diagram describing the main fluxes. In brown the inlet mass flow rate of fuel entering two out of three combustion lines of the power plant and the auxiliary fuel entering the auxiliary burner; in yellow the flue gases; in blue the water streams; in light blue the primary and secondary and the auxiliary oxidizer.

- Case B (Figure 23): the reference case is equipped with a CaL system that removes the CO2 generated by the three functioning combustion lines; in this case study the CaL heat recovery boiler generates steam which is sent to a dedicated and optimized additional turbine (4.2.3).

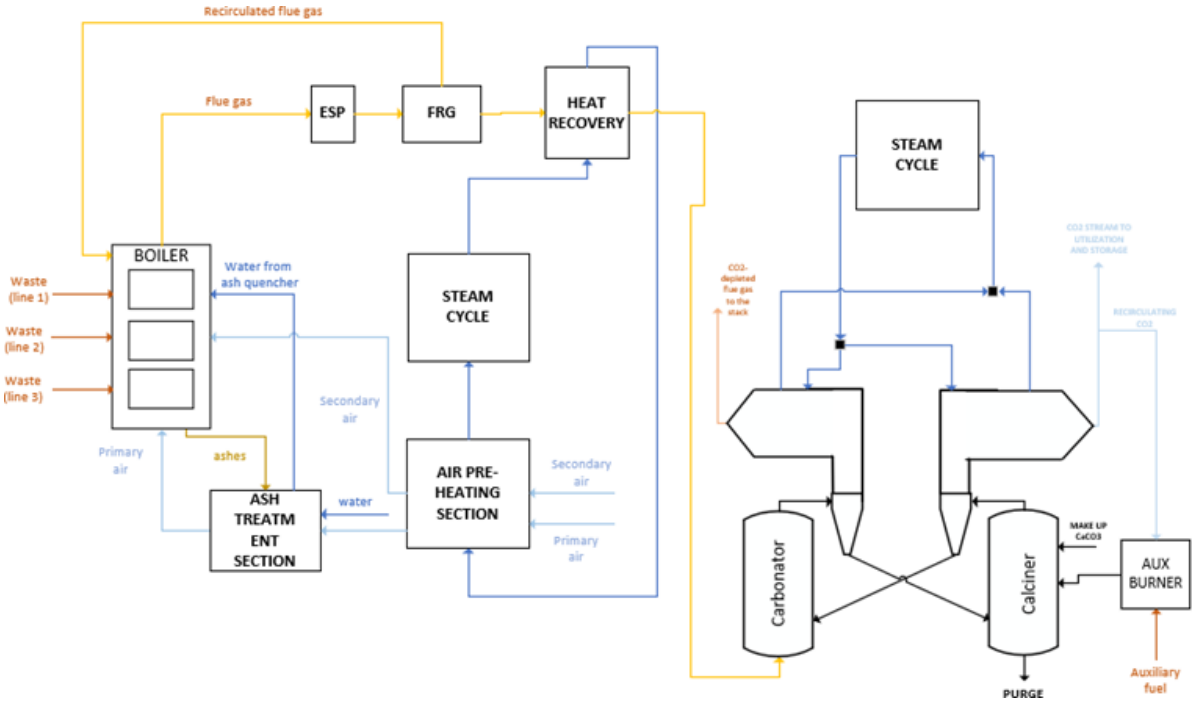

Figure 24 Case B: block diagram describing the main fluxes. In brown the inlet mass flow rate of fuel entering three combustion lines of the power plant and the auxiliary fuel entering the auxiliary burner; in yellow the flue gases; in blue the water streams to two distinguished steam cycles; in light blue the primary and secondary and the auxiliary oxidizer.

4.2.1. Base Case

The base case, also referred as "reference case", describes the thermodynamic conditions and the operating parameters of a WTE power plant working at nominal conditions.

The main assumptions are reported in Table 4.

Main assumptions		
Number of combustion lines (grate combustors)	3	
Number of steam turbines	1	
Average working hours per year	8.050	h/year
Overall fuel mass flow rate	20,49	kg/s
Overall fuel mass flow rate	73,78	t/h
Thermal input	212	MW_{th}
Flue gas recirculation	15	%
Live pressure at the inlet of the steam turbine	50	bar
Live temperature at the inlet of the steam turbine	423	°C
Evaporating pressure	54	bar
Evaporating temperature	270	°C
Primary air preheating temperature	195	°C
Secondary air preheating temperature	140	°C

Deaerator temperature	120	°C
Deaerator pressure	2	bar

Table 4 Base Case: main assumptions to evaluate the thermodynamic conditions of the system

The WTE power plant is equipped with three combustion lines with an overall inlet mass flow rate of the fuel equal to 20,49 kg/s. The overall thermal input is equal to 212 MW. The selected fuel is an MSW with a LHV equal to 10,342 [MJ/kg].

The three combustion lines are grate combustors and both a primary and secondary air flux is provided to the system, to ensure a complete oxidation: in the first stage of the combustion process, 79,29 kg/s of hot primary air are injected at a temperature equal to 195 °C and atmospheric pressure; to complete the combustion, 35,75 kg/s of hot secondary air at a temperature of 140 °C are supplied.

At the end of the combustion process the bottom ashes are separated through a wet discharge, while the flue gases are sent to the heat recovery section. The boiler's tube banks are positioned as follows: first, we have the evaporator tube banks, then the superheater's tube banks, and then the economizer's tube banks. This asset is forced by the peculiar characteristics of the flue gases in WTE power plants: due to the presence of chlorine, the flue gases increase the risk of corrosion of the tube banks with the increase of the temperature of the tube walls and with the increase of pressure. Because of this reason, the evaporator is in the hottest section, due to the fact that evaporating water has the best heat transfer coefficient. Additionally, to avoid excessive liquid formation in the last part of the turbine expansion, as well as to limit the evaporating temperature of the tube walls, the maximum evaporating pressure is set equal to 50 bar (maximum value allowed equal to 70 bar). Regarding the superheater, the maximum temperature needs to be set below 450 °C to limit the corrosion problems: in this case, the temperature of the stream (34) at the outlet of the superheater is equal to 443 °C.

	Heat transferred [MW]	Temperature at the inlet [°C]	Temperature at the outlet [°C]
ECONOMIZER	120,3	259	138,5
EVAPORATOR	33,2	270	
SUPERHEATER	39,7	423	270

Table 5 Heat transferred within the boiler's tube banks and temperature profile of the steam cycle within the heat recovery boiler

Figure 25 clearly shows the heat transfer within the heat recovery boiler. On one hand, the flue gases enter the heat recovery boiler at a temperature of 1181 °C and

exit at a temperature of 205 °C; on the other, the steam cycle temperature profile is described in Table 5.

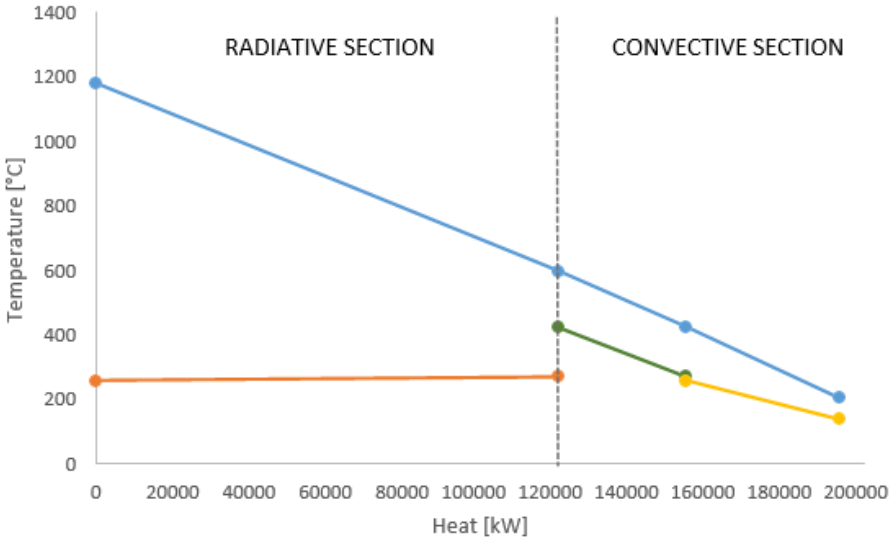

Figure 25 Simplified T-Q diagram of the WTE boiler's tube banks: in blue the flue gases are cooling; in orange the evaporator, in green the superheater and in yellow the economizer.

The steam generated in the heat recovery system is sent as superheated steam (T=423°C; p=50 bar) to a steam turbine that injects in the national grid an overall net electric power equal to 58,42 MW, with a net electric efficiency equal to 27,56%.

Electric power at generator	65,77	MW
Feedwater pump consumption	0,71	MW
Condensate extraction pump consumption	0,07	MW
Condenser auxiliaries' consumption	1,78	MW
Net electric power	63,21	MW
Auxiliaries electric power	-4,793	MW
Overall net power	58,417	MW
Net electric efficiency, $\%_{LHV}$	27,56%	

Table 6 Base Case: Power balance and Net electric efficiency of the system

Table 6 summarizes the main losses and consumptions of the system and the overall net electric efficiency.

Exiting the heat recovery boiler, a percentage equal to 15% of flue gases is separated thanks to an ESP, and it is sent back to the combustion chamber. The flue gas recirculation is a method to boost the efficiency of the system: if the fraction of FGR increases, the combustion temperature decreases, lowering the temperature of the

flue gases at the entrance of the boiler's convective section. This method allows to increase the evaporating pressure, thus, to increase the efficiency of the power cycle.

On the other hand, the percentage of not recirculated flue gases is sent to the flue gas treatment line. Finally, they are sent to the stack at a temperature equal to 135°C and atmospheric pressure.

At the stack, the specific CO2 emissions are equal to 1244,98 kg/MWh.

By assuming that 50% of the CO2 emitted is biogenic, the specific fossil CO2 emissions at the stack are equal to 622,49 g/MWh. Accordingly, the total CO2 emissions in terms of mass flow rate result to be equal to 20,20 kg/s of which 10,10 kg/s are fossil. The focus is shifted on the fossil CO2 emissions because the biogenic CO2 emissions can be considered neutral when re-emitted in the environment.

Figure 26 summarizes the CO2 impact of the reference case.

CO2 overall mass flow rate release to ambient [kg/s]	20,20
CO2 fossil mass flow rate emitted at the stack [kg/s]	10,00
CO2 biogenic mass flow rate emitted at the stack [kg/s]	10,00
CO2 total specific emissions [kg/MWh]	1244,98
CO2 fossil specific emissions [kg/MWh]	622,49

Figure 26 Base Case: CO2 emissions and CO2 specific emissions at the stack

4.2.2. Case A

This case study aims at analyzing a complete retrofitting of the CaL technology as a CO2 removal system, promoting the use of the existing steam turbine to generate power. The existing steam turbine works at the operating temperature of 423 °C and at the pressure of 50 bar. The operating mass flow rate of the steam turbine is equal to 71,56 kg/s.

To keep the same nominal conditions, the steam fed to the steam turbine comes both from the existing WTE power plant and from the Calcium Looping heat recovery boiler. With the purpose of maintaining a fixed mass flow rate, the steam toward the turbine comes from two out of three combustion lines and the calcium looping heat recovery system. Therefore, both the WTE thermal input through the combustion lines and the fuel mass flow rate are 2/3 of the reference case analyzed in the previous section. The thermal input is equal to 141 MW and the fuel mass flow rate is equal to 13,63 kg/s.

Table 7 defines the main assumptions of the WTE power plant under study: the overall functioning of the power plant doesn't change compared to the reference case.

Main assumptions		
Number of combustion lines (grate combustors)	2	
Number of steam turbines	1	
Average working hours per year	8.050	h/year
Overall fuel mass flow rate	13,63	kg/s
Overall fuel mass flow rate	49,07	t/h
Thermal input	141	MW_{th}
Flue gas recirculation	15	%
Live pressure at the inlet of the steam turbine	50	bar
Live temperature at the inlet of the steam turbine	423	°C
Evaporating pressure	54	bar
Evaporating temperature	270	°C
Primary air preheating temperature	195	°C
Secondary air preheating temperature	140	°C
Deaerator temperature	120	°C
Deaerator pressure	2	bar

Table 7 Case A: main assumptions of the WTE power plant

However, the flue gases exiting the existing treatment line are diverged to the CO2 removal system for a further treatment. The mass flow rate of the flue gases to the calcium looping system is equal to 93,86 kg/s, at a temperature of 135 °C and at atmospheric pressure.

To analyze the thermodynamic conditions and kinetics convergence of the calcium looping system, the Romano Model and the GS simulation tool have been used. A further analysis of the two models is described in Appendix A.

For what concerns the operating parameters of the CO2 removal system, they have been set to respect the main constrains, such as

1) the mass flow rate at the entrance of the steam turbine must be equal to the one of the reference case, in order to keep the same operating conditions;
2) the two main components of the CaL system, the carbonator and the calciner, are considered adiabatic and working at constant operating temperature (which has been set, accordingly to the best-practices, equal to 650 °C for the carbonator and 920 °C for the calciner);
3) kinetics convergence in the carbonator (verified through the MATLAB Romano Model).

First, the main operating parameters that must be selected are the **make-up factor** and the **solid recirculation factor**.

The first, F_0/F_{CO2}, has been set in accordance with a qualitative trade off between the reduction of the auxiliary fuel entering the calciner and the increase of the solid build-up in the system. In fact, if the make-up stream (the mass flow rate of CaCO3 entering the system) increases, the auxiliary fuel mass flow rate increases as well, because the energy required to perform the primary calcination reaction is higher.

In this specific case study, the make-up factor has been set equal to 0,08.

Second, the solid recirculation factor, F_R/F_{CO2}, has been set equal to 4,5 after an iterative procedure between the kinetics convergence of the carbonator (Romano Model) and the thermodynamic convergence (GS Model). The main purpose of the iterative procedure was obtaining a mass flow rate at the entrance of the turbine equal to the one of the reference case, ensuring that the other constraints listed above were verified. Therefore, the solid recirculation factor was decreased as much as possible, to reduce the CaO to the carbonator, thus the energy released during the carbonation reaction. Consequently, the energy recovered from the carbonator decreases together with the steam generated. As a side effect, by decreasing the reactions occurring into the carbonator, the carbonator efficiency decreases, and it results equal to 69,26%.

Figure 27 shows how the reduction of the carbonator efficiency leads to a lower energy of reaction, reducing significantly the heat recovered from the carbonator, thus the mass flow rate to the turbine. Recalling a targeted mass flow rate equal to 71,56 kg/s, it can be noticed from the graph below that the objective cannot be fully reached: with a carbonator efficiency equal to nearly 70% a minimum heat is generated to ensure a constant operating temperature in the vessel, and the corresponding overall steam mass flow rate to the turbine is equal to 75,77 kg/s. The results could be still considered acceptable because it has been assumed that the existing steam turbine can handle a mass flow rate variation lower than 5%.

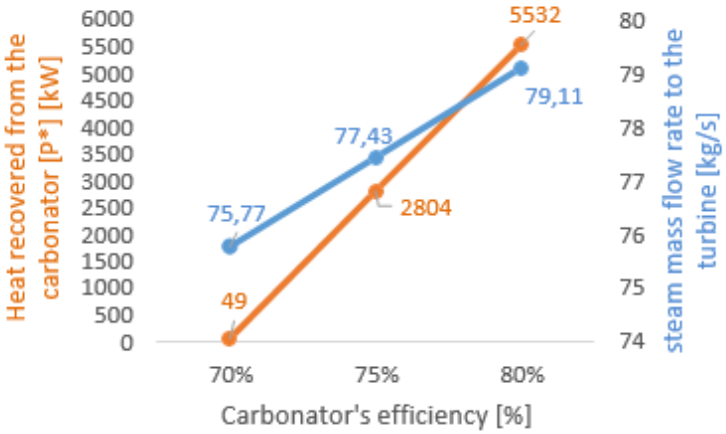

Figure 27 Dependency between the carbonator's efficiency and the heat recovered from the carbonator and the steam mass flow rate sent to the turbine

For a better understanding of the heat recovery within the CaL heat recovery boiler a deeper analysis can be done, in accordance with what described in Figure 28.

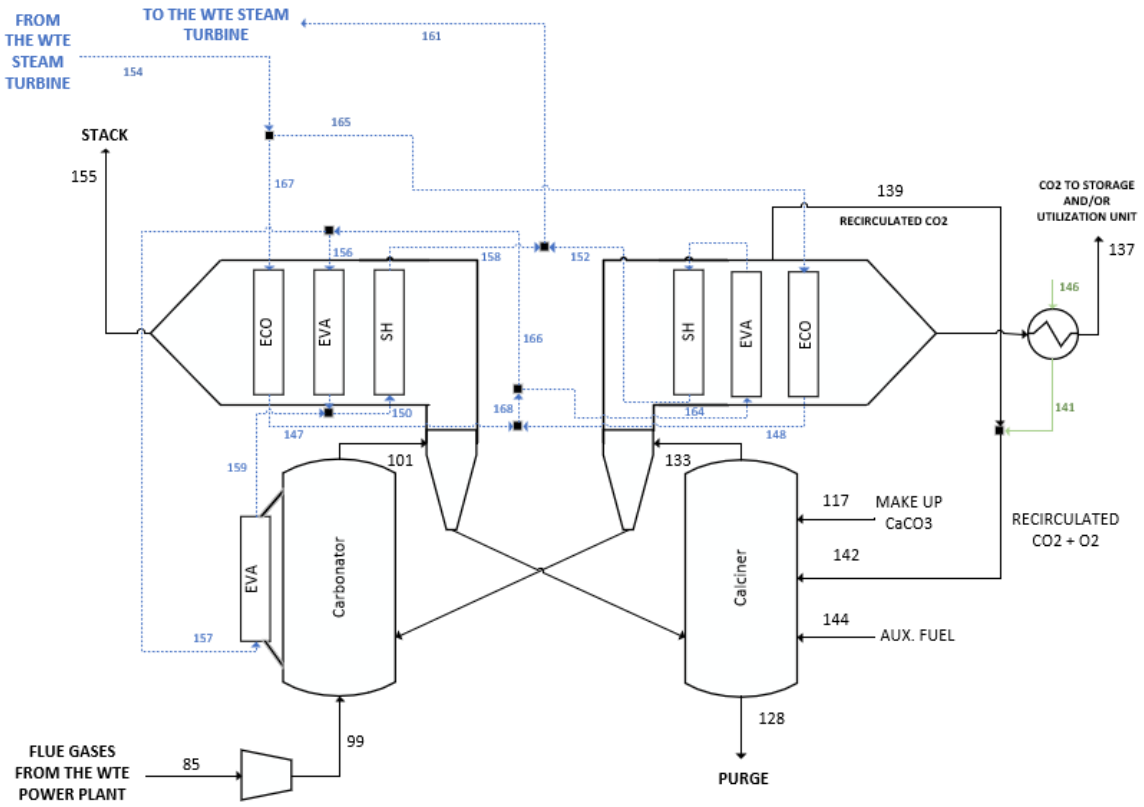

Figure 28 Calcium looping system and calcium looping heat recovery boiler

Figure 28 clearly shows that heat is recovered from the hot CO2-depleted flue gases exiting the carbonator, from the hot CO2 stream exiting the calciner and from the carbonator. It can be noticed that the boiler's tube banks are positioned differently compared to the WTE power plant and this is because the flue gases in this section are cleaner and less subject to corrosion issues: the presence of an alkaline environment ensures the additional reduction and removal of chlorine from the clean flue gases.

In particular, Figure 29 shows how the hot CO2 depleted flue gases exchange heat with one portion of the steam cycle: the possibility of decreasing this portion of generated steam was constrained by an acceptable outlet temperature of the flue gases at the stack. The resulting outlet temperature of stream 155 results to be equal to 144 °C.

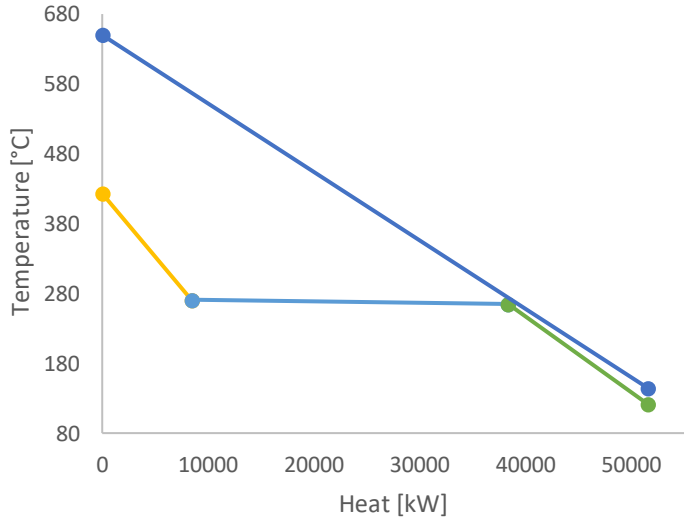

Figure 29 Case A: T-Q diagram of the carbonator-side of the CaL heat recovery boiler, in which the hot CO2-depleted flue gases exchange heat with the steam cycle

Table 8 sums up the heat transferred within each tube banks and the temperature profile of the steam cycle exchanging heat with the hot CO2-depleted flue gases: it can be clearly noticed that, at the outlet of the superheater, 20,29 kg/s of steam are sent to the WTE steam turbine at the desired temperature of 423 °C and at the pressure of 50 bar.

	Heat transferred [MW]	Temperature at the inlet [°C]	Temperature at the outlet [°C]
SUPERHEATER	8,42	271	423
EVAPORATOR	29,95	270	
ECONOMIZER	13,24	121,1	265

EVAPORATOR (carbonator heat recovery)	0,489	270

Table 8 Case A: Heat transferred within the heat recovery tube banks and temperature profile of the steam cycle (carbonator side)

On the other hand, the remaining 7,71 kg/s, are brought to the desired temperature of 423 °C and at the pressure of 50 bar by exchanging heat with the hot CO2 stream exiting the calciner, as shown in Figure 30.

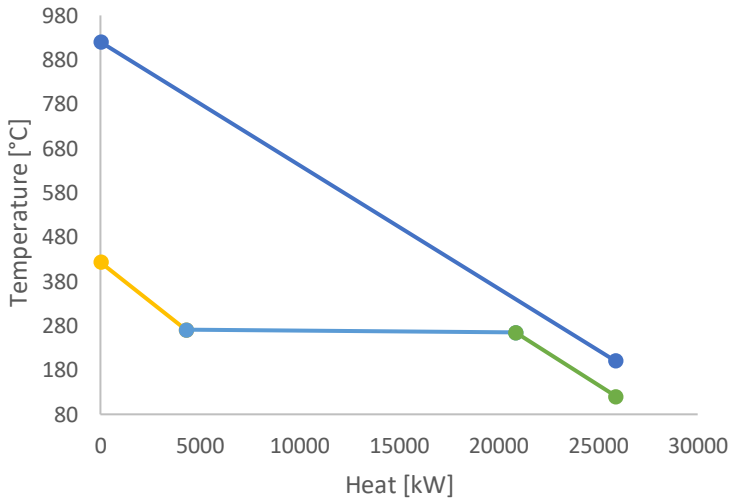

Figure 30 Case A: T-Q diagram of the calciner-side of the CaL heat recovery boiler, in which the hot CO2 exchanges heat with the steam cycle

The heat recovered and the steam generated in this section of the heat recovery boiler couldn't be lowered to reach the objective of equal mass flow rate at the turbine inlet. The main constraints of the heat exchanged in this part of the systems are:

- the CO2 recirculation stream (139) must have a temperature lower than 400°C because of thermal stress limits of the recirculation blower;
- the CO2 stream (137) is sent to the CPU at a temperature that must be lower than 200 °C, not to have excessive losses in the cooling section prior the transportation and storage phase.

Table 9 summarizes the temperature profile and the heat transferred between the hot CO2 and the steam cycle.

	Heat transferred [MW]	Temperature at the inlet [°C]	Temperature at the outlet [°C]
SUPERHEATER	4,29	271	423
EVAPORATOR	16,56	270	
ECONOMIZER	5,03	121,1	265

Table 9 Case A: Heat transferred and temperature profile of the steam cycle (calciner side)

Because of the aforementioned design of the CaL heat recovery boiler, the auxiliary fuel (144) needed to perform the complete calcination reaction in the calciner is equal to 3,32 kg/s and it is injected in the system at a temperature of 60°C. It has been assumed the use of an SRF with a lower heating value equal to 24,98 kJ/kg. Even if it has also been assumed a sulphur free fuel, in real case applications, this compound must be kept under control to avoid the additional build-up of solids in the calcination-carbonation cycles.

To ensure a complete oxidation, it is injected in the calciner a mixture of recirculated CO2, as a temperature moderator, and preheated pure oxygen. The oxygen mass flow rate required is equal to 7,74 kg/s and it is separated from air thanks to an Air Separation Unit.

Ca-Looping process	
Molar flow of fresh limestone per molar flow of CO2 (F_0/F_{CO2}) [mol/mol]	0,08
Molar flow of recirculating solids per molar flow of CO2 (F_R/F_{CO2}) [mol/mol]	4,5
Adiabatic gas/solid mixing temperature at carbonator inlet [°C]	464
Carbonator outlet temperature [°C]	650
Calciner outlet temperature [°C]	920
Recirculated CO2-rich gas temperature [°C]	420
Oxygen preheating temperature [°C]	150
Cyclone's efficiency [%]	0,99
Cyclone's ash selectivity [%]	0,90
Oxygen concentration in the oxidant flow to calciner [%vol]	6,94
Oxygen concentration in the calciner off-gas [%vol]	1,83
Fans isentropic efficiency [%]	0,82
Fans electric mechanical efficiency [%]	0,94
Percentage of biogenic CO2 [%]	50%
CaL Heat recovery system	
ASU specific consumption [kWh/tO2]	200
CPU specific power consumption [kJ/kgCO2]	396
Refrigeration system specific consumption [MWel/MWth]	0,02
CO2 lost to the atmosphere in the GPU [%]	3%
Temperature at the turbine inlet [°C]	423
Pressure at the turbine inlet [bar]	50

Superheater pressure drop [bar]	0,08
Economiser pressure drop [bar]	0,15
Condenser pressure [bar]	0,07

Table 10 Case A: Main assumptions and operating conditions of the calcium looping system of the completely retrofitted WTE power plant

Table 10 defines the main operating parameters of the designed calcium looping system.

For what concern the final overall power balance of the WTE power plant, it has been obtained a net electric power output equal to 48,7 MW and a net electric efficiency equal to 21,7 %, as shown in Table 11.

Power balance [kW]	
Total steam cycle net power output	68.870,00
Condensate extraction pump	-80,00
Condenser auxiliaries' consumptions	-1.960,00
Feedwater pump consumption	-750,00
Oxidant compression	-669,84
Ventilation consumption	-1.550,92
Other auxiliary consumptions	-3.096,07
Thermal battery's consumption*	-18,06
ASU*	-5.536,86
CO2 compression unit*	-6.528,55
Net electric power output	48.679,70
Net electric efficiency, %LHV	21,71%

Table 11 Case A: Power balance and consumption description

Due to the larger amount of steam at the inlet of the steam turbine, the actual power output is slightly larger than the reference case: however, because of the additional energy penalties, the final overall net electric power output is lower.

The additional losses are related to the additional CaL system: the main ones are related to the

- CO2 compression unit, whose specific consumption has been assumed equal to 396 kJ/kgCO2;
- The Air Separation Unit (ASU), whose specific consumption has been assumed equal to 200 kWh/tO2
- Refrigeration system prior the storage section, whose specific consumption has been assumed equal to 0,02 MWel/MWth.

It has been assessed that a change in this assumption within the best-practices range, impacts significantly neither the efficiency nor the overall power output.

Regarding the performances of the CO2 removal system, the CO2 absorption rate, Ecarb, results to be equal to 69,26% and the overall CO2 capture efficiency, Etot, results to be equal to 95,07%.

It leads to an overall CO2 mass flow rate released to ambient equal to 4,65 kg/s. Recalling the assumptions done for the reference case in which it has been considered a fossil CO2 mass flow rate emissions equal to 10,10 kg/s, it can be stated that the entire amount of CO2 emitted in the atmosphere is biogenic, therefore not impactful for the environment. Important feedback regarding the effectiveness of this CO2 removing technology is also given by the total CO2 specific emissions which result to be equal to 343,9 g/kWh.

CO2 from auxiliary fuel combustion, kg/s	6,69
CO2 from limestone calcination, kg/s	0,91
CO2 mass flow rate to storage, kg/s	16,49
CO2 overall mass flow rate release to ambient, kg/s	4,65
CO2 fossil mass flow rate emitted at the stack, kg/s	0,00
CO2 biogenic mass flow rate emitted at the stack, kg/s	4,65
CO2 total specific emissions [g/kWh]	343,89

Table 12 Case A: CO2 emissions and CO2 specific emissions of the entire system

Table 12 summarizes the CO2 emissions released in the atmosphere by the system.

Additionally, by considering that the emissions in the atmosphere are lower than the overall biogenic emissions of the reference case, the concept of negative CO2 emissions could be reported:

$$CO_2\ net\ negative\ emissions = m_{CO_{2_{captured}}} - m_{CO_{2_{fossil,ref}}}$$

The expression above gives, as a result, a mass flow rate of net CO2 negative emissions equal to 6,02 kg/s.

4.3. Case B

This case study considers a different solution for the integration of a post-combustion calcium looping system compared to Case A. Instead of only using the existing steam turbine to generate electrical power, it has been suggested the addition of a new steam turbine that recovers the heat of the CaL heat recovery boiler. Because the flue gases exchanging heat with the new steam cycle are cleaner

due to the treatments within the purification line, the thermodynamic parameters of the new steam turbine could be optimized: it has been set a live steam temperature equal to 520 °C and a live steam pressure of 70 bar.

Additionally, due to the independency of the two HRSG of the system, there aren't constrains related to the maximum steam that can be generated: on the contrary, larger is the amount of steam generated by the two steam cycles, higher is the net electric power output. Because of this reason the WTE power plant works at full load (three combustion lines are active) and the heat exchanged within the recovery boiler is maximized.

Additionally, instead of decreasing the carbonator efficiency to reduce the heat recovered within the carbonator, it has been maximized, setting a value equal to 90%.

Concerning the make-up factor and the solid recirculation factor, it has been suggested the following iterative procedure:

1) The make-up factor has been set equal to 0,2 in accordance with the average values found in literature. This parameter is an input of the system, thus is not varied.
2) Using the Romano Model on MATLAB it has been found the solid recirculation ratio that gives 90% efficiency with a fixed value of the make-up factor. Thus, the solid recirculation factor has been set equal to 7.
3) It has been verified the thermodynamic convergence with the GS simulation tool.

Figure 31 shows the configuration of the heat recovery boiler equipped with a second steam turbine.

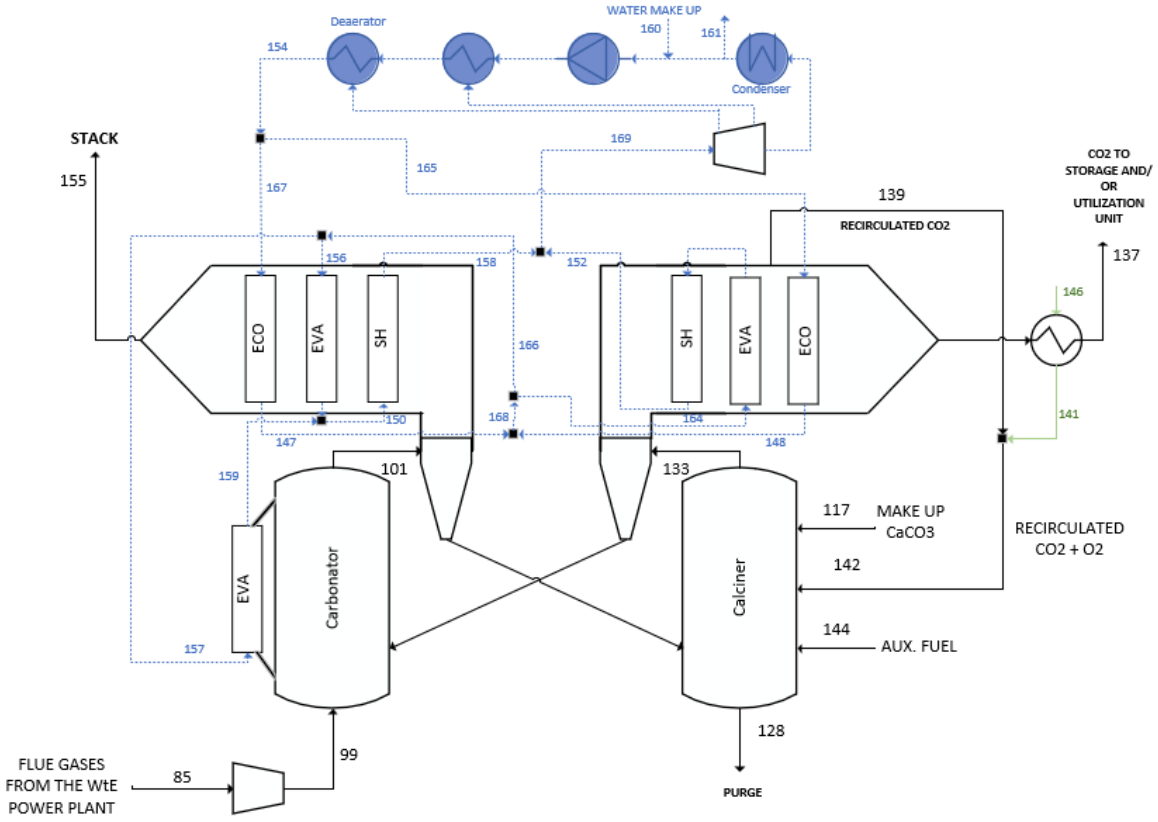

Figure 31 Calcium looping system and calcium looping heat recovery boiler equipped with a new turbine operating at 520 °C and 70 bar

Given the operating conditions, the heat exchanged within the calcium looping heat recovery boiler is schematized in Figure 32 and Figure 33.

Figure 32 defines the heat exchanged between the steam cycle and the hot CO2-depleted flue gases. The mass flow rate of water at the inlet of the carbonator-side of the boiler is equal to 40,89 kg/s and it is heated up at the temperature of 281°C by the cooler CO2-depleted flue gases. A portion of this stream, equal to 35,37 kg/s, is evaporated partially (14,24 kg/s) in the boiler's tube banks and partially (21,13 kg/s) by the heat recovered from the carbonation reaction occurring within the carbonator. The evaporator T-Q diagram refers only to the heat exchanged with the flue gases, and it doesn't show the one recovered from the carbonator. The 35,37 kg/s of water are sent to the superheater and brought to the temperature of 520 °C.

	Heat transferred [MW]	Temperature at the inlet [°C]	Temperature at the outlet [°C]
SUPERHEATER	24,47	287	520
EVAPORATOR	21,99	281	
ECONOMIZER	30,25	121,2	282

EVAPORATOR (carbonator heat recovery)	32,30	281

Table 13 Case B: heat exchanged with the CO2-depleted flue gases in the carbonator side and heat recovered from the carbonator

The flue gases, on the other hand, enter the recovery boiler at a temperature equal to 650 °C and exit at stack at the temperature of 135 °C.

It has also been set a ΔT_{PP} equal to 15 °C, and a ΔT_{SC} equal to 5 °C.

The overall heat exchanged in the carbonator-side of the boiler is equal to 109,01 MW.

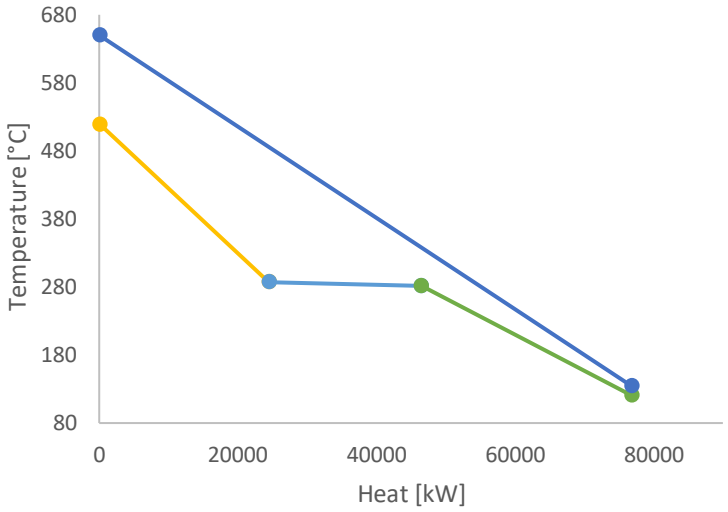

Figure 32 Case B: heat exchanged in the carbonator-side and temperature profile. In yellow it is shown the superheater profile, in light blue the evaporator profile and in green the economizer profile.

Due to a high make-up factor and a large amount of solid recirculating in the system, the fuel required for the calcination reaction is equal to 7,42 kg/s, because of the higher amount of heat required for the first calcination reaction of the Ca-based particles. This leads to a larger CO2 mass flow rate to the storage system, because a portion of CO2 emissions is generated by the auxiliary combustion in the calciner. The overall heat exchanged in the boiler in the calciner-side is equal to 56,94 MW and the contribution of each tube bank is shown in Figure 33.

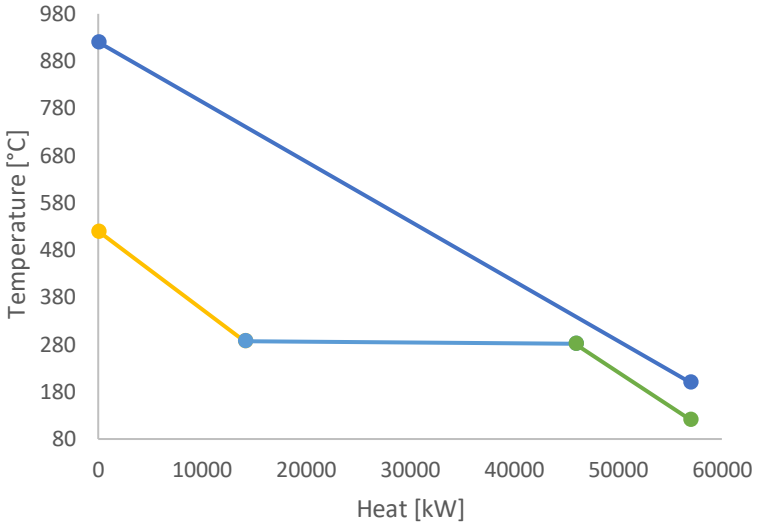

Figure 33 Case B: heat exchanged in the calciner-side and temperature profile. In yellow it is shown the superheater profile, in light blue the evaporator profile and in green the economizer profile.

The mass flow rate of water at the entrance of the boiler is equal to 15,02 kg/s and they are heated up at the temperature of 281°C. On the other hand, 20,53 kg/s of water are sent to the evaporator: the main constraint is ensuring that the hot CO2 at the outlet of the evaporator is lower than 400 °C to allow the recirculation. The water is then sent to a superheater that heats up the stream to the temperature of 520 °C.

Table 14 lists the main results of the heat exchanged within the boiler tube banks (calciner-side).

	Heat transferred [MW]	Temperature at the inlet [°C]	Temperature at the outlet [°C]
SUPERHEATER	14,08	287	520
EVAPORATOR	31,83	281	
ECONOMIZER	11,04	121,2	282

Table 14 Case B: heat exchanged within the boiler tube banks, calciner side

To summarize the design of the calcium looping technology, the main operating parameters and assumptions are reported in Table 15.

Ca-Looping process	
Molar flow of fresh limestone per molar flow of CO2 (F0/FCO2) [mol/mol]	0,2
Molar flow of solid recirculation per molar flow of CO2 (FR/FCO2) [mol/mol]	7
Adiabatic gas/solid mixing temperature at carbonator inlet [°C]	540,8
Carbonator outlet temperature [°C]	650
Calciner outlet temperature [°C]	920,1

Recirculated CO2-rich gas temperature [°C]	419,7
Oxygen preheating temperature [°C]	150
Cyclone's efficiency [%]	0,99
Cyclone's ash selectivity [%]	0,9
Oxygen concentration in the oxidant flow to calciner [%vol]	6,854
Oxygen concentration in the calciner off-gas [%vol]	1,755
Fans isentropic efficiency [%]	0,82
Fans electromechanical efficiency [%]	0,94
Percentage of biogenic C in the emitted CO2 [%]	50%
CaL Heat recovery system	
ASU specific consumption [kWh/tO2]	200
GPU specific power consumption [kJ/kgCO2]	396
CO2 lost in the atmosphere in the GPU [%]	3%
Power consumption for the refrigeration section [MWel/MWth]	0,02
Temperature at the turbine inlet [°C]	520
Pressure at the turbine inlet [bar]	70
Superheater pressure drop [bar]	0,08
Economizer pressure drop [bar]	0,15
Condenser pressure [bar]	0,07

Table 15 Case B: main assumptions and operating parameters of the calcium looping system equipped with a recovery steam turbine

Considering the design described above, the overall performances of the power plant, in terms of net power output and net electric efficiency, are summarized in Table 16.

Power balance [kW]	
Total steam cycle net power output	126.570,00
Condensate extraction pump	-140,00
Condenser auxiliaries' consumptions	-3.340,00
Feedwater pump consumption	-1.310,00
Pumps auxiliary consumption	-4,53
Oxidant compression consumption	-964,80
Ventilation consumption	-2.432,49
Other losses	-4.352,45
Refrigeration section specific consumption*	-175,79
ASU*	-12.347,14
CO2 compression unit*	-14.199,32
Net electric plant output	87.303,49
Net electric efficiency, %LHV	21,97%

Table 16 Case B: Power Balance and net electric efficiency of the WTE power plant equipped with a calcium looping technology and a recovery turbine

Considering an overall thermal input equal to 397,42 MWth and an overall net power output equal to 87,30 MWel, the total net electric efficiency is equal to 21,97%. The losses referred to the calcium looping system have been calculated as in the previous case study, maintaining the same assumptions for the specific consumptions.

For what concern the CO2 removal performances of the system, it can be stated that the overall emissions to the atmosphere are equal to 3,14 kg/s, therefore, all the emissions could be considered biogenic.[1] Thus, the fossil CO2 emissions at the stack are equal to zero. Another important parameter is the total CO2 specific emissions, which are equal to 129,59 g/kWh.

CO2 from auxiliary fuel combustion [kg/s]	14,94
CO2 from limestone calcination [kg/s]	3,73
CO2 mass flow rate to storage [kg/s]	35,86
CO2 mass flow rate released to ambient [kg/s]	3,14
CO2 fossil mass flow rate emitted at the stack [kg/s]	0,00
CO2 biogenic mass flow rate emitted at the stack [kg/s]	3,14
CO2 total specific emissions [g/kWh]	129,59

Table 17 Case B: CO2 emissions and specific emissions to the atmosphere

Table 17 summarizes the most important contributions in terms of CO2 emissions. Recalling the concept of CO2 net negative emissions, in this specific case study they resulted to be equal to 8,07 kg/s.

What would have happened in case of different assumptions for the Calcium Looping system?

The assumptions and choices of the main operating parameters have been assigned in accordance with the main constrains of the entire system.

However, the choice of the make-up factor, has been done in accordance with the bast-practices shared in literature. Because the previous operating parameter influences the overall process, it has been done a brief evaluation of the different main results that would have been obtained in case the make-up factor was varied in a range between 0,15 and 0,25.

[1] As specified in the previous case study, the reference fossil CO2 emissions to the atmosphere are equal to 10,10 kg/s and the overall emissions are equal to 20,20 kg/s. Therefore, it could be assumed that the entire amount of CO2 emitted to the atmosphere is biogenic.

For all the values of the make-up factor, it has been assessed the kinetic and thermodynamic convergence of the system maintaining fixed both the solid recirculation factor (F_R/F_{CO2}=7) and the carbonator efficiency (E_{carb} = 90%).

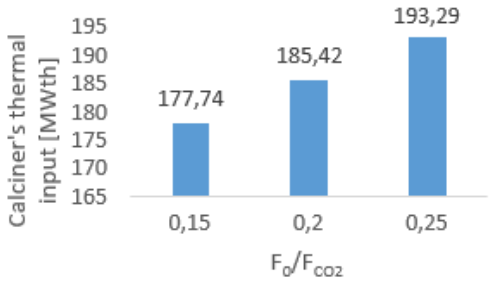

Figure 34 Calciner's thermal input variation with the make-up factor

As expected, and as shown in Figure 34, by reducing the make-up factor, the auxiliary fuel required for the calcination reaction reduces, reducing the thermal input of the entire system, effecting positively the net electric efficiency of the system.

Because of this reason, while the heat exchanged within the carbonator's tube banks side remains nearly constant, the heat exchanged in the calciner side decreases significantly with the make-up reduction. Therefore, as a consequence, the steam mass flow rate toward the CaL turbine decreases, as shown in Figure 35.

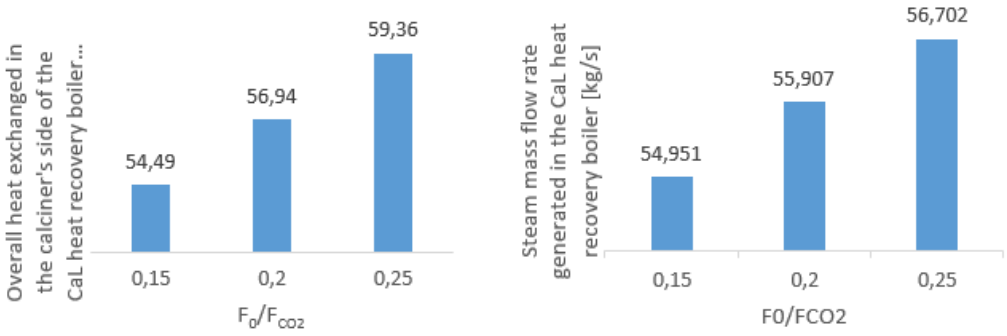

Figure 35 (left side) Overall heat exchanged in the calciner side of the CaL heat recovery boiler VS make-up factor; (on the right) steam mass flow rate to the CaL turbine VS make-up factor

Additionally, a reduction in the calciner's thermal input reduces, on one hand, the oxygen requirement to fulfil the completeness of the combustion in the auxiliary burner, and, on the other, reduces the CO2 generated during the auxiliary combustion, lowering the CO2 mass flow rate to the storage/utilization system. Consequently, both the ASU consumption and the CO2 compression unit

consumption decrease with the reduction of the make-up factor, leading to lower electric losses of the system (Figure 36).

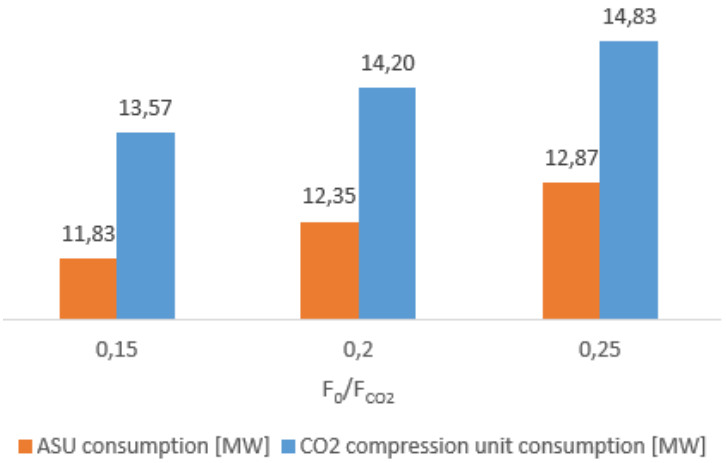

Figure 36 ASU consumption and CO2 compression unit consumption VS make-up factor variation

In the end, the overall balance of the positive and negative contributions with the reduction of the make-up factor results in an increase in both the overall net power output and the net electric efficiency. However, in Figure 37, it is also clearly shown how the net electric efficiency is more influenced by the make-up factor compared to the overall electric power output, and this is because of the impact of the reduced electric and thermal losses of the system.

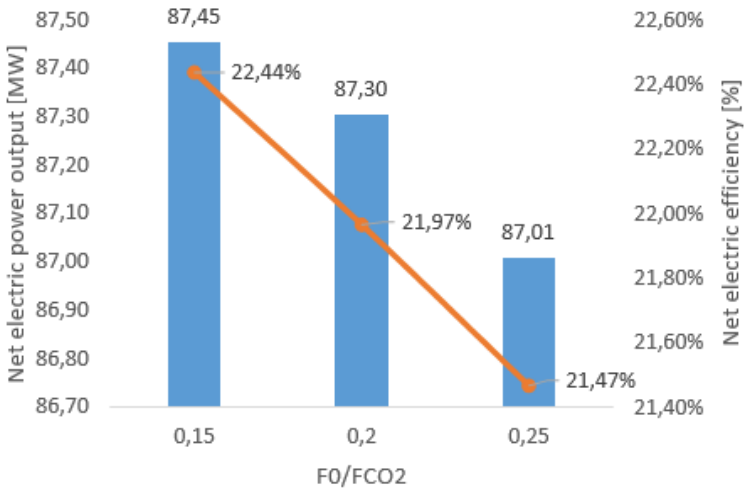

Figure 37 Net power output and net electric efficiency VS the make-up factor variation

4.4. Case studies comparison

The following paragraph has the purpose of comparing the main results of the three different cases under study. To make a proper comparison of the improvements and problems of each design the KPIs have been used.

4.4.1. KPIs introduction and definition

The aim of this thesis was assessing the energy performances of the reference WTE power plant when equipped with a calcium looping post-combustion CO2 removal system: the following chapter analyses the main results obtained and allows comparison thanks to the evaluation of the main KPIs. For the sake of clarity, the main Key Performance Parameters (KPIs) used in the comparison are the following:

1) **Specific Primary Energy Consumption for CO2 Avoided (SPECCA):** starting from the obtained values of specific CO2 emissions, the SPECCA coefficient can be calculated as follows:

$$SPECCA\ [\frac{MJ_{LHV}}{kg_{CO_2}}] = \frac{3600\left(\left(\frac{1}{\eta}\right)-\left(\frac{1}{\eta_{ref}}\right)\right)}{e_{CO_{2_{ref}}} - e_{CO_2}}$$

where ηref and $eCO2ref$ represent the electric efficiency and the specific CO2 emissions of the reference case. This performance parameter is needed to evaluate the quality of the energy performances of the CCS unit, and it is highly used when comparing different technologies.

It has also been considered a modified approach in the evaluation of the SPECCA coefficient, which takes into consideration the additional power generated and sent to the grid [21] by the Calcium Looping turbine, as described in the expression below:

$$SPECCA^{*}\left[\frac{MJ_{LHV}}{kg_{CO_2}}\right] = \frac{\frac{1}{\eta_{WTE\ with\ CCUS}}-\left(x_i\left(\frac{1}{\eta net_i}\right)-(1-x_i)\left(\frac{1}{\eta ref_{WTE}}\right)\right)}{\left((1-x_i)e_{CO_2 ref,WTE}+x_i e_{CO_2,i}\right)-e_{CO_{2WTE\ with\ CCUS}}}$$

where the xi is the share of the additional power that is supplied to the grid by the CaL technology and η_{net_i} and $e_{CO2,i}$ are the state-of-art plant's relative net electric efficiency and specific CO2 emissions to the atmosphere ($\eta_{net,i}$ = 25%; $e_{CO_{2_{i,fossil}}}$ =771 g/kWh).

2) The **Carbon Capture Ratio (CCR):** the CO2 is not only generated by the main fuel, but also by fresh limestone calcination: assuming that the CO2 from limestone calcination is entirely captured, and that the residual CO2 emitted at the stack is associated only with the waste combustion process, the CCR is evaluated as follows:

$$CCR[\%] = 1 - \frac{G_{CO2_{stack}}}{G_{waste}\, e_{CO2_{waste}}}$$

were $e_{CO2_{waste}}$ is the CO2 emission factor from waste incineration, which means the kg of CO2 generated burning a ton of waste. I have evaluated this parameter in the reference case, and it resulted to be equal to 986 kg_{CO2}/ton_{waste}.

3) **Avoided CO2**: this parameter considers the amount of fossil CO2 avoided compared to the reference case to produce a MWh of electricity.

$$CO_2\ avoided = e_{CO_{2_{refcase}}} - e_{CO_{2_{case,i}}}$$

The biogenic avoided CO2 is not taken into consideration because it is neutral when emitted into the atmosphere.

4) **The Efficiency Penalty ($\Delta\eta$):** the addition of a post-combustion CO2 removal technology implies extra consumption and/or energy penalties. Because of this reason it is important to evaluate the system efficiency penalty in the electricity generation compared to the reference case. This parameter can be considered as the "cost" to be paid to reduce the emissions.
The Efficiency Penalty is evaluated as follows:

$$\Delta\eta = \eta_{refcase} - \eta_{case,i}$$

4.4.2. Analysis of the case studies

Starting from the concepts introduced in the previous paragraph a deeper analysis of the advantages and disadvantages of each solution needs to be address.

	Base Case	Case A	Case B
Total fuel consumption, MW_{LHV}	212	223,95	397,42
Total gross power output, MW	65,77	68,87	126,57
Gross electric efficiency, %	31,02%	30,75%	31,85%
Total net power output, MW	58,42	48,67	87,30
Net electric efficiency, %	27,56%	21,71%	21,97%

Table 18 Comparison of the overall net electric power output, the net electric efficiency of the three case studies and the total fuel consumption

The overall net electric power output and the net electric efficiencies listed in Table 18 are represented in Figure 38.

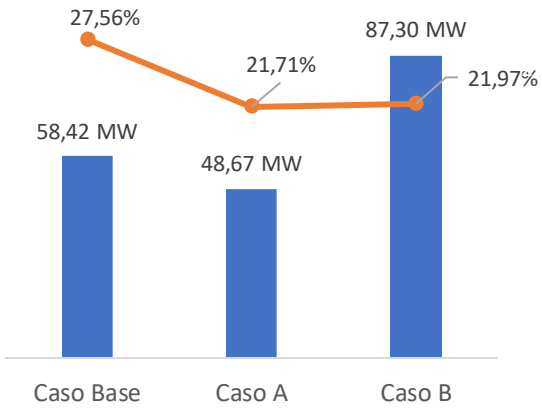

Figure 38 Net electric power output and net electric efficiency comparison

The reference case is linked to a net power output equal to 58,42 MW: because case A doesn't include an additional turbine, the overall power output depends only on the main turbine. Even if the steam mass flow rate at the entrance of the steam turbine is higher than the reference case, the additional power generated doesn't compensate the additional losses related to the calcium looping system, such as the ASU, the CO2 compression unit, and the refrigeration system. Figure 39 clearly shows the path from an electric power at the generator equal to 68,87 MW to a net electric power output equal to 48,67 MW.

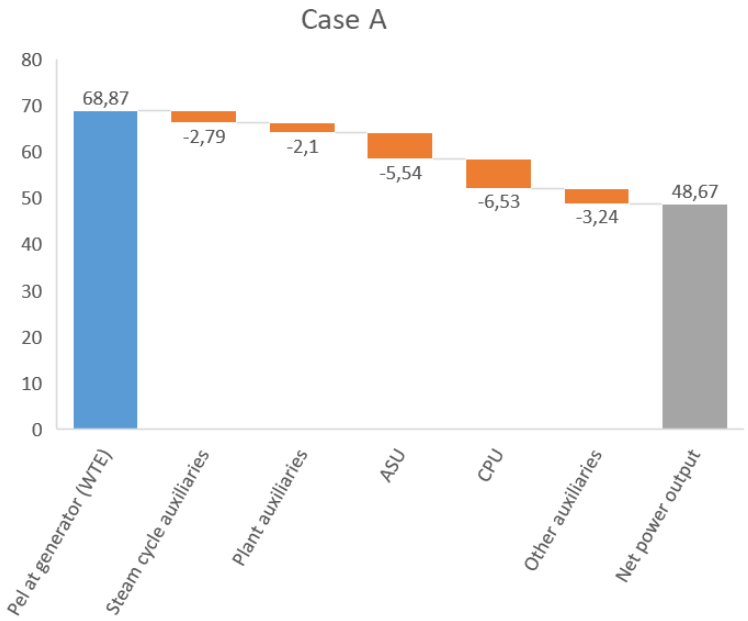

Figure 39 Case A power breakdown showing the different losses leading to the final net power output

On the other hand, case B, is equipped with an additional steam turbine which provides an additional contribution to the net electric power output.

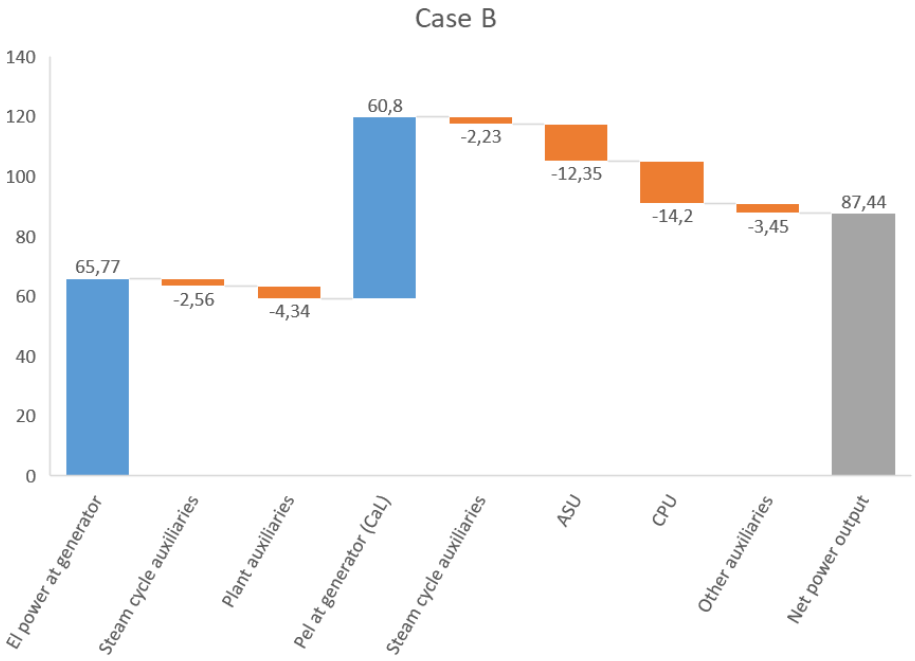

Figure 40 Case B power breakdown showing the different losses leading to the final net power output

Figure 40 shows that the contribution of the main turbine is equal to the one of the reference case, while, the additional turbine generates 60,8 MW: the overall net electric power output is equal to 87,44 MW.

For what concern the overall thermal input, Table 18 lists a value slightly higher than the one of the reference case for case A, while, concerning case B, a value almost doubled (Figure 41).

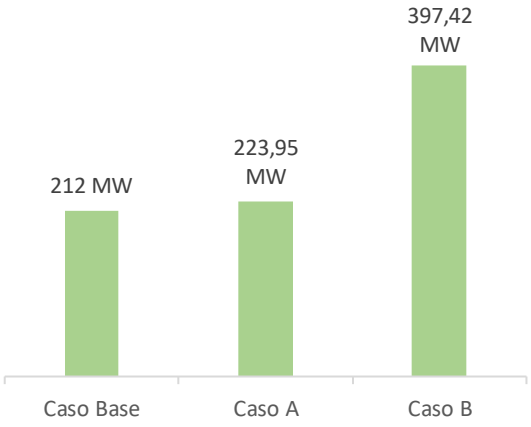

Figure 41 Thermal input comparison

Comparing the net electric efficiency, case B has an efficiency slightly higher than case A because the additional steam cycle added to the system has better thermodynamic characteristics. Compared to the reference case they both register an energy penalty slightly lower than 6%pt.

Table 19 compares the three different case studies in accordance with the considerations done above.

	Base case	Caso A	Caso B
Fuel consumption			
WTE plant, MW_{LHV}	212	141	212
Calciner CaL, MW_{LHV}	0	82,95	185,42
Power Balances			
WTE plant			
Electric power at generator, MW	65,77	68,87	65,77
Steam cycle auxiliaries, MW	-2,56	-2,79	-2,56
Plant auxiliaries, MW	-4,79	-2,10	-4,34
Net power output of WTE, MW	58,42	63,98	58,87
CaL power plant			
Electric power at generator, MW	0	0	60,80
Steam cycle auxiliaries, MW	0	0	-2,23
Air separation unit, MW	0	-5,54	-12,35
CO2 compression unit, MW	0	-6,53	-14,20
Other auxiliary consumptions, MW	0	-3,24	-3,45
Overall WTE + CaL power plant			
Total fuel consumption, MW_{LHV}	212	223,95	397,42
Total gross power output, MW	65,77	68,87	126,57
Gross electric efficiency, %	31,02%	30,75%	31,85%
Total net power output, MW	58,42	48,67	87,30
Net electric efficiency, %	27,56%	21,71%	21,97%

Table 19 Power balance and fuel consumption comparison for the three different case studies

Additionally, it needs to be introduced the difference between the total gross power output and the net power output of the two case studies: while the gross power output corresponds to the electricity generated at terminal of the generator, the net power output is the net electricity transmitted from a power plant to the grid. Therefore, while the net electric efficiency considers the losses occurring within the plant in terms of auxiliaries' consumption and flue gas treatment systems, the gross electric efficiency gives an understanding of the quality of the process beside those losses.

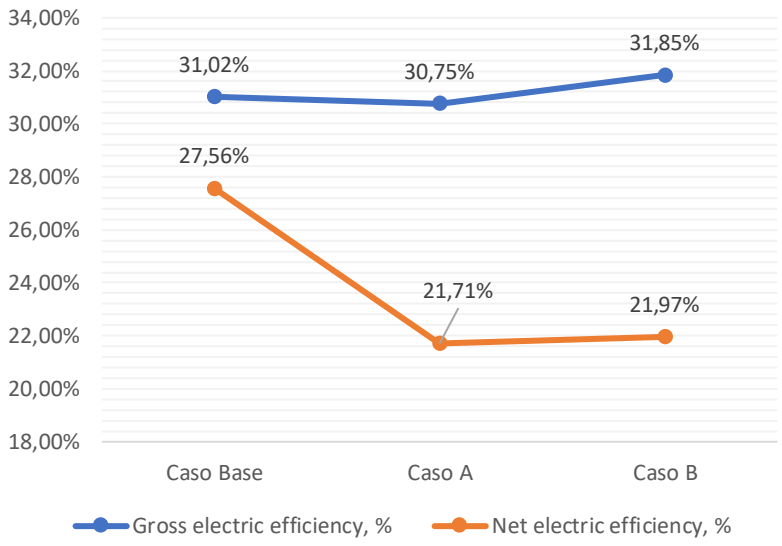

Figure 42 Net electric efficiency VS gross electric efficiency

In fact, Figure 42 shows the different trends of the net electric efficiency and the gross electric efficiency of the models under study: the former decreases steeply from the reference case due to the additional losses linked mainly to the post-combustion CO2 treatment section (i.e. the air separation unit and the CO2 compression unit); the latter shows even an increase in the process' quality for case B, because the additional steam turbine works at improved thermodynamic conditions.

Finally, a brief analysis of the CO2 emissions and the related KPIs needs to be addressed, to also understand the quality and the penalties of the CO2 treatment section, whose operating conditions are listed in Table 20.

	Caso A	**Caso B**
Make-up factor F0/FCO2 [mol/mol]	0,08	0,2
Solid recirculation factor FR/FCO2 [mol/mol]	4,5	7
Carbonator efficiency [%]	69%	90%

Table 20 Case A and case B main operating parameters of the calcium looping system

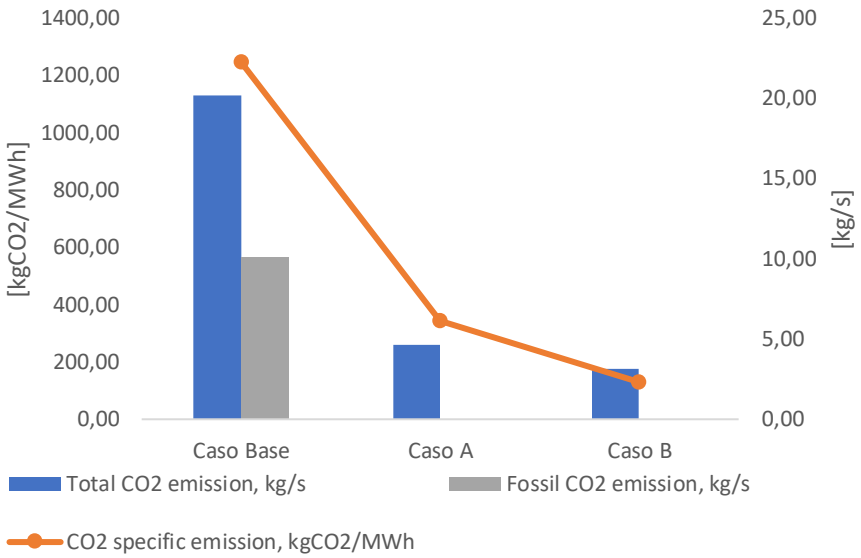

Figure 43 CO2 emissions and specific CO2 emissions comparison

Figure 43 shows the total CO2 emissions in the first case and in the two case studies with the CO2 capture system: it can be noticed that, while the former has 10,10 kg/s of fossil CO2 emitted in the atmosphere, Case A and Case B have only environmentally neutral emissions, because they can be considered totally biogenic. Additionally, by looking at the CO2 specific emissions trend, it can be noticed that the increased power output of Case B allows a deeper decarbonization of the system.

	Base Case	**Case A**	**Case B**
Direct CO2 emission at stack, kg/s	20,20	4,51	2,03
CO2 vented from CO2 compression, kg/s	0	0,14	1,11
Total CO2 emission, kg/s	20,20	4,65	3,14
Fossil, kg/s	10,10	0,00	0,00
Biogenic, kg/s	10,10	4,65	3,14
CO2 specific emission, kg/MWh	1244,98	343,89	129,59
Fossil, kg/MWh	622,49	0,00	0,00
Biogenic, kg/MWh	622,49	343,89	129,59
Fossil CO2 avoided, kg/s	0	10,10	10,100
Specific fossil CO2 avoided, kg/MWh	0	343,89	622,49
Net CO2 negative emissions, t_{CO2}/year	0	-74936,73	-233779,28
CO2 grid emissions, kg/s	0	3,48	-10,31
CO2 from limestone calcination, kg/s	0	0,91	3,73
CO2 sent to storage, kg/s	0	16,49	35,86

Table 21 CO2 main fluxes of the system in the three different case studies

Table 21 CO2 main fluxes of the system in the three different case studiesgives a better overview of the main CO2 fluxes involved in the two different case studies. Among the values described above, it is interesting to make a further comment about the CO2 grid emissions: this value is useful to better understand the SPECCA* index: the SPECCA* index evaluates, based on the different power output of the case study compared to the reference case, the amount of extra CO2 that is emitted in the atmosphere to compensate the energy not generated by the WTE power plant. Because case A has a net power output lower than the one of the reference case, based on the Italian energy mix, it will be emitted in the atmosphere 3,48 kg/s of CO2 by the national grid. On the contrary, because case B design leads to a higher net power output, the "additional emissions of the grid" become an additional contribution of CO2 avoided.

This last reasoning can be shown also through the evaluation of the SPECCA* coefficient, whose purpose is evaluating the consumption of primary energy per unit of CO2 avoided weighted with the amount of extra energy injected in the grid system. Thus, lower the SPECCA* coefficient, lower the energy losses to capture CO2.

	Caso A	**Caso B**
SPECCA [MJ_{LHV}/kg_{CO2}]	3,91	2,98
SPECCA, fossil [MJ_{LHV}/kg_{CO2}]	5,66	5,35
SPECCA* [MJ_{LHV}/kg_{CO2}]	1,74	0,95

Table 22 SPECCA coefficient evaluation

Table 22 shows batter results for Case B because directly dependent on the specific CO2 emissions to the atmosphere: in the table there are also the values related to the SPECCA coefficient that doesn't take the extra power injected in the grid into account. As also shown in Figure 44, the SPECCA evaluated only on the fossil emission doesn't allow a proper comparison that consider all the advantages and disadvantages of the two technologies in terms of energy penalties of the CO2 removal system: the two values are slightly different. On the other hand, both the evaluation of the entire CO2 emitted in the atmosphere and the SPECCA weighted on the power injected into the grid give a better understand of the better performances of Case B.

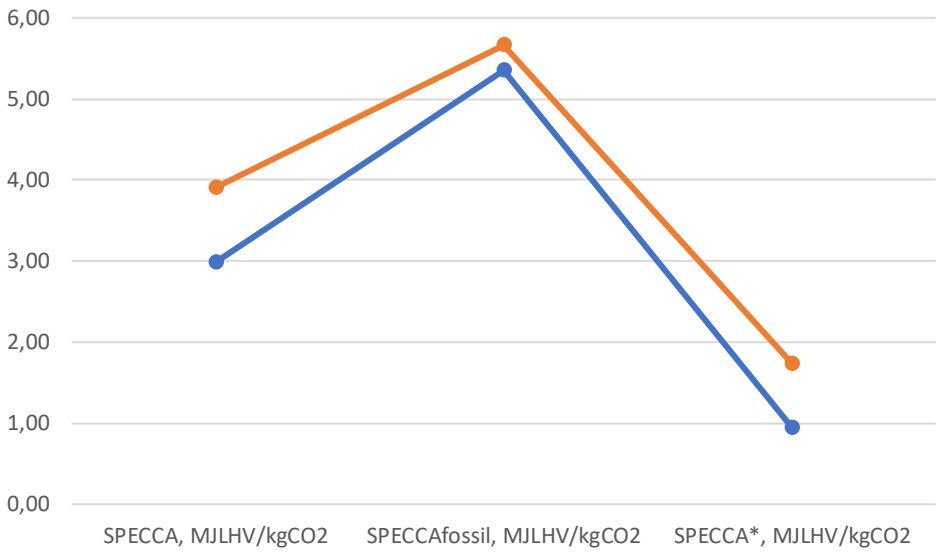

Figure 44 SPECCA evaluation and comparison

Another parameter to be considered when evaluating the quality of the carbon capture technology is the CCR, Carbon Capture Ratio, and the Avoided CO2 emissions, whose results are listed in Table 23.

	Caso A	**Caso B**
Overall CCR [%]	65,47%	84,44%
Specific fossil CO2 avoided [kg_{CO2}/MWh]	343,89	622,49

Table 23 CCR and specific fossil CO2 avoided

5 Chapter five: simplified economic analysis

The technical constraints and improvements of the two different case studies need to be coupled with an economic analysis, even if simplified, to address a financial point of view to the results discussed in Chapter four.

One of the side effects of post-combustion solutions is the additional costs linked to the CO2 capture process. These additional costs can be evaluated in terms of the costs required to avoid a certain amount of CO2 emissions in the atmosphere. Thus, lower is this value, more suitable, in economic terms, will the system be.

5.1. Evaluation of the CAPEX and OPEX of case A and case B

This section is going to target the procedure to evaluate the total costs of adding a calcium looping technology with the two different designs explained in Chapter four.

In order to discuss deeper the analysis of the calcium looping related costs, it has been assumed that the LCOE of a WTE power plant of this size is equal to 80 €/MWh (20). This assumption will be used for both the designs because the project has been defined as a retrofitting solution that doesn't make major structural changes of the existing WTE power plant.

Therefore, it has been estimated the calcium looping system total cost of investment (TCI) following a bottom-up approach, which means that it has been derived by the sum of all the additional components that need to be included in the CO2 capture system. Table 24 reports the empirical and regressed equations which consider experience and the scale effect of small size non-standard components.

Non-standard component	Direct cost model [k€]
Carbonator	$474 * Transferred\ thermal\ power\ [MW_{th}] + 8.360 * \left(\frac{internal\ diamenter[m]}{4,7}\right)^{0,6}$
Calciner	$415,3 * (Fuel\ thermal\ input\ [MW_{th}])^{0,65}$
Heat recovery boiler (Case A)	$434,6 * \left(\frac{Carbonator\ Heat\ duty\ [MW]}{1361}\right)^{0,85} + 130,5 * \left(\frac{Calciner\ Heat\ duty\ [MW]}{496,9}\right)^{0,8^r}$
Heat recovery and steam production system (Case B)	$26.875 * \left(\frac{Overall\ heat\ recovery\ duty\ [MW]}{266}\right)^{0,67}$
Sealed fan (<500 kW)	$63 * \left(\frac{Volumetric\ flow\ rate\ \left[\frac{m^3}{h}\right]}{25.000}\right)^{0,5} + 303 * \left(Power\ \frac{[kW]}{75}\right)^{0,65}$
Air separation unit	$63.645 * \left(\frac{Mass\ flow\ of\ oxygen\ \left[\frac{tO2}{d}\right]}{2.717}\right)^{0,6}$
CPU	$101 * \left(\frac{CO2\ mass\ flow\ rate\ \left[\frac{kg}{s}\right]}{164,5}\right)^{0,624}$

Table 24 Capital cost experimental functions to evaluate the non-standard components characterizing the calcium looping system. Sources (19) (20) (21)

Therefore, the evaluation of the non-standard components has been derived by the following considerations:

1) **carbonator costs**: it has been considered, in accordance with Haaf et al. work, two terms: the former (heat recovery term) is dependent on the heat transferred within the carbonator because it considers the heat recovery surfaces; the latter (size term) is dependent on the size of the carbonator's vessel. The internal diameter is a parameter that depends on the kinetics of the carbonation reaction, therefore, it has been evaluated using the Romano Model, which gives, as output, the area of the carbonator, considering the velocity of the flue gasses within the vessel. Additionally, the heat transferred has been considering the heat of the carbonation reactions taking place in the carbonator;
2) **calciner costs:** it is only dependent on the thermal input, thus on the amount of auxiliary fuel needed to perform the calcination reaction;
3) **heat recovery boiler costs**: Table 24 reports two different functions for the evaluation of the heat recovery boiler. The former considers only the heat recovery boiler (case A), while the latter, also considers the presence of the additional steam turbine (case B);
4) **sealed fan costs**: the costs of the sealed fan are both related to the volumetric flow rate of the CO2 recirculating at 400°C and the electric power consumption of the fan itself;
5) **ASU and the CO2 compression unit costs**: their cost is dependent on the oxygen mass flow rate needed to perform the auxiliary combustion and the

CO2 mass flow rate to storage because they are strictly related to the electric consumption of the two systems.

The main results are described in Table 25.

	Case A [k€]	Case B [k€]
Carbonator (Size term)	9.011,32	10.175,04
Carbonator (Heat recovery term)	23,18	15.310,20
Calciner	7.338,25	12.378,38
Heat recovery and steam production system	11.255,09	19.591,27
Sealed fan (<500 kW)	162,53	252,02
Air separation unit	27.338,59	44.234,35
CPU	28.541,19	46.529,74
TOTAL COSTS [k€]	83.670,15	148.470,99

Table 25 Main results of the total cost of investment evaluation for non-standard components for case A and case B

The total costs of capital investment described in the table above are characterized in Figure 45 and Figure 46, in terms of TCI breakdown: as it can be noticed from the two graphs below, the major expenses are linked to the CPU and ASU for both case studies. The different costs of the two solutions are related to the different mass flow rate of oxygen and CO2 for the two case studies. On one hand, case B is linked to a higher CO2 captured ($E_{carb,A}$=70%, $E_{carb,B}$=90%) and a higher amount of CO2 generated during the auxiliary combustion process, therefore, a higher mass flow rate of CO2 ($m_{CO2,A}$=16,49 kg/s, $m_{CO2,B}$=35,86 kg/s) is sent to the storage system; on the other, due to the higher thermal input registered in case B, the oxygen required to perform a complete combustion is more than doble the one of case A ($m_{O2,A}$=7,69 kg/s, $m_{CO2,B}$=17,15 kg/s). These two considerations justify the difference between the two solutions proposed in this work.

Additionally, case B registers a percentage of the total cost related to the carbonator significantly higher than the one of case A (17% compared to 11%): this is another consequence of setting a carbonator efficiency of case B higher than the one of case A. First, the area of the section of the vessel obtained for the two case studies is different: the internal diameter of case A resulted equal to 5,33 m^2, while the one of case B resulted equal to 6,52 m^2. However, the major cause of the different carbonator cost is the heat transferred: while case A had the aim of minimizing the heat transferred in the evaporator exchanging heat with the carbonator (to minimize the steam generation due to steam cycle constrains), case B had been designed to maximize the steam generated to increase the electric power output of the new

additional steam turbine (no specific constraints related to the steam cycle mass flow rate). This reasoning can be clearly seen in Table 24: in fact, the term related to the size doesn't change significantly from case A to case b; what changes is the cost related to the heat recovery surfaces, due to the significant difference among the two solutions.

Regarding the calciner costs, the main difference is caused by the different auxiliary thermal input related to the two case studies: while case A has a thermal input equal to 82,95 MW, case B has 185,42 MW.

One important difference between the calciner and the carbonator is that, while the calciner had a scaling factor equal to 0,65 (the wide difference between the two case studies is not related to a linear increase of the costs), the heat transferred, which mostly impacts the carbonator costs, is linearly related to them.

Moreover, for what concerns the heat recovery boiler expenses, the main difference between case A and case B is related to the costs of the additional steam turbine present only in case B.

Finally, it can be also noticed that the cost of the sealed fan, compared to the other costs of the calcium looping system, is negligible.

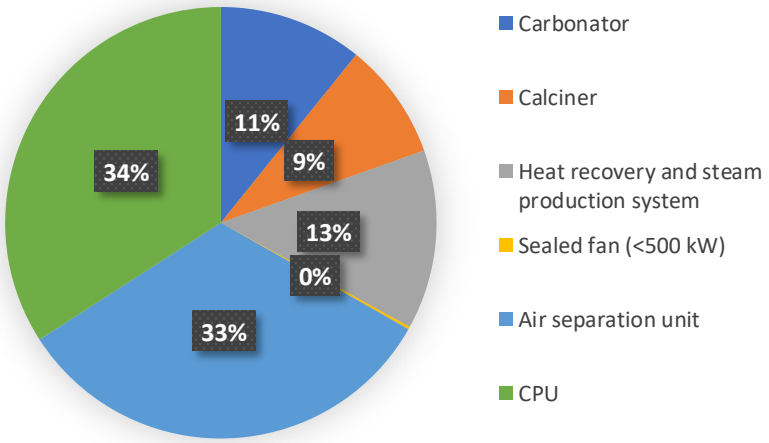

Figure 45 Case A: TCI breakdown showing the impact of the different contributions of the main non-standard components

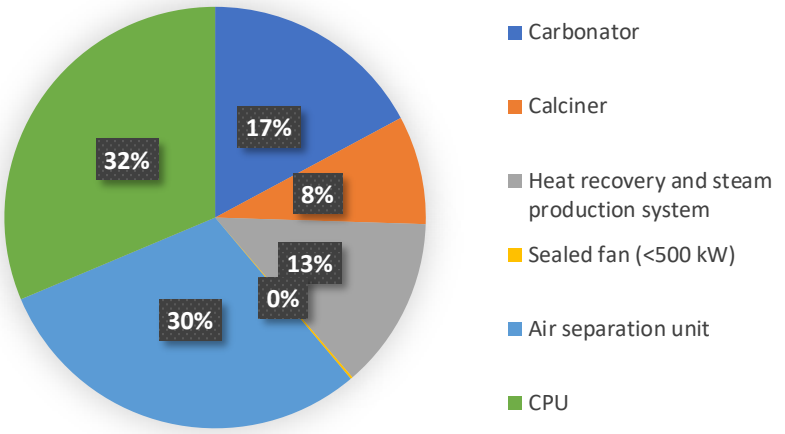

Figure 46 Case B: TCI breakdown showing the impact of the different contributions of the main non-standard components

To evaluate the yearly share of the overall CApital EXpenditures (CAPEX), a capital carrying charge (CCR) needs to be taken into consideration: because of the small size of the power plant under study and the innovative nature of the technology, the CCR could be estimated equal to 0,15. Even if this assumption is a plausible first guess, the nature of this value is complex: it requires detailed information of the breakdown between equity and debt, nominal return on equity and nominal return on debt, the inflation rate, the duration of construction and duration of the project, allowances for funds used during construction, etc. .

Therefore, the yearly costs of the two case studies can be evaluated by the following expression:

$$CAPEX, i = TCI, i * CCR$$

Thus, $CAPEX_{,case\ A}$ is equal to the 12.550,52 k€/year, and $CAPEX_{,case\ B}$ is equal to 22.270,65 k€/year.

To evaluate the overall total costs per year linked to the addition of a calcium looping technology, the operating expenses need to be considered as well.

Table 26 reports the assumptions of the specific costs and credits needed to evaluate the OPerating EXpenses (OPEX) of the calcium looping technology.

Cost of Limestone	[€/ton]	30
Cost of SRF	[€/ton]	- 10
Cost of MSW	[€/ton]	- 75
Cost of CO2 transport and storage	[€/ton]	7

Table 26 Specific variable costs assumptions for the evaluation of the operating expenses

The results are reported in Table 27: case B is linked to operating costs that are significantly higher due to the higher make-up factor, a bigger amount of fuel needed to perform the calcination reaction in the auxiliary burner, the nominal operating conditions of the power plant working with three combustion lines active, and the larger quantities of CO2 captured and sent to storage.

In fact, the cost of make-up is directly dependent on the mass flow rate of CaCO3 entering the system: the mass flow rate of make-up of case A is equal to 70.914 ton_{CaCO3}/year, while the mass flow rate of make-up of case B is equal to 265.863 ton_{CaCO3}/year, a value that is almost 4 times bigger than the one of case A. One possible way to cut this term of the operating expenses is considering the usage of carbide slag, described in paragraph 3.4, as a sorbent of the calcium looping system. Because it is considered a non-valuable material, it is nearly free of charge and all the expenses related to the cost of make-up listed above could be significantly reduced or even become negative.

This concept is applied in the use of SRF as auxiliary fuel, instead of natural gas or coal: the SRF is a waste flux therefore the operating costs can become credits because a waste management service is offered. In this specific work, it has been selected an SRF characterized by a particularly high LHV, therefore it has been assumed an auxiliary fuel gate fee (credits) significantly low compared to other waste fluxes. However, the idea was leaving the analysis open for future reasonings, in which a lower quality SRF could be chosen in order to increase the economic advantages related to this technology[2]. Additionally, it can be noticed that the increased amount of auxiliary fuel used in case B (96.213 ton_{SRF}/year for case A and 215.089 ton_{SRF}/year for case B) becomes economically advantageous.

Cost of make-up	2.127,42	7.975,88
SRF calciner	-962,14	-2.150,90
CO2 transport and storage cost	4.403,48	9.637,27
TOTAL COSTS [k€/year]	5.568,77	15.462,25

Table 27 Results of the operating costs evaluation

Finally, the costs related to the CO2 transport and storage are different because the CO2 mass flow rate of case B is nearly double the one of case A, as reported in the above considerations.

[2] It must be underlined that the aim of this assumption was showing the economic advantages of selecting this technology compared to others. However, there are some studies available, such as the Haafa et al. (20), that consider high quality fuels with positive costs. The purpose of this study was trying to address a case study that could better respect the real costs found in the market right now.

Knowing the operating costs (OPEX) and the capital expenditures (CAPEX), the total additional costs of a system equipped with a CO2 removal system can be evaluated as follows:

$$\Delta\ Costs\ \left[\frac{€}{year}\right] = TCI * CCR + OPEX$$

The resulting additional costs of the two case studies are

A. Case A: 18,12 M€/year
B. Case B: 37,73 M€/year

By recalling the assumption made for the WTE power plant ($LCOE_{ref}$ = 80 €/MWh), the concept of the levelized cost of electricity could be introduced: the LCOE is an index that is used to compare the costs related to different technologies and helps establishing which technology is economically convenient. It approximates the average discounted electricity price over the project duration that would be required as income to match the net present value of the overall project costs.

The reference LCOE has been defined assuming a gate fee for the MSW equal to 75 €/ton, which can be considered an average value.

To evaluate the overall LCOE [€/MWh] of the WTE power plant equipped with a CCS technology, the following expression could be used (20):

$$LCOE_{CCS_{case,i}}\left[\frac{€}{MWh}\right] = \frac{LCOE^*_{ref} * E^*_{ref} + CAPEX_{CCS} + OPEX_{CCS}}{E_{WTEwithCCS}}$$

where $LCOE^*_{ref}\ and\ E_{ref}$ refer to the reference case, $CAPEX_{CCS}\ and\ OPEX_{CCS}$ refer only to the calcium looping technology evaluated above and $E_{WTEwithCCS}$ refers to the overall energy generated by the WTE power plant equipped with the calcium looping technology in a year. $LCOE^*_{ref}$ is a weighted value of the $LCOE_{ref}$ based on the ton of fuel injected in each case study. The reference case and case B are both referred to the same fuel mass flow rate at the inlet of the WTE power plant, therefore, the reference LCOE used is equal to 80 €/MWh. On the other hand, for what concern case A, the LCOE used is equal to 117,06 €/MWh.

The LCOE for the two case studies resulted to be equal to

A. $LCOE_{CCS_{CASE\ A}} = 200{,}13\,\frac{€}{MWh}$
B. $LCOE_{CCS_{CASE\ B}} = 107{,}64\,\frac{€}{MWh}$

The big difference is not only related to the lower net power output registered in case A, but it is also related to the fact that case A has a lower mass flow rate of fuel

injected into the system, both in terms of SRF in the auxiliary burner and of MSW in the main combustion chamber.

Knowing the reference LCOE and the LCOE obtained with the implementation of a carbon capture technology, it can be introduced the concept of the Cost of CO2 avoided, which represents the average CO2 tax over the duration of the project that would be required as income to match the net present value of costs due to the added CO2 capture system. The CAC (Cost of Avoided CO2) is evaluated as follows:

$$CAC = \frac{LCOE_{CCS_i} - LCOE_{ref}}{e_{CO2_{ref}} - e_{CO2_{CCS_i}}}$$

By recalling the obtained specific CO2 fossil emissions defined in the previous chapter, it has been estimated that the CAC for the two case studies is equal to

A. $CAC_{CASE\ A} = 92{,}18\ €/ton_{CO2}$
B. $CAC_{CASE\ B} = 24{,}78\ €/ton_{CO2}$

The values obtained are competitive compared to the carbon capture benchmark technologies now available on market.

Because the designed WTE facilities equipped with CCS, in addition to the thermal treatment of waste and the delivery of electrical power also ensures net negative emissions, there is the prospective of obtaining a carbon credit equal to the CAC, promoting a cost-effective solution. A carbon credit, or carbon tax, is a tax paid by the companies, industries and power plants that produce carbon dioxide through their operations. The tax aims at reducing the CO2 impact, pushing on green investments that allow the reduction of CO2 emissions of the industries. It works as a sort of pollution tax that makes more expensive the use of fossil-base fuels.

Because the carbon tax has been shaped as the cost to the society through the harm that it causes to the environment, the possibility of having a negative emissions power plant opens the doors on negative carbon taxes, thus to a carbon credit.

5.2. Gate fee evaluation

The aforementioned results consider that the main fuel (MSW) costs and the SRF costs are not to be considered costs but credits. In real operating conditions, WTE power plants have an additional source of revenue, called “gate fee”, which is related to the waste management service offered.

A gate fee is the charge dependent on the quantity of waste received at a waste processing facility. The fee can be charged per load, per ton, or per item depending on the source and type of waste. In the following analysis, the gate fee is going to be referred as euros per ton of waste, as defined in Table 25.

In order to evaluate the gate fee, there are two different approaches that can be adopted: (i) fixing the desired cost of electricity and consequently evaluating the gate fee or (ii) fixing the gate fee and evaluating the cost of electricity. In this work, the second approach has been selected. Higher is the gate fee, lower is the cost of electricity needed to pay back the costs.

To better explain how it has been considered the MSW gate fee in this work, the $LCOE^*_{ref}$ evaluation must be explained.

First, it has been assumed a levelized cost of electricity for the reference power plant equal to 80 €/MWh and a gate fee equal to 75 €/MWh. Knowing that the ton/h of waste injected in the reference WTE power plant is equal to 73,78 ton/h, the overall yearly revenues had been evaluated as follows:

$$Yearly\ revenues = 80\ \left[\frac{€}{MWh}\right] + 75\ \left[\frac{€}{ton}\right] * \frac{m_{MSW_{in_{ref}}}\left[\frac{ton}{h}\right]}{P_{ref}[MW]}$$

Knowing that, by definition, the gate fee is the price required to have

$$Yearly\ costs - Yearly\ revenues = 0$$

the yearly cost of the refence case (CAPEX*CCR + OPEX) has been found and it resulted to be equal to 82 M€/year.

Once the yearly costs have been found, the $LCOE^*_{ref_A}$ is equal to

$$LCOE^*_{ref_A} = \frac{Yearly\ costs_{ref}\left[\frac{€}{year}\right]}{8050\left[\frac{h}{year}\right] * P_{WTEcaseA}[MW]} - \frac{gate\ fee\ \left[\frac{€}{ton}\right] * m_{MSW_{caseA}}\left[\frac{ton}{h}\right]}{P_{WTEcaseA}\ [MW]}$$

Therefore, the reference LCOE for case A is equal to 117,06 €/MWh. Because the WTE power plant works at nominal condition in case B, the LCOE remains the same.

By looking at the above results, it is clear how the use of waste streams increases the economic advantages of this technology, making it competitive not only compared to other carbon capture solutions applied to WTE power plants, but also compared to other BECCS technologies.

6 Conclusions

This thesis has the aim of exploring a possible solution to enhance the energy transition through the implementation of a BECCS system. By adding a CO2 capture system to a WTE power plant it is possible to promote a net negative emissions technology that could be a game changer in the next years.

The advantages of promoting such a technology are linked to a steep increase in the energy demand and waste production, but also to the urge of changing the energy mix due to environmental and political reasons. This technology could lead the transition due to the high reliability, predictability, and ancillary services that could provide, emitting an amount of CO2 equivalent emissions that is way below the actual regulations.

The two case studies, case A and case B, analyzed in this thesis are both a post-combustion CO2 capture system, but they suggest two different integrations of the calcium looping technology, the process selected to capture the CO2.

Case A promotes an integration that sees, as unique addition, the calcium looping main components, limiting the capital expenses and, consequently, the operating costs. However, due to the worst thermodynamic characteristics of the processes involved and due to the lower carbon capture efficiency, the final expenses of the overall carbon capture system are comparable to a much more sophisticated asset (case B) that leads to a higher power output and a higher efficiency.

Case B has an additional steam turbine integrated into the system that works at better thermodynamic conditions, reducing the exergy losses of the system. Additionally, due to the reduction of operating constraints, it is possible to set the carbonator's efficiency equal to the maximum efficiency (Ecarb = 90%), minimizing the CO2 emissions to the atmosphere and increasing the mass flow rate of CO2 sent to storage, which can be considered as a valuable stream. Moreover, the main KPIs analyzed confirm that this case study leads to better performances.

From the economical point of view, a specific comparison has been addressed to verify which solution leads to lower expenses: through the evaluation of the LCOE it has be stated that the integration of two different waste streams as fuel input make the costs related to the additional technology affordable and cost-effective, leading to a levelized cost of electricity for case B, which is significantly lower than the one obtained for case A. This is because of the incentives related to the gate fee (which

are more significant due to a higher MSW mass flow rate and SRF mass flow rate) and the better performances of the system.

Table 28 summarizes the main results of the analyzed solutions, facilitating a comparison and understanding both the economic and the KPIs results described in Chapter four and Chapter five.

	Base case	**Caso A**	**Caso B**
Fuel consumption			
WTE plant, MW_{LHV}	212	141	212
Calciner CaL, MW_{LHV}	0	82,95	185,42
Power Balances			
WtE plant			
Electric power at generator, MW	65,77	68,87	65,77
Steam cycle auxiliaries, MW	-2,56	-2,79	-2,56
Plant auxiliaries, MW	-4,79	-2,10	-4,34
Net power output of WTE, MW	58,42	63,98	58,87
CaL power plant			
Electric power at generator, MW	0	0	60,80
Steam cycle auxiliaries, MW	0	0	-2,23
Air separation unit, MW	0	-5,54	-12,35
CO2 compression unit, MW	0	-6,53	-14,20
Other auxiliary consumptions, MW	0	-3,24	-3,45
Overall WTE + CaL power plant			
Total fuel consumption, MW_{LHV}	212	223,95	397,42
Total gross power output, MW	65,77	68,87	126,57
Gross electric efficiency, %	31,02%	30,75%	31,85%
Total net power output, MW	58,42	48,67	87,30
Net electric efficiency, %	27,56%	21,71%	21,97%
CO2 emissions			
Direct CO2 emission at stack, kg/s	20,20	4,51	2,03
CO2 vented from CO2 compression, kg/s	0	0,14	1,11
Total CO2 emission, kg/s	20,20	4,65	3,14
Fossil, kg/s	10,10	0,00	0,00
Biogenic, kg/s	10,10	4,65	3,14
CO2 specific emission, kg_{CO2}/MWh	1244,98	343,89	129,59
Fossil, kg_{CO2}/MWh	622,49	0,00	0,00
Biogenic, kg_{CO2}/MWh	622,49	343,89	129,59
Fossil CO2 avoided, kg/s	0	10,10	10,100

Specific fossil CO2 avoided, kg_{CO2}/MWh	0	343,89	622,49
Net CO2 negative emissions, t_{CO2}/year	0	-74936,73	-233779,28
CO2 grid emissions, kg_{CO2}/s	0	3,48	-10,31
KPIs			
Net electric efficiency penalty, %pts.	0	5,85%	5,60%
Carbonator's efficiency	0		90%
Overall CCR, %	0	65,47%	84,44%
SPECCA, MJ_{LHV}/kg_{CO2}	0	3,91	2,98
SPECCA fossil, MJ_{LHV}/kg_{CO2}	0	5,66	5,35
SPECCA*, MJ_{LHV}/kg_{CO2}	0	1,74	0,95

Table 28 Summary of the main results obtained

7 Bibliography

1. **IEA.** *The role of CCUS in low-carbon power systems.* 2020.

2. —. *Carbon capture in 2021: Off and running or another false start?* Paris : https://www.iea.org/commentaries/carbon-capture-in-2021-off-and-running-or-another-false-start, 2021.

3. *Application of CCUS to the WtE sector.* **Vincenzo Tota, Manuele Gatti, Federico Viganò, Monica Garcia.** Adu Dhabi, UAE : s.n., March 2021. 15th International Conference on Greenhouse Gas Control Technologies, GHGT-15.

4. **Prag, Andrew.** Sustainable Development Scenario. *World Energy Outlook 2018 (IEA).* 2018.

5. **PROGRAMME, IEA GHG R&D.** *IEAGHG Technical Report.* 2020.

6. **IEA.** *Exploring Clean Energy Pathways, The role of CO2 storage.* July 2019.

7. **D. Coleman, J. Davison, C. Hendrinks, O. Kaarstad, M. Ozaki.** *IPCC Special Report on Carbon dioxide Capture and storage, Transport of CO2.*

8. *The technological and economic prospects for CO2 utilization and removal.* **C. Hepburn, E. Adlen, J. Beddington, E. A. Carter, S. Fuss, N. Mac Dowell, J.C. Minx, P. Smith, C.K. Williams.** 575, 2019, Nature , p. 87 - 97 .

9. **Institute, Global CCS.** *Global of CCS 2020.* 2020.

10. **Bank, The World.** [Online] 2019. https://datatopics.worldbank.org/what-a-waste/trends_in_solid_waste_management.html.

11. **ambiente, a2a.** *Relazione annuale sul funzionamento e la sorveglianza dell'impianto (Periodo: 1/1/2020 - 31/12/2020), IMPIANTO DI TERMOVALORIZZAZIONE RIFIUTI "SILLA 2".* Marzo 2021.

12. **J. Sthrole, M. Junk, J. Kremer, A. Galloy, B.Epple.** *Caronate looping experiments in a 1 MWth pilot plant and model validation.* 2014.

13. *CO2 Capture Capacity of CaO in Long Series of Carbonation/Calcination Cycles.* **Abanades, Gemma S. Grasa and J. Carlos.** 2006, Ing. Eng. Chem. Res., Vol. 45, p. 8846 - 8851.

14. *Surface area reduction during isothermal sintering.* **Gernam, M.R.** 1976.

15. *On the Decay Behavior of the CO2 Absorption Capacity of CO2-based sorbents.* **J.Wang, E. Anthony, E.J.** 2005, Ind. Eng. Chem. Res.

16. **Spinelli, Maurizio.** Advanced technologies for CO2 capture and power generation in cement plants. s.l. : Doctoral thesis, 2016.

17. **Mordor Intelligence. [Online] 2021. https://www.mordorintelligence.com/industry-reports/calcium-carbide-market.**

18. ***Modeling the carbonator of a Ca-looping process for CO2 capture from power plant flue gas.*** **Romano, Matteo C. 257-269, s.l. : Chemical Engineering Science , 2012, Vol. 69.**

19. ***CO2 capture from waste-to-energy plants: Techno-economic assessment of calcium looping technology.*** **Martin Haafa, Rahul Anantharaman, , Simon Roussanaly. s.l. : Resources, conservation and recycling , 2020, Vol. 164.**

20. Cinti, G., et al. ***Deliverable D4.4 Cost of critical components in CO2.*** **s.l. : CEMCAP, 2018.**

21. ***Improved flexibility and economics of calcium looping power plants by thermochemical energy storage.*** **Astolfi, Marco. 140-155, s.l. : International Journal of Greenhouse Gas Control, 2019, Vol. 83.**

22. ***Simultaneous CO2/HCl removal using carbide slag in repetitive absorption/desorption cycles.*** **Yingjie Li, Wenjing Wang, Xingxing Cheng. 142, 2015, Vol. Fuel.**

23. Yingjie Li, Rongyue Sun, Changtian Liu, Hongling liu, Chunmei Lu. ***CO2 capture by carbide slag from chlor-alkali plant in calcination/carbonation cycles.*** **China : International Journal of Greenhouse Gas Control, 2012.**

24. ***Waste-to-Energy network synthesis for municipial solid waste.*** **Wendy Pei Qin Ng, Hon Loong Lam, Petar Sabev Varbanov. 85, 2014, Vol. Energy Conversion and Management.**

25. Romano, Matteo C., et al. Guidelines for modeling and simulation of Ca-looping processes. [Online] 2012. [Riportato: 19 10 2020.] https://researchgate.net/profile/dursun_ozcan/publication/278847528_guidelines_for_modeling_and_simulation_of_ca-looping_processes/links/5586c28c08aef58c03a00a5e.pdf.

26. Prag, Andrew. World Energy Outlook 2018 : Sustainable Development Scenario. s.l. : IEA, Dicember 2018.

27. P. Tilak, M.M.El-Halwagi. ***Process integration of Calcium looping with industrial plants for monetizing CO2 into value-added products*** **. s.l. : Carbon Resources Conversion, 2018.**

28. ***The role of CO2 capture and utilization in mitigating climate change.*** **Niall Mac Dowell, Paul S. Fennell, Nilay Shah & Geoffrey C. Maitland. s.l. : Nature Climate Change, 2017, Vol. 7.**

29. ***Process simulation of Ca-lopping process: review and guidelines*** **. Matteo C. Romano, Isabel Martìnez, Ramon Murillo. 2013, Energy Procedia 37, p. 142-150.**

30. ***Combustion of solid recovered fuels within the calcium looping process*** **. Martin Haafa, ⁎, Jens Petersa. 2020, Experimental thermal fluid science 113.**

31. ***Improved flexibility and economics of Calcium Looping power plants by thermochemical energy storage.*** **Marco Astolfi, Edoardo De Lena, Matteo C. Romano. 2019, International Journal of Greenhouse Gas Control 83, p. 140-155.**

32. M.Zhao, A.Minett, A.Harris. ***A review of techno-economic models for the retrofitting of conventional pulverised-coal power plants post-combustion capture (PCC) of CO2.*** **s.l. : Energy and Environmental Science , 2013.**

33. M.Romano, M.Spinelli, S.Campari, S.Consonni, G.Cinti, M.Marchi, E. Borgarello. ***The Calcium looping process for low CO2 emission cement and power*** **. s.l. : Energy Procedia 37, 2013.**

34. ***Design and erection of a 300 kW indirectly heated carbonate looping test facility.*** **M. Reitz, M. Junk, J. Strohle, B. Epple. s.l. : Energy Procedia, 2014, Vol. 63.**

35. ***Waste-to-Energy in the EU:the effects of plant ownership, waste mobility, and decentralization on Environmental Outcomes and Welfare.*** **Laura Levaggi, Rosella Levaggi,Carmen Marchiori, Carmine Trecroci. 2020, Vol. Sustainability.**

36. ***A perspective on environmental sustainability in the cement industry.*** **Joshua O. Ighalo, Adewale George Adeniyi. s.l. : Waste Disposal & Sustainable Energy, July 2020.**

37. ***Thermodynamics and kinetics analysis of Ca-lopping for CO2 capture: application of carbide slag.*** **Jie Yang, Liping Ma, Hongpan Liu. 242, 2019, Vol. Fuel.**

38. Intelligence, Mordor. ***CALCIUM CARBIDE MARKET - GROWTH, TRENDS, COVID-19 IMPACT, AND FORECASTS (2021 - 2026).***

39. Institute, Global CCS. Transporting CO2 - Fact Sheet.

40. —. *Global status of CCS 2021: CCS ACCELERATING TO NET ZERO.* 2021.

41. IEA, International Energy Agency. *About CCUS.* Paris : https://www.iea.org/reports/about-ccus, April 2021.

42. IEA. *Global Energy & CO2 impact 2019.* 2019.

43. —. *Cement.* June 2020.

44. H.Dieter, A.Bidwe, G. Varela-Duelli. *Development of the calcium looping CO2 capture technology from lab to pilot scale at IFK,University of Stuttgard.* s.l. : Fuel 127, 2014.

45. *A thermodynamic and kinetic study of the de- and rehydration of Ca(OH)2 at high H2O partial pressures for the thermochemical heat storage.* F. Schaube, L. Koch, A. Wörner , H. Müller-Steinhagen. s.l. : Thermochimica Acta, 2012, Vol. 538.

46. *The 21st-century cement plant: Greener and more connected.* Eleftherios Charalambous, Thomas Czigler, Ramez Haddadin, Sebastian Reiter, and Patrick Schulze. s.l. : McKinsey & Company, September 2020.

47. Dr. Ella Adler, Prf Cameron Hepburn. Carbon Brief, Clear on climate. [Online] July 2019. https://www.carbonbrief.org/guest-post-10-ways-to-use-co2-and-how-they-compare.

48. Corporation, International Finance. *The impact of COVID-19 on the cement industry.* August 2020.

49. Consoli, Christopher. *Bioenergy and Carbon Capture and Storage).* s.l. : CCS Global Institute, 2019.

50. *Aspen Plus process simulation of Calcium Looping with different indirect calciner heat transfer concepts.* Chaamera K. Jayarathna, Anette Mathisen, Lars Erik Oi, Lars-André Tokheim. s.l. : Energy Procedia, 2017, Vol. 114.

51. *Transformation technologies for CO2 utilisation: Current status, challenges and future prospects* . Ariane D.N. Kamkeng, Meihong Wang, Jun Hu. 409, s.l. : Chemical Engineering Journal, 2021.

52. *The maximum capture efficiency of CO2 using a carbonation/calcination cycle of CaO/CaCO3.* Abanades, Juan Carlos. 2002, Chemical Engineering Journal, Vol. 90, p. 303-306.

53. A. Martinez, Y. Lara, P. Lisbona, L. Romeo. *Energy penalty reaction in the calcium looping cycle.* **s.l. : International Journal of greenhouse gas control, 2012.**

54. IEA. [Online] Aprile 2021. https://www.iea.org/reports/about-ccus.

55. *https://www.ecoprog.com/publications/energy-management/waste-to-energy.htm.* **2020.**

56. *https://oilandgasclimateinitiative.com/knowledge-base/talking-transition-podcast-highlights/#podcast-4.*

57. *https://ec.europa.eu/eurostat/statistics-explained/index.php/Municipal_waste_statistics.*

58. *HS Markit's Chemical Economics Handbook–Calcium Carbide.* **2020.**

59. *calcium carbide market size, COVID-19 impact analysis, by application, by end user, and by regional forcast 2020-2027.* **s.l. : Furtune business insights, 2020.**

A Appendix A

A.1. Base Case: GS simulation

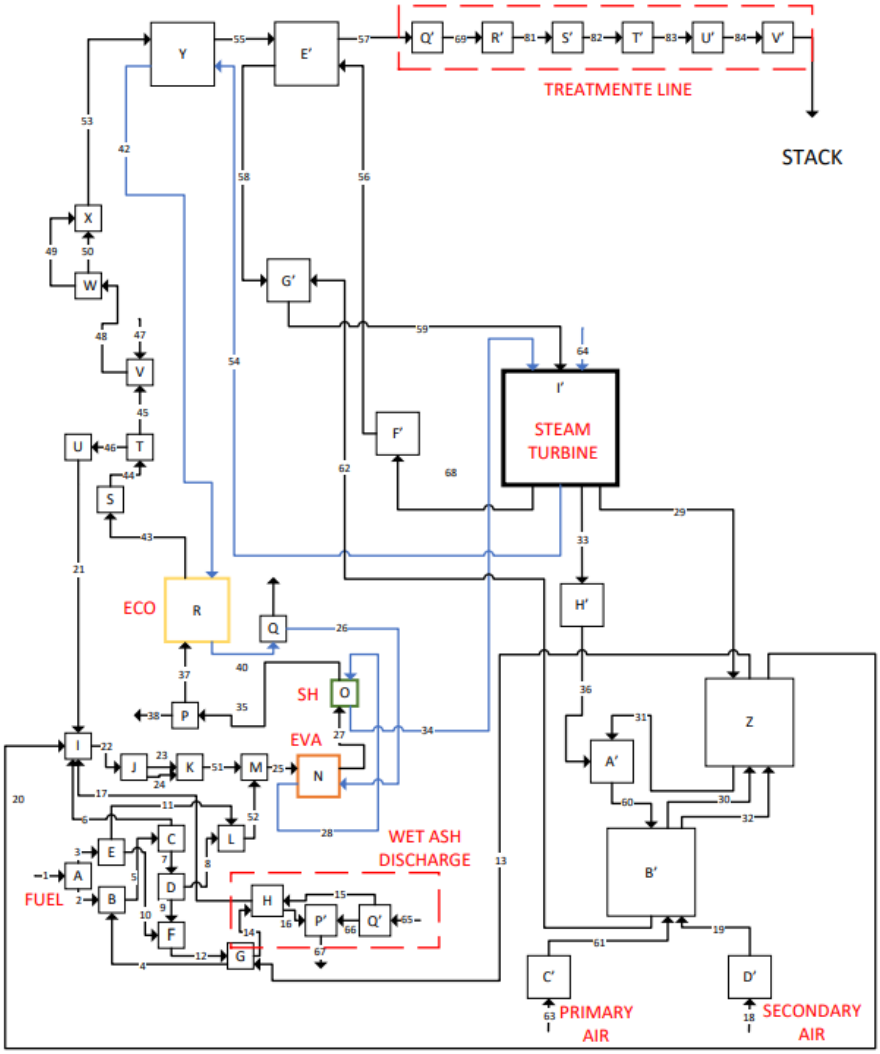

Figure 47 Base case: GS block flow diagram coherent with the flows and components described in the GS model

Figure 47 describes the GS model of the base case, schematizing a the WTE power plant like the "Silla 2" based in Milan.

Flow (1) is the waste stream (fuel) entering the combustor through the feeding system. The fuel mass flow rate at the inlet of the WTE power plant has an average LHV equal to 10,342 [MJ/kg]. In order to model this kind of fuel, it has been defined an equivalent composition of the fuel, using the most common molecules found in common fuels, with the addition of an invented species, CH4($$) necessary to model the right lower heating value. The equivalent composition of the fuel is reported in Table 29.

COMPONENT	[mol/s]	COMPONENT	[mol/s]
Ar	0	**H2S**	0
CH4	0	**NH3**	0
CO	117.66	**N2**	7.5118
COS	0	**O2**	13.021
CO2	22.373	**C4H10**	0
C2H2	0	**CH4($$)**	126.66
C2H4	0	**S(G)**	0
C2H6	0	**SO2**	0
C3H8	0	**H2O(L)**	341.01
H2	142.14	**C(S)**	172.41
H2O	0	**Ah**	56.224

Table 29 Fuel's equivalent composition with a LHV equal to 10,342 MJ/kg

After the fly ashes' separation in splitter [A], the fuel (1) is sent to the combustor [B]. The hot primary air (4) is needed to ensure a proper oxidation process and it is fed to the combustor after it has been heated up by heat exchanger [G]. After the combustion process, the flue gases (6) exit the combustor and they are split in splitter [C] in gaseous flue gases (6) and ashes (7), which are further spitted by component [D] in fly ashes (17) and unburned carbon (9). The bottom ashes (10) and the unburned (9) are mixed together in [F] and then they are sent to two heat exchangers in series: the former, heat exchanger [G], exchanges heat with primary combustion air (4) fed to the combustor; the latter, heat exchanger [H], produces steam. The steam produced, the secondary air (20), the recirculated flue gases (21), and the gaseous flue gases (6) are then mixed by mixer [I]. On the other hand, the bottom ashes are first mixed with water and then purged (67).

Going back to [I], a stream (22) of flue gases exits the mixer and it is cooled down in the boiler section of the power plant. The boiler's tube banks (shown in Figure 25) are positioned as follows: first, we have the evaporator [N], then the superheater [O], and then the economizer [R].

Before the economizer, the fly ashes (38) are separated by [P], and, after the economizer, the flue gas stream is sent to an ESP [S] to allow the recirculation to the combustion chamber of a fraction of flue gases (46). In this specific case, the percentage of FGR is set equal to 15%.

On the other hand, the percentage of not recirculated flue gases, first, mixes with ambient air (47) entering the treatment line due to not perfect sealing, then is sent to the flue gas treatment line. To evaluate the performances of the treatment line, splitter [W] and [X] have been introduced: they are not real plant components, but they are used to separate water and ashes from the flue gases to find the oxygen fraction in dry flue gases. This parameter is needed to evaluate if the power plant is respecting the emission limits according to the regulations. Then the virtual flows are mixed back together to perform the calculation on the heat recovery section. The flue gas heats up the feed water (54) in the heat exchanger [Y], while heat exchanger [E'] is used to heat up the feed water coming from the condensate extraction pump [F']. Then, thanks to the fan [O'], the flue gases are sent to the flue gas treatment line: mixer [R'], [S'], [T'], [U'] and [V'] represent the main components of the treatment line for the removal of the acid compounds, SOx and NOx (in this specific simulation they are inactive).

Finally, stream (85) exits the treatment line, and it is sent to the stack.

A.2. Case A: GS simulation model

Figure 48 shows the GS simulation model and highlights the main components of the system.

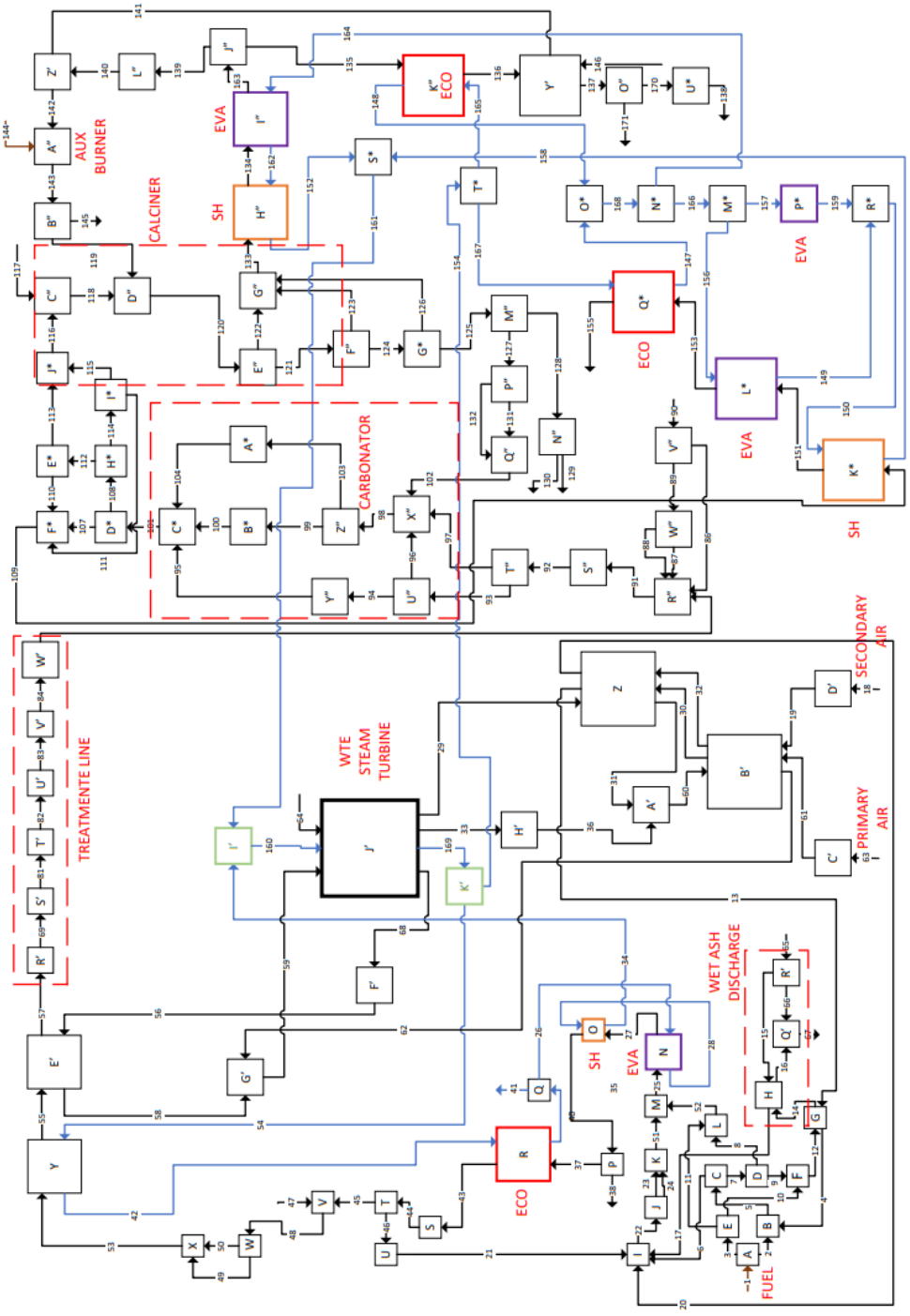

Figure 48 Case A: GS block diagram definition

In case A stream (85) is not sent directly to the stack, as occurs in the reference case, but it is subject to the CaL CO2 removal section.

Stream (85) enters [R"] and, thanks to the blower [S"], is sent to the splitter [T"], a virtual component needed to divide the CO2 present in the flue gases (93) and the flue gases without CO2 (97). In this model [T"] has an important role: by changing the split fraction f in the GS input file, it was possible to qualitatively simulate a different carbon capture efficiency within the carbonator. In this case it has been obtained a carbonator's efficiency equal to 69,26%, recovering a minimum amount of heat.

To model the carbonator operating conditions, the following components are used: splitter [U"] is a virtual component needed to diverge the CO2 that is subject to the carbonation reaction to the carbonator (96) and the one which is unconverted to a bypass section. On one hand, the unconverted CO2 is heated up to the temperature at the exit of the carbonator, which is equal to 650 °C, and then mixed with the stream exiting the carbonator in mixer [C*]; on the other, the CO2, that will be fully converted in the carbonator, is mixed with the stream of recirculated CaO, coming from the calciner, in mixer [X"]. Stream (98) is sent to [Y"] which is a virtual mixer that separates the CaO that actually partakes in the carbonation reaction, going into stream (99), and the one that is unconverted (103). The unconverted CaO is sent first to mixer [A*] and then it is mixed with the unconverted CO2 (95) and the flue gases coming out of the carbonator [B*] in mixer [C*]. Stream (101) is characterized by the presence of flue gases, CaCO3, unconverted CaO, unconverted CO2, and ashes. Thanks to a cyclone, the hot CO2 depleted flue gases (109) and the solid compounds (116) are separated. The selectivity for the removal of ashes has been assumed equal to 90%, while the one for the calcium compounds was assumed equal to 99%.

The CaCO3 formed, the unconverted CO2 and CaO (solid compounds) are then sent to the calciner, whose purpose is addressing the calcination reaction to obtain again CaO and CO2. Because the calciner [D"] needs to operate at a temperature of 920 °C, an auxiliary burner [A"] is used to supply additional heat. The composition of the solid recovered fuel (144) burned within the auxiliary burner, as defined in the GS input file, is summarized in Table 8. It has been assumed a sulfur free fuel, however, in real case applications, this compound must be kept under control to avoid the additional built up of solids in the calcination-carbonation cycles.

Additionally, the fuel considered is a high-quality fuel because of its LHV, that is equal to 24,982 [kJ/kg].

Table 30 define the equivalent auxiliary fuel composition, needed to model the SRF used in the auxiliary burner.

COMPONENT	[mol/s]	COMPONENT	[mol/s]
Ar	0	**H2S**	0
CH4	332.26	**NH3**	0
CO	74.598	**N2**	12.917
COS	0	**O2**	42.583
CO2	0.03239	**C4H10**	0
C2H2	0	**CH4($$)**	0
C2H4	0	**S(G)**	0
C2H6	0	**SO2**	0
C3H8	0	**H2O(L)**	117.09
H2	0.69201	**C(S)**	397.60
H2O	0	**Ah**	22.224

Table 30 Auxiliary fuel equivalent composition

Nearly pure oxygen (141), preheated in heat exchanger [Y'], is also supplied to the auxiliary burner as an oxidizer together with stream (140) of recirculated CO2, used as a fluidization medium and temperature moderator. It has been assumed a CO2 recirculation temperature equal to 400 °C, because of technical constraints mainly linked to the maximum blower's thermal stress.

At the exit of the calciner, the CO2 stream (122) is separated by splitter [E"] while the CaO is recirculated to the carbonator to be reused. The selectivity of the calciner's cyclone is assumed equal to the carbonator's one. Additionally, a percentage of CaO is purged (128) by splitter [M"] because of the deactivation of limestone occurring after a certain number of operating cycles.

The hot CO2 separated from the calciner (133) is then cooled down to be stored or set up for utilization.

In the steps previously described, two hot streams can be identified as outputs: the hot CO2 separated from the calciner, at a temperature equal to 920 °C, and the hot CO2 depleted flue gases (109) exiting from the carbonator, at a temperature equal to 650 °C.

The hot CO2 stream is cooled down by three different heat exchangers: heat exchangers [H"] and [I"] are respectively a superheater and an evaporator, and they are used to cool down the CO2 (163) to a temperature of 400 °C to perform the recirculation in the auxiliary burner; then, heat exchanger [K"], an economizer, brings the CO2 (136) at the targeted temperature of 200 °C (value forced by the convergence variables). The CO2 stream (137) is then sent to a filter [O"] for the residual ashes removal and it is then sent to a refrigeration section [U*] to reach the desired temperature of 60°C, required by the CO2 storage/transportation/utilization system.

On the other hand, the hot CO2 depleted flue gases (109) exiting the carbonator exchange heat with superheater [K*], with evaporator [L*], and then with economizer [Q*]. The constraints defined in the model regard the ΔT_{PP} set equal to 15 °C, and the ΔT_{SC} set equal to 5 °C. The flue gases are released into the environment at a temperature of 144,2°C.

Additionally, one last heat exchanger is present into the CaL heat recovery section: the evaporator [P*], in parallel with evaporator [L*], recovers the heat lost during the exothermic carbonation reaction.

The resulted mass flow rate of stream (161), steam generated in the CaL heat recovery section, resulted equal to 28 kg/s. The steam generated in the CaL heat recovery section is sent to the main steam cycle: the live steam temperature is set equal to 443 °C and the live steam pressure equal to 50 bar; the overall mass flow rate of the steam going into the turbine results to be equal to 75,7 kg/s, which means an increase in the mass flow rate equal to 5% compared to the reference case.

A.3. Case B: GS simulation model

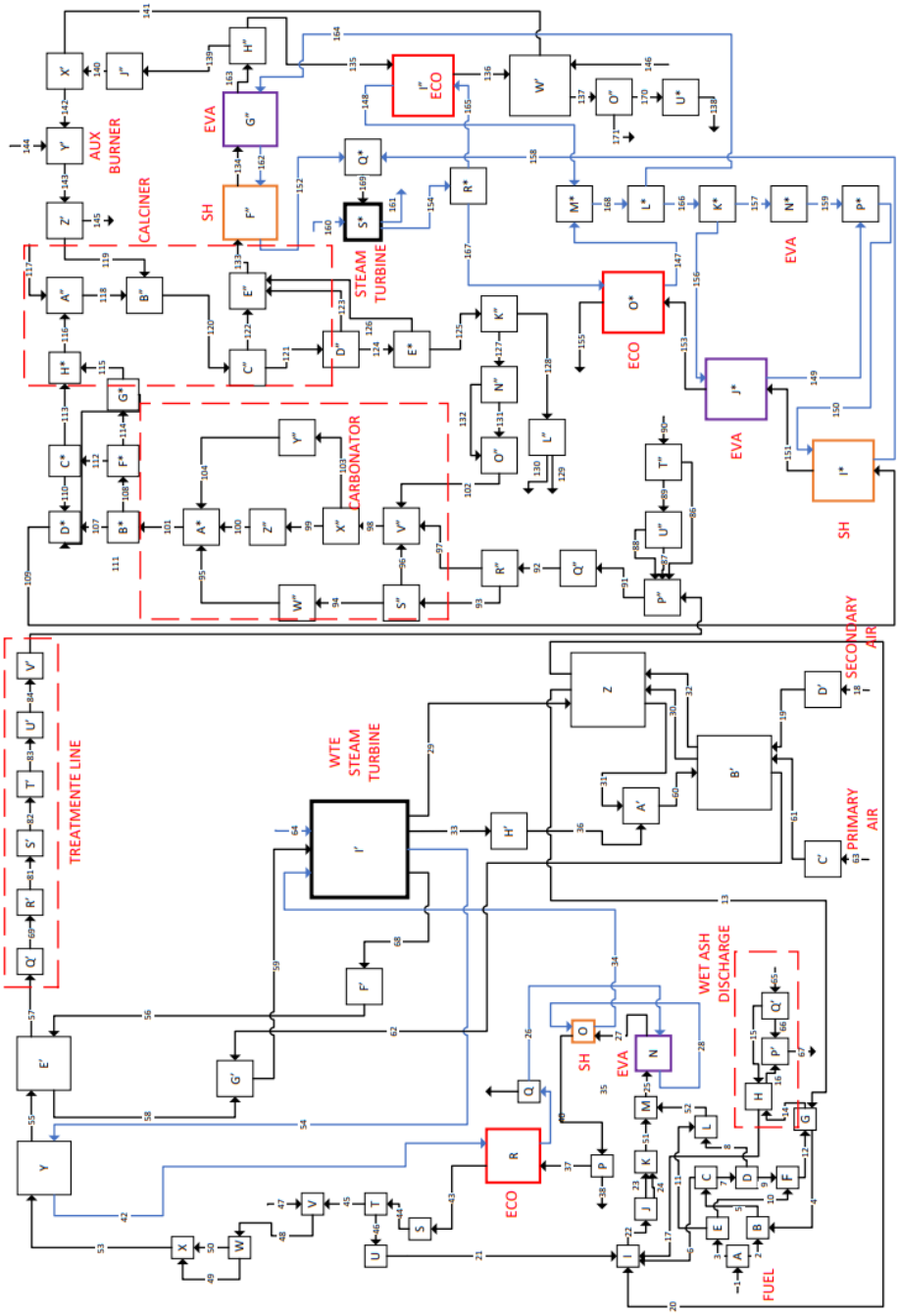

Figure 49 Case B: GS block flow diagram and flows identification

Case B has been modelled in accordance with the previous case studies. The main difference of this model is the presence of the additional component [S*] which is the additional turbine of the calcium looping heat recovery section. Stream (169) entering the steam turbine is at the live steam temperature of 520 °C and at 70 bar.

Stream (160) and (161) are the water make-up and water discharge of the steam cycle under st

List of Figures

List if Tables